Spring 1-1-2010

Assessing feasibility of electrochromic space suit radiators for reducing extravehicular activity water consumption

Jonathan Glen Metts
University of Colorado at Boulder, metts@colorado.edu

ASSESSING FEASIBILITY OF ELECTROCHROMIC SPACE SUIT RADIATORS
FOR REDUCING EXTRAVEHICULAR ACTIVITY WATER CONSUMPTION

by

JONATHAN GLEN METTS

B.S., Auburn University, 2004

M.S., Auburn University, 2006

A thesis submitted to the

Faculty of the Graduate School of the

University of Colorado in partial fulfillment

of the requirement for the degree of

Doctor of Philosophy

Department of Aerospace Engineering Sciences

2010

The thesis entitled:

Assessing Feasibility of Electrochromic Space Suit Radiators for Reducing

Extravehicular Activity Water Consumption

written by Jonathan Glen Metts

has been approved for the Department of Aerospace Engineering Sciences

_____

David M. Klaus, Ph.D. (Chair)

_____

James A. Nabity, Ph.D.

Date _____

The final copy of this thesis has been examined by the signatories, and we

Find that both the content and the form meet acceptable presentation standards

Of scholarly work in the above mentioned discipline.

Metts, Jonathan Glen (Ph.D., Aerospace Engineering Sciences)

Assessing Feasibility of Electrochromic Space Suit Radiators for Reducing
Extravehicular Activity Water Consumption

Thesis directed by Associate Professor David M. Klaus

Water consumption for space suit thermal control is a limiting factor on long-term
space exploration missions. A concept is proposed for an integrated, flexible suit
radiator using infrared electrochromic materials for modulated heat rejection from
the suit. Properties of electrochromic materials, the structure of electrochromic
devices, and relevant heat transfer processes are presented as background
information. Analytical methods are employed to bound theoretical performance
and determine required emissivity ranges for lunar surface operations. Case studies
are presented incorporating Apollo program and Advanced Walkback Test
metabolic and environmental data to estimate sublimator water consumption and
hypothetical water savings with the electrochromic radiator. Concepts are
presented and analyzed for integrating an electrochromic radiator with existing and
future space suit designs. A preliminary systems-level trade analysis is performed
with the Equivalent System Mass metric used to compare this technology with the
legacy sublimator and other extravehicular activity cooling technologies in
development. Experimental objectives, procedures, and results are presented for
both bench-top and thermal vacuum testing of electrochromic radiator materials.

This thesis is dedicated to my parents, Glen and Susan Metts, for their support and patience throughout my education.

Acknowledgements

Finally, I am very thankful for the guidance of my thesis committee:

- David Klaus, CU-Boulder (Chair)
- Brian Berland, ITN Energy Systems
- Se-Hee Lee, CU-Boulder
- James Nabity, TDA Research
- Jeffrey Thayer, CU-Boulder

TABLE OF CONTENTS

TABLES

FIGURES

EQUATIONS

Chapter 1 – Introduction

During extravehicular activities (EVAs), astronauts generate metabolic heat proportional to their levels of exertion. There are also incident external thermal loads and heat generated by the space suit's Portable Life Support System (PLSS). All of this heat must be redistributed away from the human in order to maintain thermal equilibrium and to ensure safe and comfortable working conditions in the space suit.

Current space suits maintain thermal balance by using a liquid cooling and ventilation garment (LCVG) to collect heat from the skin via convection and conduction, where it is transferred to a water heat exchanger. The heat is then transported via closed water loop to a sublimator, which exposes a stream of feed water to vacuum, where it is frozen into ice and then sublimated into vapor. The heat is stored in the vapor through the phase change, and the vapor is allowed to vent away from the suit, carrying the heat with it.

Sublimated water is a considerable consumable mass during an EVA, and the amount of consumable water required increases with duration and intensity of activity. The problem of water loss is of particular concern for lunar missions, because the current cost per kilogram to launch anything to the Moon is at least an order of magnitude greater than the cost to launch that same mass into low Earth orbit (LEO). One study estimates that the cost to launch enough feed water for a single lunar EVA could equal up to $1 million U.S. dollars (Jones, 2008). Reducing or eliminating this mass consumption offers potential system-level benefits to suit operations as well as to overall mission design trades.

Radiators offer a possible alternative or supplement to the sublimator for thermal control. The primary advantage of a radiator is that it can reject heat from the suit without consuming any mass. To date, although used extensively on spacecraft, radiators have not been used on space suits due to increased mass, limited available surface area, and reduced operational performance capacity compared

to the sublimator. The objective of this research is to determine whether electrochromic materials may be feasible as an integrated space suit radiator to reduce or eliminate the amount of water consumed for EVA thermal control. A simplified comparison of each technology's mass/energy flows is depicted in Figure 1-1 below.
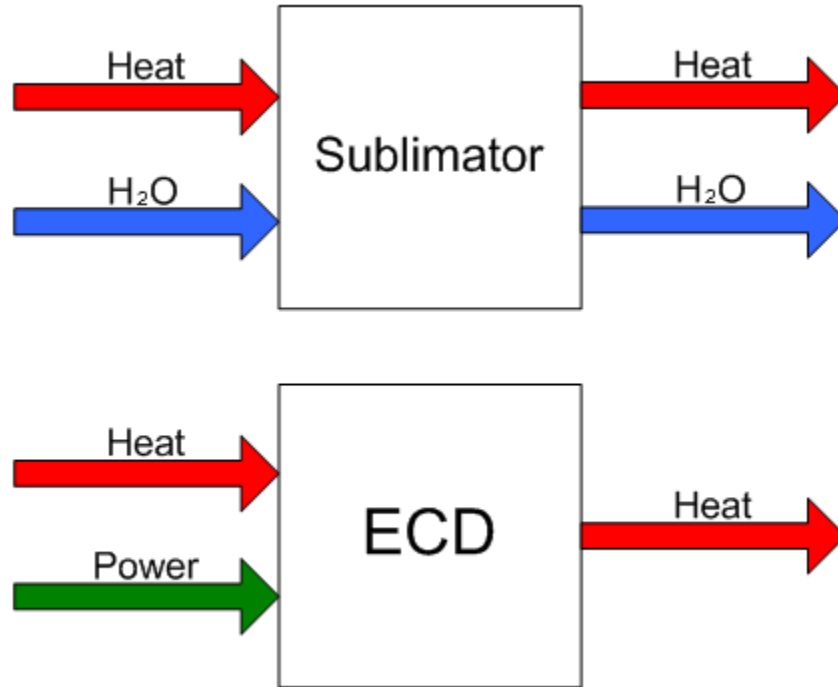
Figure 1-1: Mass/Energy Flow Comparison

In many respects, the U.S. Extravehicular Mobility Unit (EMU) and Russian Orlan space suits currently onboard the Space Shuttle and International Space Station are extremely similar to the suits worn by Apollo and Soyuz astronauts in the 1960s and 70s. They were not designed for long-term missions (station suits are frequently replaced) or for the type of activities and environments that will be encountered on Mars. NASA's Institute for Advanced Concepts (NIAC) funded a report on a concept for a radically different, next-generation space suit to be developed over the next few decades. Directed by Edward Hodgson, Jr. of Hamilton-Sundstrand, the contractor responsible for designing the EMU suit, this

report outlines an advanced space suit with fundamental differences from the traditional designs. Whereas past and current suits have completely isolated and protected an astronaut from the space or lunar environment, the "Chameleon Suit" incorporates numerous technologies that facilitate interaction among the astronaut, the suit itself, and the environment. The diagram below provides an overview of life support functionality for this suit concept and recommends specific technology development areas to enable milestones towards realization of this new system (Hodgson, 2001; Hodgson et al., 2004).
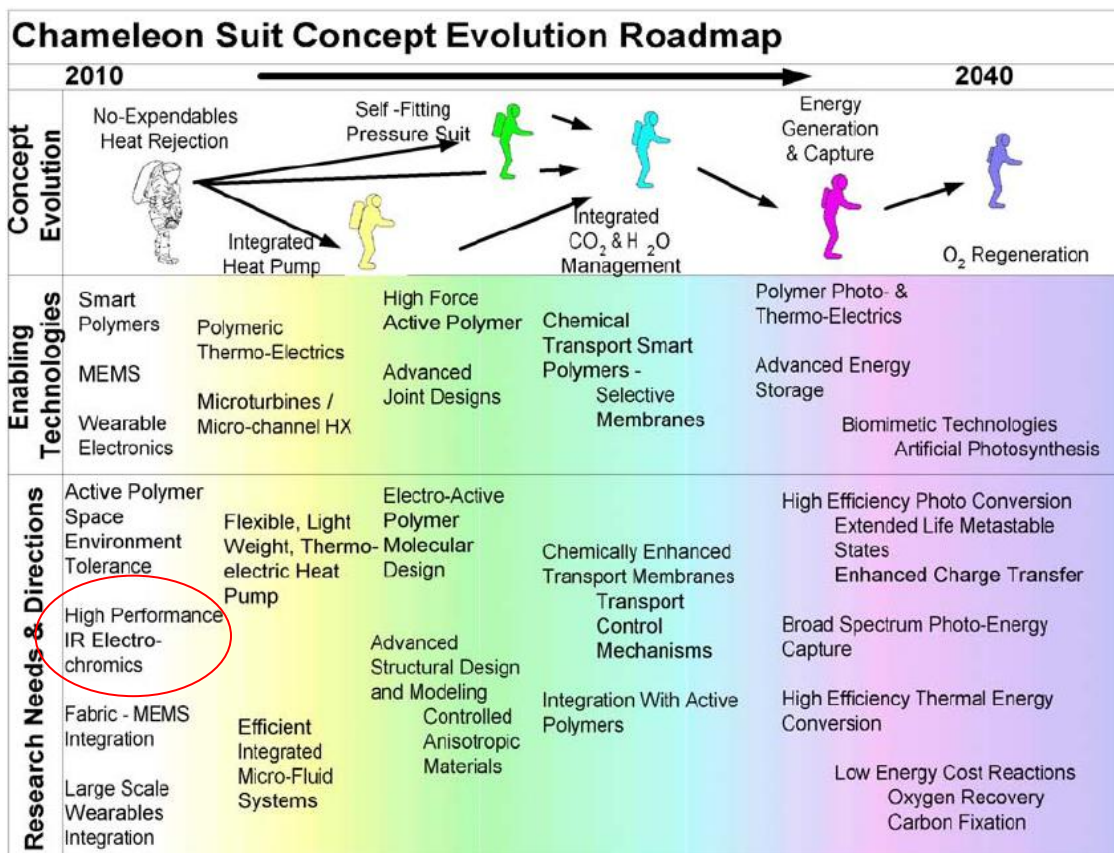
Figure 1-2: Chameleon Suit Roadmap (Hodgson et al., 2004)

The Chameleon Suit NIAC report provided the inspiration for this research topic. The area being investigated in this research is high performance, infrared electrochromics for "No Expendables Heat Rejection" is circled in red. As described by Hodgson, the goal is to integrate flexible radiators into the

fabric of the suit, allowing heat to flow into the environment in a controlled manner while still protecting the astronaut from incoming thermal radiation. Although the Chameleon Suit may never be realized to the extent envisioned in the NIAC reports, it represents a target concept whose constituent, enabling technologies may prove valuable to any future space suit design. In other words, the realistic value of these reports is to encourage investigation of advanced life support technologies, and that is exactly what it has accomplished by providing the motivation for the present research.

Electrochromic materials have been studied on a fundamental physio-chemical basis for many years, but practical applications are a recent development. Most commercial and industrial electrochromic products involve modulation in the visible spectrum of light; infrared electrochromics are a less mature technology. NASA and other organizations have been conducting and funding research on applied electrochromics for several years, but these studies have focused on satellite and spacecraft applications to replace traditional radiators. Trimble et al. (2000) characterize infrared electrochromics and propose applications in satellite radiators. Additional recommendations for small satellite applications are made by Kislov et al. (2004), and counter-measures against performance degradation by the space environment are proposed. Considerations for practical spacecraft applications are outlined by electrochromic manufacturer Ashwin-Ushas in a presentation by Paris et al. (2005). Tuan & Birur (2006), in a report for Johnson Space Center, characterized the endurance of Ashwin's electrochromic materials (along with other material coupons) in the harsh space environment. Another manufacturer, Eclipse Energy Systems, Inc., has characterized its own infrared ECD prototype for satellite applications in Demiryont et al. (2006). As opposed to these recent studies at the government and industry levels, my research is unique in its focus on space suit applications, where radiators of any type are still unproven in actual missions.

Key to the integrated suit radiator concept is the flexibility of the electrochromic devices. Although the electrochromic film itself and most other layers of the ECD are naturally flexible, they are

4

usually deposited on rigid silicon substrates that are not conducive to fabric-level integration. However, Bessiere et al. (2002) and Kislov et al. (2003) have investigated flexible substrates for electrochromic devices and confirmed that performance is similar to that of devices on rigid substrates.

NASA is investigating other types of radiators for space suits, some of them including innovative heat exchangers and rechargeable heat sinks. A concept for a rechargeable phase-change heat exchanger was tested in 1988 by Klaus at Johnson Space Center. Haddad et al. (2007) have investigated spacecraft radiators with thermochromic material coatings, whose optical properties passively change based on temperature. Pu et al. (2004) consider generic radiator performance for space suits in the Mars environment. Research by Izenson et al. (2008) describes a comprehensive new concept for space suit thermal control that includes an alternative cooling garment, rechargeable desiccant, and a backpack radiator to remove the heat of absorption from the desiccant. Another type of freezable heat exchanger for space suits is considered by Nabity et al. (2008), with the potential to interface with either a backpack-type radiator or an integrated, flexible radiator system. There is also mature ongoing research for non-radiator heat rejection technologies, such as a new sublimator with less sensitivity to contamination and an evaporator with consumable feed water that is effective in an atmospheric planetary environment such as Mars. (Vogel et al., 2008; Leimkuehler & Stephan, 2008) This research will include a preliminary system-level trade to estimate the performance, system mass, and cost of a notional electrochromic radiator system and compare such factors to those of competing technologies and the traditional sublimator.

Technology Readiness Level (TRL) is defined by NASA as "a systematic metric/measurement system that supports assessments of the maturity of a particular technology and the consistent comparison of maturity between different types of technology" (Mankins, 1995). Nine levels are defined, with increasing fidelity and confidence as the technology is further analyzed, built, and tested in various environments. The table below provides a summary description of each level.

Table 1-1: Technology Readiness Level Definitions (Mankins, 1995)

TRL 1	Basic principles observed and reported
TRL 2	Technology concept and/or application formulated
TRL 3	Analytical and experimental critical function and/or characteristic proof-of-concept
TRL 4	Component and/or breadboard validation in laboratory environment
TRL 5	Component and/or breadboard validation in relevant environment
TRL 6	System/subsystem model or prototype demonstration in a relevant environment (ground or space)
TRL 7	System prototype demonstration in a space environment
TRL 8	Actual system completed and "flight qualified" through test and demonstration (ground or space)
TRL 9	Actual system "flight proven" through successful Mission operations

As of the Chameleon Suit final report in 2004, the application of electrochromic materials to space suit heat rejection could be considered TRL 2. The basic principles of electrochromic materials had been observed and reported in various materials studies in previous decades, and the Chameleon Suit authors had put forth the concept and outlined potential benefits.

One of the goals of this research thesis can be summarized as increasing the TRL of the electrochromic space suit radiator. Achieving TRL 3 was accomplished through performance analysis and experimental verification of the critical function (electronically regulating heat rejection by means of the electrochromic effect). Furthermore, advancing the technology to TRL 4 was partially achieved by preliminary testing of electrochromic devices in a laboratory (bench-top) environment, although not all test objectives could be met, for reasons explained in Chapter 8. Finally, an attempt at moving toward TRL 5 was made through thermal vacuum testing, but hardware problems prevented this step from being completed. Objectives and a protocol were established, however, that should prove useful for future testing.

Chapter 2 – Background

Since the Apollo program, space suits without umbilical connections have relied on a portable life support system (PLSS) that uses water sublimation to reject heat that would otherwise rapidly build up within the suit (NASA, 2006). Sources of heat include the astronaut's metabolic output, power required for the suit's avionics and PLSS components, and any environmental heat flux into the suit. Heat is collected throughout the suit's interior by a Liquid Cooling and Ventilation Garment (LCVG), which interfaces with a water and air heat exchanger in the PLSS, and from which the collected heat load is transferred to a self-regulating sublimator device. A porous metal plate exposes feed water to the low temperature and near-vacuum of space to create a thin sheet of ice that in turn sublimates directly to the vapor phase, thus removing heat collected by the LCVG. This vapor is vented away from the suit, carrying the rejected water mass and accompanying thermal energy as latent heat of sublimation.

The current US Extravehicular Mobility Unit (EMU) and Russian Orlan suits have similar thermal control subsystems, consisting of a liquid cooling and ventilation garment (LCVG), multi-layer insulation (MLI) and thermal micrometeoroid garment (TMG) to minimize heat leakage and/or environmental heat flux absorption, a heat exchanger with both liquid water and oxygen gas loops interfaced with an ice sublimator connected to a separate feed water tank. Most of the metabolic heat is conducted to water-filled Tygon tubing laced throughout the LCVG or convected/exhaled/perspired into the oxygen stream. The remainder is radiated from the skin or LCVG toward the MLI, which transmits only a small percentage of that heat out to the environment. Internal heat reflected by the MLI is eventually absorbed by the skin or LCVG. In steady-state operation, nearly all metabolic heat is ultimately rejected by the sublimator, while radiative heat leakage is a minor factor by design. Likewise, heat absorbed from the environment (e.g., solar flux, albedo from planetary bodies, and thermal radiation from nearby

spacecraft) is low, due to the high reflectivity of the MLI and other materials in the outermost layers of the suit.

NASA is currently developing the Space Water Membrane Evaporator (SWME) to replace the sublimator (Bue et al., 2009). SWME is designed to be effective in pressurized environments where sublimation does not occur, such as in the Martian atmosphere, as well as to be less prone to feed water contamination issues. The overall concept of rejecting heat using water consumption, however, remains similar to that of the sublimator. In contrast to the operational advantages that SWME offers, the evaporative phase-change process uses slightly more water for a given heat load than the legacy sublimator.

Suit radiator concepts have been proposed that would cover only the relatively flat PLSS backpack with a radiator panel, but this approach offers limited heat rejection capability due to the small surface area and the dynamic reorientation (i.e., changing sink temperature) associated with EVA operations (Sompayrac et al., 2009). Variations on this theme have also been considered that rely on partial radiation heat transfer coupled with a regenerable phase change material to modulate the net heat flux (Roebelen et al., 1983). To date, however, radiators have not been used on any operational EVA suit designs.

The Chameleon Suit, a futuristic space suit concept described by Hodgson et al. (2004), introduced the novel approach of integrating electrochromic material into the entire suit's external surface as a potential means of providing thermal control without relying on water consumption. Funded by the NASA Institute for Advanced Concepts (NIAC), the report lays out an evolutionary roadmap that defines and is dependent on various innovative enabling technologies, including flexible electrochromic material. It does not, however, provide detailed performance requirements or conduct an operational feasibility analysis of the proposed solution. Hodgson et al. (2004) concluded that "while there is substantial research and progress in the field (of electrochromic materials), the current target

applications differ dramatically in requirements from the Chameleon Suit." Those requirements were partially defined to include a ratio of maximum-to-minimum emissivity of at least 2:1, a minimum emissivity of less than 0.4, and flexibility for integration with curved surfaces across the entire suit. Otherwise, the report does not offer detailed design parameters or provide thermal analysis data specific to the proposed electrochromic radiator aspect of the Chameleon Suit.

Our current study was designed to further analyze the feasibility of incorporating variable infrared (IR) emissivity electrochromic radiators for space suit thermal control applications. In order to maintain thermal equilibrium in the space suit, total heat rejection must equal the sum of all heat inputs. This balance is represented by the following equation:

$$Q_{out} = Q_{met} + Q_{solar} + Q_{PLSS} + Q_{inc}$$

Equation 2-1

Q_{out}: Heat rejected from space suit

Q_{met}: Heat generated by astronaut's metabolic activity

Q_{solar}: Heat absorbed directly from solar irradiance

Q_{PLSS}: Heat generated by PLSS electronics and chemical processes

Q_{inc}: Incident heat absorbed from natural and artificial surfaces

The EMU outer covering is designed to be highly reflective, minimizing Q_{solar} and Q_{inc} under most conditions. Q_{PLSS} is fairly constant over the duration of a typical EVA. Q_{met} varies considerably based on the individual astronaut and his or her level of exertion. For instance, Q_{met} for a lunar mission may be quite different than for an International Space Station (ISS) mission, since the astronaut is walking under gravity, but it might also be reduced if the astronaut is riding on a lunar rover. Heuristic data exists for

both Apollo and shuttle/station EVA, and this information will provide boundary conditions for thermal analysis. NASA has also conducted a simulation called the "Advanced Walkback Test" in which subjects, wearing lunar suit mock-ups and suspension gear to approximate the effects of reduced lunar gravity, walk for 10 km on a treadmill. This test is designed to simulate the worst-case scenario for lunar EVA, in which the astronauts have ventured far away from the spacecraft or base and must walk back due to a rover malfunction (NASA, 2006).

Combining the terms for metabolic rate, solar flux, and PLSS heat generation allows for an estimation of Q_{out} under various conditions. The current sublimator method of heat rejection has been used since Apollo in all non-umbilical EVAs. This technology exploits the low pressure and temperature of space to utilize the heat of sublimation for water, as shown below.
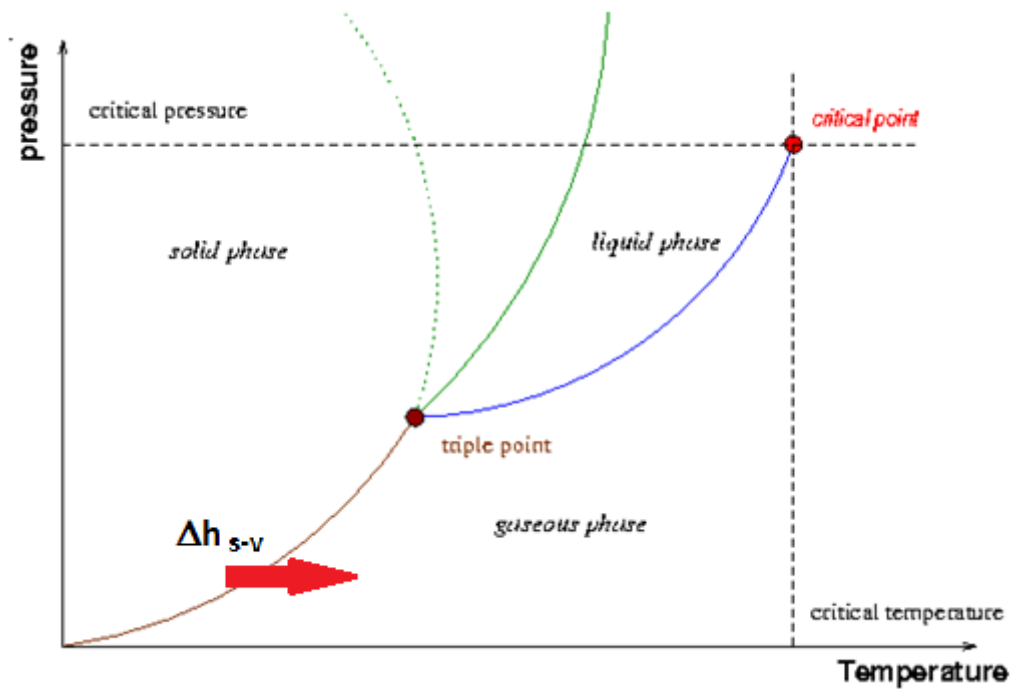
Figure 2-1: Phase Diagram for Water (Adapted from Wikimedia Commons, 2008)

For the Extravehicular Mobility Unit (EMU) sublimator currently used by NASA for shuttle and ISS missions, the heat rejection capacity is 922 W (Tongue & Dingell, 1999). The device is self-regulating, so feed water is automatically supplied to the sublimator on demand. Therefore, the amount of water consumed depends largely on the astronaut's metabolic rate.

Radiators do not consume mass for heat transfer, but the heat rejection potential is constrained by the emissivity of the surface materials and the external temperature. Emissivity ranges from $0 < \varepsilon < 1$ and is defined as the ratio of a material's emissive potential to that of a perfect black body. In other words, a material with low emissivity is a poor radiator, while a material with high emissivity approaches the performance of a black body, which is a theoretical, perfect radiator. All real materials are considered gray bodies, with emissivity somewhere between the two extreme values. The governing equation for gray body radiation to vacuum is the Stefan-Boltzmann Equation:

$$Q_{out} = E = \sigma A \varepsilon (T_s^4 - T_e^4)$$

Equation 2-2

In the above formula, Q_{out} is the total radiated heat, which is equal to $E_{?}$, the infrared emissive power of the radiating body. σ is the Stefan-Boltzmann constant. A (total surface area) is relatively constant and depends on the space suit design. ε is the surface emissivity. T_s is the external surface temperature, and T_e is the environment temperature determined by solar exposure and other mission factors (Planck, 1906; Wiebelt, 1966; Kreith & Black, 1980; Siegel & Howell, 2002).

A more sophisticated treatment of the problem must include view factors, which take into account the orientation of the radiator towards its line-of-sight external environment. For instance, if the radiator is partially facing a spacecraft or the lunar surface, it will be less effective than if it is facing deep space. NASA is currently investigating a Lunar Lander radiator design with more desirable view factors relative to the highly reflective lunar surface. (Ochoa et al., 2008) Traditional orbital spacecraft

radiators, along with solar panels that are normally maintained at an orthogonal angle, are mechanically controlled for nominal performance throughout the mission profile. This approach is not feasible for a space suit radiator, because the astronaut's position and orientation are so variable over a short period of time. Additionally, an integrated suit radiator would have multiple surfaces of various orientations. Such issues complicate any consideration of view factors for this application.

Under steady-state conditions (constant temperatures) with typical materials, there are no variables in Equation 2-2. Some spacecraft radiators use mechanical louvers to change the surface area of the radiator, thus allowing for modulation of the heat rejection based on changing thermal conditions (Darrin et al., 2000). However, mechanical louvers are generally considered too heavy and complex for space suit applications. Many spacecraft also have supplementary thermal control technologies, such as sublimators, evaporators, and complex heat exchangers, which provide a buffer against the radiators' performance limitations (Tongue & Dingell, 1999; Leimkuehler et al., 2008). Some of these supporting technologies are undesirable for EVA, whether for mass/volume reasons or because they involve toxic fluids that do not meet NASA safety standards for human-rated interfaces.

With electrochromic devices, emissivity becomes a variable in Equation 2-2, thus allowing the radiator to adapt to thermal conditions in order to maintain equilibrium. It should be noted that, unlike sublimator technology, electrochromic devices are not self-regulating and therefore require an electronic controller. The basic definition of an electrochromic material is one whose optical properties change under a voltage differential (Granqvist, 1995; Mortimer, 1997). There are many types of electrochromic materials, many of them effective in the visible portion of the electromagnetic spectrum. For this application, candidate materials are limited to those with infrared modulation.

Of the many organic and inorganic electrochromic materials, a thin film of crystalline tungsten trioxide (WO_3) has the most desirable infrared properties (Hale et al., 1998; Hale & Woollam, 1999; Granqvist, 2000; Wang et al., 2001). In order to take advantage of the electrochromic characteristics, the

material is sandwiched into a stack of other thin films (see diagram below) to support the electrical processes that modulate emissivity (Fang et al., 2001; Demiryont et al., 2006). The infrared emissivity of the ECD is modulated by activating a small voltage potential over the two electrodes. The voltage pulls ions from the storage material into the WO_3 layer and "colors" the device (increases emissivity) relative to infrared wavelengths. This process is known as intercalation and is both continuous and reversible. State-of-the-art WO_3 ECDs, such as those manufactured by the Ashwin-Ushas Corp., exhibit tunable emissivity range of $0.2 < \varepsilon < 0.7$ (a ratio of 3.5) over wavelengths of $15 \ \mu m < \lambda < 40 \ \mu m$. The required voltage for full intercalation is less than 5 V with power requirements of 40 μW per cm^2 (Ashwin-Ushas, 2008).
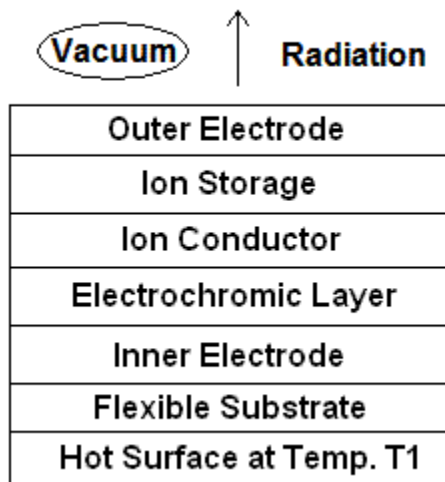
Figure 2-2. Diagram of Infrared Electrochromic Radiator (Adapted from Fang et al., 2001)

The figure above shows a typical electrochromic device layout, with the full stack of thin films required for operation. The hot surface contains the heat to be rejected through the electrochromic radiator. In the space suit application, it may be transport water from the Liquid Cooling and Ventilation Garment (LCVG), some other heat exchanger fluid, or a solid heat conductor connected to the astronaut's skin, depending on the design of the thermal control system. Both electrode layers must be

electrically conductive and thermally transparent, such as gold or aluminum. The electrochromic

material is almost always a thin film of crystalline WO_3 in devices optimized for infrared modulation.

The ion conductor is preferably also an electrical insulator, such as tantalum oxide (Ta_2O_5). This helps to

maintain intercalation with minimal power input (i.e. spectral stability). The ion storage material should

contain small ions, such as hydrogen (H+), Lithium (Li+), or Sodium (Na+). Again, thermal transparency is

necessary in all layers of the ECD except the electrochromic film itself.

Electrochromic materials and the other layers that make up a complete electrochromic device

are all flexible thin films. However, ECDs must be deposited on a substrate that may or may not be

flexible as well. This is typically irrelevant in spacecraft radiator studies, but flexibility is a necessity for

ECD integration into the external layers of a space suit. Recently, advancements have been made

towards the development of fully flexible substrates for ECDs that maintain performance and durability

of the devices. Studies indicate that electrochromic switching performance is minimally affected by the

use of flexible Kapton (a common, space-rated material) as opposed to hard silicon for the

electrochromic device substrate (Bessiere et al., 2002; Kislov et al., 2003).

Electrochromic materials have a number of unique properties that offer potential for use as

radiators. By definition, ECDs can be optically modulated by applying a voltage differential (Granqvist,

1995). The actual electrochromic material consists of a thin film that is sandwiched between supporting

layers, enabling ion transport to take place; this assembly is collectively what is known as the

electrochromic device, shown in Figure2-2. Certain types of ECDs, particularly those incorporating

tungsten trioxide (WO_3) as the electrochromic layer, exhibit electrochromism in the infrared

wavelengths where thermal radiation is active. These infrared ECDs typically have $\Delta\varepsilon > 0.5$, and the

effect is both continuous and reversible (Granqvist, 2000). Two commercial fabricators have been

identified as possible suppliers: Ashwin-Ushas Corp. in Lakewood, NJ and Eclipse Energy Systems, Inc.,

based in St. Petersburg, FL. Both of these companies produce custom infrared ECDs in small batches,

and both offer solar reflective coatings of the kind used on typical spacecraft radiators. The infrared

electrochromic capability of an Eclipse ECD is shown in Figure 2-3.
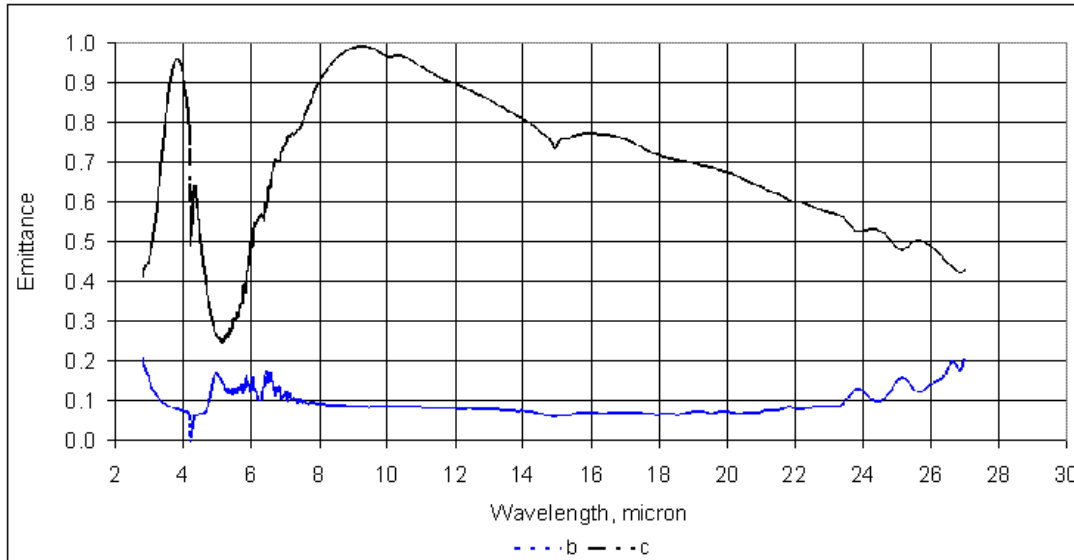
Figure 2-3. Infrared Performance of Eclipse ECD in Bleached (Low ε) and Colored (High ε) Modes. (Image

courtesy of Eclipse Energy Systems, Inc., with permission.)

Electrochromic radiators promise certain advantages over traditional spacecraft radiators. The

emissive power of ECDs can be adjusted quickly as mission operations and environmental conditions

change, and the effective surface area can also be varied if the radiator panels are controlled in parallel.

Furthermore, these changes do not involve any physical mechanisms, which may translate to reduced

mass and improved reliability compared to mechanical louvers and/or gimbals as typically used on

traditional radiators. These properties suggest that ECDs may be particularly appropriate for EVA, in

which heat loads, orientation, and environmental conditions change frequently and abruptly, and since

relative attitude stability, system mass and surface area constraints differ from those of a larger

spacecraft. A thorough trade analysis based on the Equivalent System Mass (ESM) metric will be

conducted in an upcoming study to weigh overall costs and benefits.

15

For detailed thermal analysis of electrochromic radiator performance, both heat load data and environmental parameters are required. Both are readily available from extensive documentation of the Apollo lunar missions. Furthermore, space suit radiators are particularly well-suited to lunar operations, due to relatively stable environmental temperatures, predictable suit orientation under partial gravity, and the extreme expense of launching any mass (including consumables) to the lunar surface.

NASA documents typically define "average" EVA metabolic rates for mission planning, classified as minimum/nominal/maximum values (BVAD, 2008). This approach is not sufficiently granular to accurately determine heat rejection needs over the course of a real EVA. Unpublished Apollo medical data from Waligora (1972-1975) were compiled and correlated to specific EVA operations by Carr & Newman (2008). This historical data includes detailed, minute-by-minute metabolic rates for each individual Apollo surface EVA, allowing for comparison among the various astronauts and even individual excursions within a particular mission. (Note: The primary collection of documents was missing data for Apollo 16, Lunar Module Pilot, EVA-3. The omitted data has been reconstructed in a similar format, though from a different source (Waligora, 1975), by correlating timestamps to the Apollo Lunar Surface Journal and assigning one of three associated metabolic rates based on a description of the LMP's activities.)

For the radiator analysis, lunar sink temperatures were required for each specific Apollo surface EVA. On the lunar surface, environmental sink temperature is a function of topography and solar elevation angle. The former is simple to account for in this study, because all Apollo landing sites were in the equatorial plains region. Astronauts walked and drove the lunar rover near crater rims but did not actually enter any craters, partly due to thermal concerns. Solar elevation angles are catalogued in various mission documents found within the Apollo Lunar Surface Journal. These angles can be correlated with environmental sink temperature according to the results of a "flux cube radiation" analysis by Sompayrac et al. (2009).

As a method for comparison, Equivalent System Mass analysis is a form of trade study in which disparate performance characteristics and specifications are converted to a unified, quantifiable metric that is easily compared among multiple candidates that may be extremely diverse and otherwise difficult to evaluate in a traditional trade study.

The central idea of Equivalent System Mass is based on the principle that spacecraft are propelled by launch vehicles with finite payload mass capability. All else being equal, reducing the mass of a spacecraft (or any of its subsystems or components) either increases total propulsion capability, opens up an overall mass margin that can be used to launch additional payload, or in some cases allows for the use of a smaller, less expensive launch vehicle. The ESM methodology involves applying "infrastructure costs" to convert volume, power, cooling, and even crew time into units of mass, which are then added to the actual system mass and any consumable mass to obtain the total ESM value for a particular candidate. Infrastructure costs, which are published and updated periodically in NASA's Basic Values and Assumptions Document (BVAD), depend heavily on mission destination, launch vehicle, power generation efficiency, system cooling efficiency, etc. For example, a mission to Mars utilizing solar panels would have higher infrastructure costs for power requirements than a similar mission to the Moon, because less solar power can be generated near Mars than at the Moon.

The ever-changing nature of infrastructure costs means that ESM analysis does not represent a hard-and-fast evaluation but rather a thorough comparison of technologies based on the best available information at the time. Furthermore, since ESM analysis often involves advanced technologies that may not be fully tested or characterized, all assumptions must be clearly documented and referenced to the best available sources. Over time, the results of an ESM analysis may change if repeated with updated specifications, performance data, and/or infrastructure costs.

During the Apollo lunar surface missions, lunar dust inhibited performance of space suits due to its small particle size and jagged, mechanically adhesive topography (Gaier, 2007). This research

assumed that protective measures can be taken to protect electrochromic radiators from physical damage caused by lunar dust. However, the accumulation of lunar dust may also affect thermal performance of the radiators due to surface coating. Data from the Apollo missions shows that lunar dust has similar infrared emissivity to traditional radiators (ε = 0.8), but the much higher solar absorption increases the temperature of the radiator and thus reduces performance (Gaier & Jaworske, 2007).

While many additional design trades and operational considerations ultimately remain to be evaluated to determine an optimal design solution, this thesis takes initial steps toward assessing feasibility of using variable-emissivity electrochromic radiators as a means of providing thermal control for a future lunar surface space suit. The following chapters correspond to individual publications on various studies addressing different feasibility factors, and therefore, some of the above material is reiterated as relevant background in the ensuing chapters.

Chapter 3 – Thesis Objectives

Based on the original concept in the Chameleon Suit report, several research objectives were identified for this thesis. Theoretical performance analysis is needed to predict electrochromic radiator performance in EVA operating conditions and to determine emissivity requirements for material development (Chapter 4). In order to study the technology separately from the many other advanced concepts in the Chameleon Suit report, it is necessary to understand how an electrochromic radiator might be used in conjunction with the existing space suit and the sublimator system. Therefore, a water consumption impact study is needed to determine how much water could be saved with the use of an electrochromic radiator in realistic conditions (Chapter 5).

The two performance analyses described above could answer the question of the technology's effectiveness, but there are also questions about how to integrate an electrochromic radiator with current and future space suits (Chapter 6). Furthermore, assuming that the technology is both effective and can be implemented, there is still a question of whether it is viable in comparison to other technologies being developed for the same purpose (EVA heat rejection). A full trade study would require knowledge of the entire suit design and mission profile, but a precursor, systems-level analysis can be performed by applying the Equivalent System Mass metric (Chapter 7) to electrochromic radiator concepts as well as to the legacy sublimator and other EVA cooling technologies under development.

Finally, empirical data is needed to validate the analytical results and to provide accurate performance data for future trade studies. Experiments may be conducted in a "bench-top" laboratory setting (Chapter 8) or a thermal vacuum chamber to simulate the space environment (Chapter 9).

Chapter 4 – Theoretical Performance Analysis

Abstract

Variable emissivity electrochromics have been proposed as an enabling technology for integrating a radiator capability into a space suit in order to augment or replace the traditional means of heat rejection achieved via water sublimation. Thermal analysis was performed to establish design trade spaces and to provide operational guidelines and performance specifications for electrochromic technology development. Based on using the available surface area of an entire space suit as a radiator and the projected infrared emissivity modulation capability of state-of-the-art electrochromic material, the proposed application for space suit heat rejection suggests the potential exists to reduce or eliminate reliance on water consumption for thermal control within a defined range of metabolic and environmental boundary conditions.

Background

Since the Apollo program, space suits without umbilical connections have relied on a portable life support system (PLSS) that uses water sublimation to reject heat that would otherwise rapidly build up within the suit (NASA, 2006). NASA is currently developing the Space Water Membrane Evaporator (SWME) to replace the sublimator (Bue et al., 2009). SWME is designed to be effective in pressurized environments where sublimation does not occur, such as in the Martian atmosphere, as well as to be less prone to feed water contamination issues. The overall concept of rejecting heat using water consumption, however, remains similar to that of the sublimator. In contrast to the operational

advantages that SWME offers, the evaporative phase-change process uses slightly more water for a given heat load than the legacy sublimator.

The Chameleon Suit, a futuristic space suit concept described by Hodgson et al. (2004), introduced the novel approach of integrating electrochromic material into the entire suit's external surface as a potential means of providing thermal control without relying on water consumption. Funded by the NASA Institute for Advanced Concepts (NIAC), the report lays out an evolutionary roadmap that defines and is dependent on various innovative enabling technologies, including flexible electrochromic material. It does not, however, provide detailed performance requirements or conduct an operational feasibility analysis of the proposed solution. Our current study was designed to further analyze the feasibility of incorporating variable infrared (IR) emissivity electrochromic radiators for space suit thermal control applications.

Rationale

The goal of this research is to advance our understanding of the performance requirements needed to effectively incorporate electrochromic radiators into a space suit. This is achieved by characterizing their capability for offsetting water consumption for traditional EVA heat rejection over a range of realistic metabolic profiles and environmental conditions.

Both the sublimator and proposed SWME consume water from a feed tank, resulting in a thermal control process that is non-self-sustaining over time (also known as open-loop). Water is usually a valuable commodity during space flight, although in many past and current missions, supplies for EVA water consumption have been adequately met by fuel cell water generation, resupply logistics, condensate recovery, or other recycling logistical measures. However, as space expeditions venture farther from Earth and/or experience longer durations between resupply opportunities, water mass

consumption for extravehicular activity (EVA) heat rejection becomes a limiting factor in mission planning. Studies suggest that EVA water consumption alone, as anticipated from launch mass costs with planned usage rates, will account for billions of U.S. dollars for return expeditions to the Moon. The cost of expending water for EVA's on a Mars voyage would likely be even higher (Nabity et al., 2008; Jones, 2008). Thus, a renewable (or no-consumables) method of heat rejection offers a highly desirable trade option for future needs of sustainable space exploration, either as a replacement for, or supplement to, existing sublimator or evaporator technologies.

Radiators, which reject heat without mass loss, are commonly used on almost all orbital spacecraft and deep space probes (Kreith, 1962). Radiators work by exposing a hot surface to a cooler environment (known as the heat sink). The amount of heat flux transferred from the radiator depends on the temperature difference, surface area, and a material property known as emissivity. Because surface area and emissivity are essentially fixed parameters, radiators can be designed to provide reliable rates of heat rejection for missions that have reasonably predictable thermal environments (e.g. an orbiting satellite) and consistent internal heat production (e.g. electronics).

There are notable differences between such traditional radiator-supported spacecraft and a space suit, however, most obviously the addition of a crew member as the primary thermal mass and heat source. Space-suited crew members also move around quickly and unpredictably through various thermal environments, and their heat generation is directly proportional to their highly variable metabolic activity, which can change by a factor of 5 or more during a given EVA. In addition, a crew member's metabolic heat is dominant relative to the electronics and other sources in the small volume of a space suit, thus making for a very dynamic profile throughout which the comparable heat rejection process is required to maintain a reasonable level of thermal equilibrium. The metabolic heat alone can vary from 70 to 730 W on a lunar EVA based on activity and other factors (Nabity et al., 2006; Williams et al., 1973).

Problem Statement

There are no existing design boundary conditions for developing electrochromic space suit radiators. While the application has been proposed, it has not studied in detail. By combining electrochromic device vendor specifications with average EVA metabolic loads and lunar environment data, the radiator's capability to reject heat in a given situation can be assessed by thermal analysis.

We consider the radiative surface area to include the entire space suit and also the impact of adding the ability to vary IR emissivity to actively modulate radiator heat flux. The preliminary success criteria for this proposed solution include rejecting a non-trivial percentage of the internal heat load at various metabolic activity levels, allowing operation in multiple environments of interest, and demonstrating a capacity to significantly reduce water consumption for heat rejection.

The proposed, integrated electrochromic radiator has the potential to not only maximize heat rejection with reduced consumable mass requirements, but also to provide the rapid response and versatile performance range needed to maintain acceptable thermal equilibrium inside a space suit being operated under dynamic metabolic loads and varying external environmental conditions.

Electrochromic materials have the ability to enable such a solution by virtue of their variable, actively controlled optical properties and geometric compliance when mounted on a flexible substrate. The chemical properties of electrochromic thin films cause emissivity to change when an applied voltage forces ions into or out of the electrochromic layer. Emissivity modulation is reversible as well as stable for most existing devices (Granqvist, 1995; Mortimer, 1997). This exotic property means that radiators with electrochromic surfaces can be regulated using a rapid, reversible, solid-state electronic process. The range of achievable emissivity depends on the kind of electrochromic material and the particular fabrication method employed in manufacturing. As emissivity approaches zero, the radiator is

essentially deactivated, because it will emit (or absorb) little or no heat. This functional property can potentially be harnessed to allow fine thermal control by designing the radiator system to have multiple electrochromic pixels with independent circuitry, so that the effective surface area becomes independently variable.

The aforementioned Chameleon Suit report further suggests incorporating electrochromics directly into the fabric of the space suit, providing maximum surface area by using the entire suit as a radiator, not just the relatively small PLSS backpack shell. Such a fully integrated suit-radiator concept requires that the electrochromic material be sufficiently flexible to accommodate irregular and changing suit surfaces. Electrochromic devices can already be built onto flexible substrates (e.g., Kapton film) with little or no effect reported on their performance (Bessiere et al., 2002; Kislov et al., 2003). Determining where to place the electrochromics within the complex multilayered suit fabric and designing pathways for transporting waste heat to the distributed radiator surface, however, present additional implementation challenges. To some extent, these decisions depend on specific suit design factors, but preliminary concepts for electrochromic integration and heat delivery to the radiators have been outlined as part of this ongoing research (Metts and Klaus, 2009).

Electrochromic technology has been in development for decades but has only recently matured to the point of commercial viability. There are multiple classes of electrochromics, distinguished by base material type, fabrication techniques, and the wavelength (spectral) dependency of their optical properties. Visible-spectrum electrochromics are already commercially available and used for applications such as "smart windows" and automotive rear-view mirror night vision, but devices with broadband infrared (IR) modulation (required for practical heat rejection) are less mature. At least two U.S.-based firms are currently fabricating infrared electrochromics for space applications: Ashwin-Ushas Corp. and Eclipse Energy Systems. Ashwin's performance specifications indicate an infrared emissivity range of $\Delta\varepsilon > 0.56$ with power consumption of 40 μW/cm^2 and switching times < 1 s (Ashwin-Ushas,

24

2010). Eclipse specifications show $\Delta\varepsilon = 0.7$ in the 8-12 micron electromagnetic spectrum, with power consumption ~0.1 mW/cm^2 (Demiryont & Moorehead, 2009). Due to the very low power requirements and optical stability of either company's devices, the total power of the fully integrated radiator is expected to be less than 20 W. Additionally, both Ashwin and Eclipse note the flexibility of their electrochromic products.

Current Work

A first-order, feasibility assessment was undertaken to determine if it is theoretically possible to achieve adequate thermal control in a space suit, provided that the entire outer surface could act as a radiator with variable IR emissivity properties. This analysis was conducted to bound the problem using available data and simplifying assumptions, and also to derive specification requirements for future electrochromic development. This process involved predicting the ideal heat rejection capacity of an integrated radiator as a function of environmental temperatures and total surface area across a range of expected emissivity values, then comparing this capacity to the heat rejection requirements of a space suit for various relevant environments and metabolic heat loads. The results are specified as the theoretical heat load that can be rejected by using an integrated electrochromic radiator as an offset to what can be regulated by sublimation. Thermal control performance in terms of water mass savings can then be predicted for given EVA metabolic and environmental profiles. This information serves as a basis for enabling a more detailed, system-level trade study to then be conducted to assess any theoretically possible performance gains in terms of their practical application based on a cost-benefit analysis.

This initial feasibility analysis was conducted using various lunar conditions, because the lunar surface offers a stable thermal-vacuum environment with near-continuous light and dark cycles

compared to low Earth orbit (LEO) or the Mars surface, thus making it a good case study for using radiators in a baseline, steady-state thermal analysis.

A single lunar day is approximately 28 Earth days in length, divided into roughly two Earth weeks each of light and darkness. The moon does not have an atmosphere to disperse heat by convection, so the surface temperature is primarily a function of location and time within the lunar day. Average surface temperatures for various lunar conditions and locations are compiled in Table 4-1 (Sompayrac et al., 2009). These sink temperatures were determined by NASA's "flux cube" method, which uses standard soil and surface properties to determine the steady-state temperature of a volumetric unit on the lunar surface. The moon's surface at the polar regions are always exposed to the sun, regardless of lunar time, while deep polar craters can be continuously shadowed. Therefore, these locations provide the most consistent thermal environments on the moon, as well as being among the most desirable landing sites for scientific reasons. However, the dynamic nature of EVA operations means that even such stable environments do not translate to stable, uniform thermal conditions for the space suit. During an actual EVA, there will be transient effects due to the crew member moving in and out of shadows, changing orientation with respect to the sun, and dynamic metabolic heat loads. The present study, however, is focused on conducting a first-order, steady-state thermal analysis in order to establish performance limits. The ultimate transient effects will be bounded within those limits and the electrochromic properties should allow for the quick responses needed to maintain thermal equilibrium.

Table 4-1: Lunar Environment Thermal Conditions (Adapted from Sompayrac et al., 2009)

Environment	Temperature (K)
Lunar Equator (Night)	175
Lunar Equator (Noon)	336
Moon 88° Latitude (Illuminated)	187
Moon Polar Crater (Shaded)	95

Aside from the geographic location and external environment exposure, which determine sink temperature, another key radiator design parameter is the heat load to be rejected, which is highly variable for space suit applications due to individual physiology and the dynamic nature of the operations being performed. In this analysis, heat rejection requirements are based on total internal heat load, which is the sum of metabolic rate plus a constant 120 W for PLSS electronics heat (Sompayrac et al., 2009). The majority of the heat load comes from metabolic waste, which varies constantly with activity and is also unique to each crew member's physical characteristics. NASA's baseline metabolic rates for LEO, Apollo, and the Lunar Walkback Test are shown in Table 4-2 (NASA, 2006). The Lunar Walkback Test was a simulation conducted at the Johnson Space Center to collect metabolic data and experimental suit performance data in a worst-case contingency scenario. It represents a situation in which a lunar rover becomes disabled at its maximum range from the base and the astronauts must walk back to the habitat before their life support consumables are depleted. Due to the demanding physical activity and psychological stress associated with being in survival mode, the astronauts experienced a higher metabolic rate during the Walkback Test than in normal lunar EVA operations, thus representing a time-constrained, upper-limit metabolic scenario.

Table 4-2: Standard EVA Metabolic Loads (NASA, 2006)

Operational Environment	Metabolic Rates (W)		
	Minimum	Nominal	Maximum
μ Gravity (ISS and STS)	169	264	644
Apollo Lunar Surface EVA	144	286	724
Lunar Walkback Test	491	696	880

Radiator surface temperature is determined by a number of factors. In terms of optimal performance, a radiator should be as hot as possible to reject the maximum amount of heat per a given emissivity setting, and absorb the minimum amount of heat in an inverted temperature gradient (when

27

the environment is hotter than the suit) based on its reflectivity and/or absorptivity properties. However, there are additional operational, safety and material interface issues that translate to practical upper limits for suit surface temperatures. In traditional spacecraft radiators, external surface temperature is determined by heat exchanger flow control and environmental conditions. For this study, the radiator surface temperature is assumed to be 300 K, similar but slightly less than that of the average human skin temperature, which is approximately 303 K (Benedict, 1919). Since most of the heat load is transported from the skin to the radiator by the LCVG or some other distributed heat transport system, the radiator surface must operate at least slightly colder than the skin itself in order to facilitate heat transfer. Radiator temperature serves as a control point that is easier to monitor than the crew member's internal (core) or skin temperature. Emissivity of the electrochromic surface is dynamically set such that the radiator surface temperature remains at or near 300 K, which indicates that thermal equilibrium is established and thus the internal heat load is being rejected at the same rate it is generated.

The emissivity range considered for this study, $0.1 \leq \varepsilon \leq 0.9$, represents the minimum and maximum values achievable with state-of-the-art infrared electrochromic devices. Although certain currently available devices may reach either the high or low end of this range, no single electrochromic device was found that covers the entire range alone. For instance, Ashwin-Ushas offers infrared electrochromics tailored to any "window" of $\Delta\varepsilon = 0.5$ within the overall device limitations of $0.18 \leq \varepsilon \leq 0.89$ (Ashwin-Ushas, 2010). Eclipse Thin Films offers devices with emissivity range up to $\Delta\varepsilon = 0.7$; the device's emissivity spectra over 3-27 μ wavelength shows modulation up to $\Delta\varepsilon = 0.93$, but only at a specific wavelength, with decreased modulation for other infrared wavelengths (Demiryont et al., 2009; Eclipse Energy Systems, 2010). In short, there is no currently known electrochromic device with broadband infrared emissivity across the entire range of $0.1 \leq \varepsilon \leq 0.9$; however, the values defined by these limits are partially achievable by certain electrochromic devices under certain conditions, and are

thus included in the present analysis as ideal performance limits. A detailed analysis based on actual experimental data, carried out by by Ashwin-Ushas Corp. shows the theoretical emissivity range of their technology to be $0.1 < \varepsilon < 0.88$ on a single device fabricated with the best, currently achievable techniques and materials (Chandrasekhar et al., 2002; Chandrasekhar, 2010). The thrust of present electrochromic development for space applications is to refine fabrication techniques such that the delta-ε performance is maximized to handle extreme shifts in temperature that may be experienced in space.

Analytical Methods and Results

$$Q'_{load} - Q'_{rad} - Q'_{sub} + G'_{abs} = 0$$

Equation 4-1

Assuming no external conduction or convection occurs, the overall heat balance of an exposed thermal surface in the vacuum of space or the lunar surface is given by Eq. 4-1, where Q'_{load} is the suit's heat load to be rejected, Q'_{rad} is the radiator's emissive power, Q'_{sub} is the heat rejected by the sublimator (or evaporator) and G'_{abs} is absorbed solar irradiance with the assumptions that $G'_{abs} = 0$ (ideal solar reflectance) and Q'_{load} is comprised of metabolic and PLSS electronics heat. In practice, some solar flux is outside the visible wavelengths that are specifically blocked by a solar-reflective coating, and thus the infrared portion of solar flux may be absorbed by the suit exterior (and electrochromic radiators) in certain conditions. However, the primary effect of solar flux is on the lunar environment itself, which absorbs solar flux and re-radiates that energy at infrared wavelengths; this effect is accounted for in the sink temperatures and the flux cube method used to compute them. For the purposes of this study, we consider absorbed infrared flux (as opposed to visible-wavelength solar flux)

29

to be accounted for by a negative Q'rad term in Eq. 4-2, which results when the sink temperature exceeds radiator surface temperature.

$$Q'_{rad} = \sigma A \varepsilon \, (T_s^4 - T_e^4)$$

Equation 4-2

Radiative power is governed by the Stefan-Boltzmann relationship shown in Eq. 4-2, in which Q'_{rad} is heat transfer, $\sigma = 5.67e\text{-}08 \ W/m^2/K^4$ is the Stefan-Boltzmann constant, A is radiator surface area, ε is emissivity, T_s is radiator surface temperature, and T_e is environment temperature (Gilmore, 2002). View factors and lunar soil properties are not explicitly considered in this study because their effects are already implicitly considered in the flux cube methodology used to evaluate the sink temperatures in Table 1 that are used throughout this analysis. If the sink temperature is greater than the radiator temperature, Q'_{rad} will be negative, indicating that the radiator is absorbing heat from the environment, therefore, no net heat is being rejected. The radiator surface temperature T_s is set to 300 K as previously explained.

For the integrated, full-suit radiator, surface area A is based on the outer surface of the existing Extravehicular Mobility Unit (EMU) suit. The average surface area of that suit is 3.90 m^2, or approximately twice that of an average nude human (Tepper, 1991). However, some surfaces of the suit are occluded, particularly within joints. A refined estimate of the active surface area is based on the concept of radiation area as described by Guibert & Taylor (1952), who empirically analyzed the ratio of exposed radiation area to total body surface area. The ratio for a medium-sized male was determined to be 0.88, and this value was found to be insensitive to clothing. Assuming this ratio to be valid for an average suited crew member, the effective radiation area of the EMU, used for A in Eq. 4-2, is 3.43 m^2.

Suit designers may find that this much radiator surface area is impractical and/or unnecessary, but it is useful as a maximum value for bounding the problem.
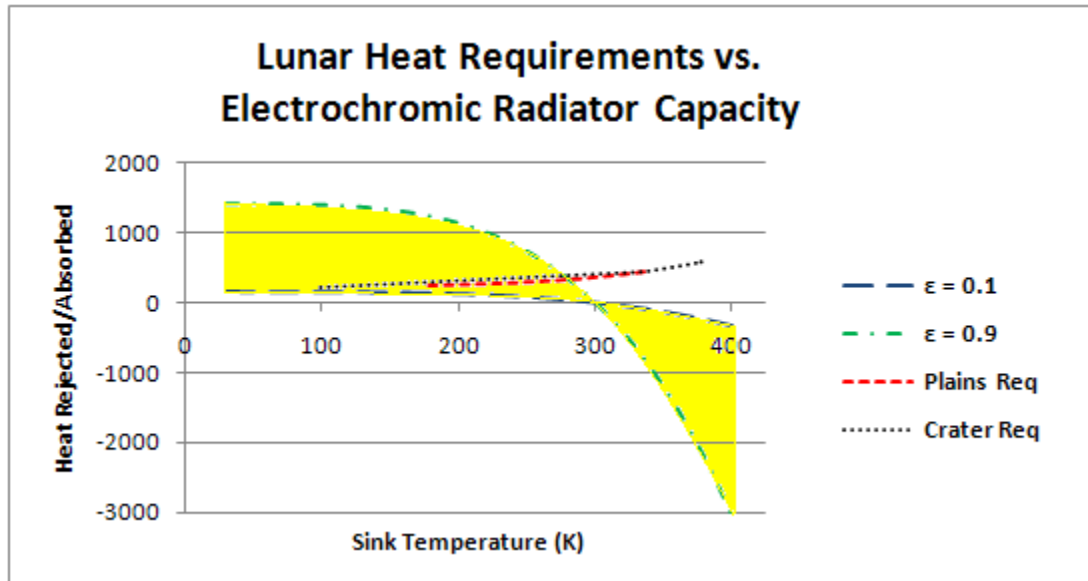
Figure 4-1: Electrochromic radiator performance envelope. The shaded area represents a performance range theoretically achievable using a 3.43 m^2 electrochromic radiator in lunar surface thermal environments (adapted from Sompayrac et al., 2009).

In Figure 4-1, average heat loads that must be rejected during a lunar surface EVA are plotted against lunar surface temperatures in the plains and craters, as adapted from Sompayrac, et al. (2009). Also, heat rejection capacity, as calculated using Eq. 4-2, is plotted for an integrated radiator with 3.43 m^2 surface area and surface temperature of 300 K at $\varepsilon_{min} = 0.1$ and $\varepsilon_{max} = 0.9$, the assumed emissivity limits. The shaded area defines the functional envelope in which the conceptual electrochromic radiator can operate at the given emissivity range. The radiator heat flux becomes zero when surface temperature equals sink temperature, and the flux is negative at higher sink temperatures. In this hot case, the radiator will not only be incapable of rejecting any internal heat, but it will also absorb some

environmental flux in addition to the internal heat load that will then have to be rejected by some other means, such as sublimation or evaporation. Although the radiator ceases to be effective over 300 K, these higher lunar sink temperatures only occur in particularly hot times/latitudes and can be avoided with proper mission planning.
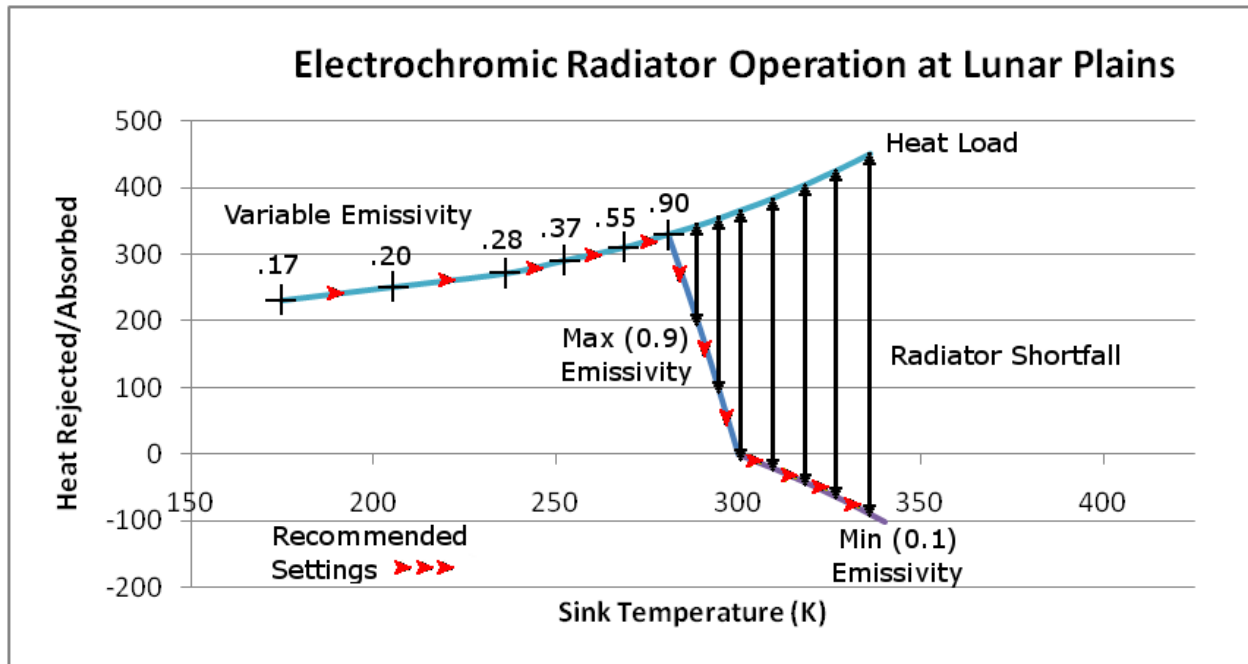
Figure 4-2: Notional electrochromic radiator operation scheme. An example heat load in the lunar plains (adapted from Sompayrac et al., 2009) is compared to electrochromic radiator performance over a range of sink temperatures. Red arrowheads indicate suggested emissivity settings. Vertical black arrows represent heat that must be removed by supplemental cooling.

These results suggest an operational configuration for electrochromic suit radiators, which can be adjusted to the desired emissivity within the material limits. A conceptual set point profile is illustrated in Figure 4-2. It should be noted that even if the sink temperature increases (e.g., the astronaut steps out of a shadow) and the radiator is no longer able to reject heat, it can at least be

switched to a minimum emissivity to reduce heat absorption from the environment. Also note that between the requirement/capability crossover point and the x-intercept, the radiator is still capable of rejecting some portion of the heat load; thus, it can reduce (though not eliminate) water consumption, if sublimation or evaporation is used for backup thermal control. If for some reason emissivity is higher than the suggested values in Figure 4-2, too much heat will be rejected (the astronaut may become cold) or, in the hot case, even more heat will be absorbed (more supplemental cooling is required); the converse results apply if emissivity is lower than prescribed.

To establish performance bounds for this analysis, the heat rejection capacity of an integrated electrochromic suit radiator was determined from the assumed parameters and compared to total heat load requirements, consisting of historical Apollo data and Lunar Walkback Test (worst-case scenario) metabolic rates (Table 4-2) with a constant PLSS electronics heat load of 120 W (Sompayrac et al., 2009). Depending on the specific combination of environmental sink temperature and internal heat load, the radiator is shown to be capable of rejecting all or some fraction of the net heat load from the suit and then, even when the capacity to reject is exceeded in the worst case hot scenario, at least helping to reduce the amount of environmental heat absorbed.

Radiator Capacity, Polar Shadowed Crater (95 K)

Radiator Capacity, Equator Night (175 K)
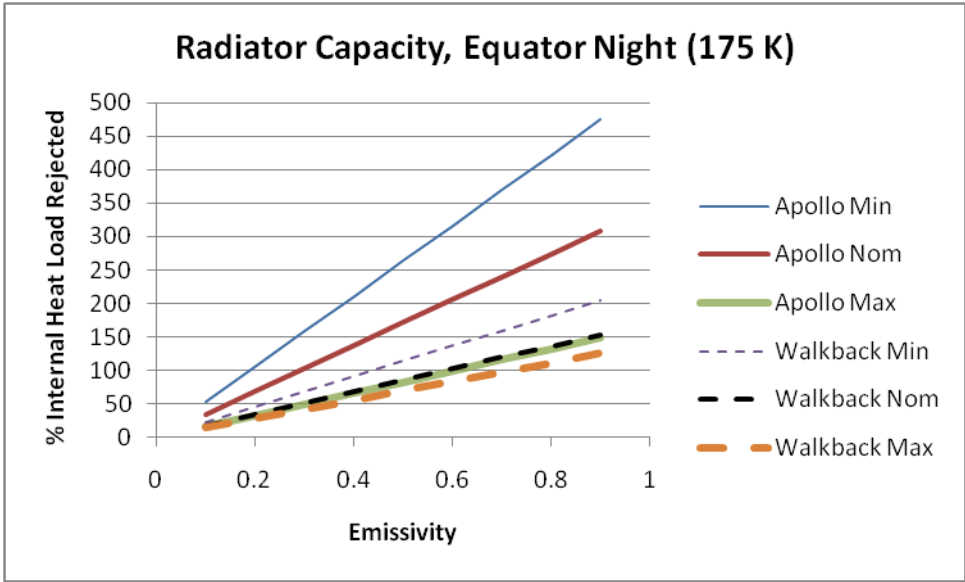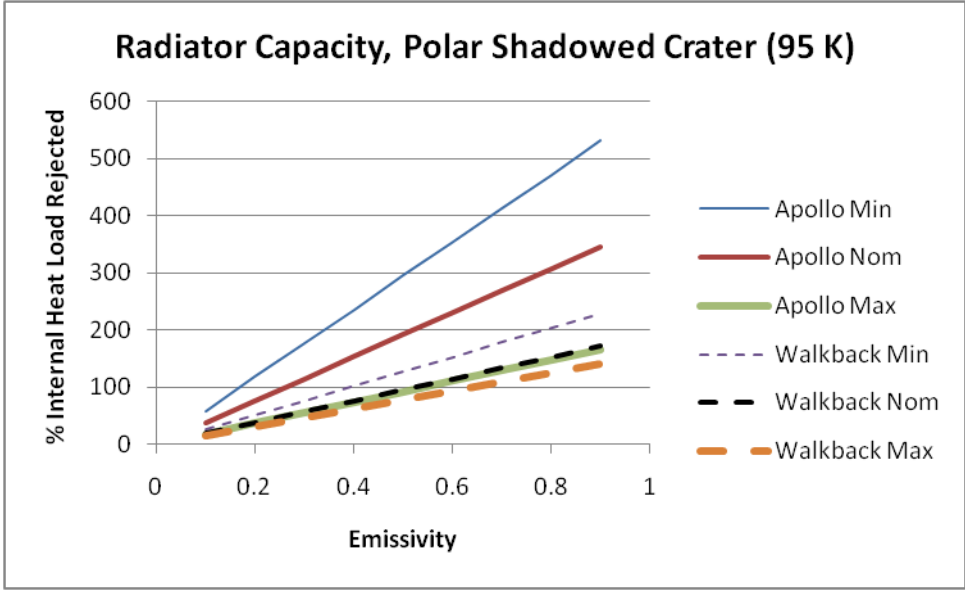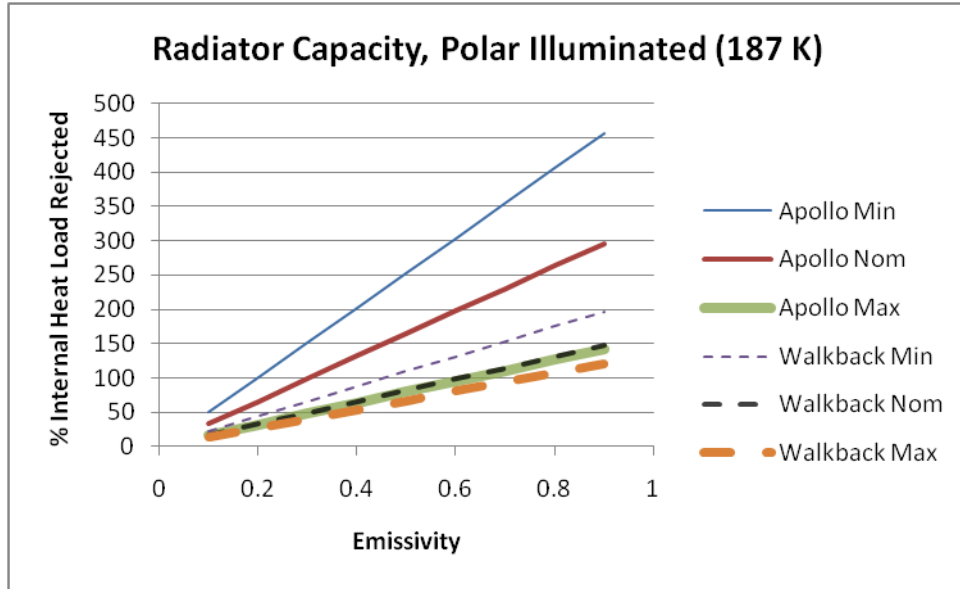
Figure 4-3: Electrochromic radiator performance in favorable conditions. For a given metabolic rate, the emissivity should be set to a value that will achieve 100% heat rejection, or as close as possible.

This performance capability is shown in Figure 4-3. The electrochromic radiator's heat rejection capacity in the three favorable lunar conditions is plotted as a function of emissivity. The primary goal of space suit thermal control is to maintain a comfortable thermal equilibrium in the suit, so in favorable environmental conditions (when the sink temperature is less than the radiator surface temperature of 300 K), the electrochromic radiator should be set to the emissivity needed to achieve 100% heat rejection. If sink temperature increases (i.e. the sun ascends overhead during EVA), the curves in Figure 4-3 will increase in slope such that higher emissivity settings are required to maintain 100% heat rejection. In some cases, the sink temperature could increase enough that supplemental cooling would be required because radiator performance would not reach 100% heat rejection at the maximum emissivity.
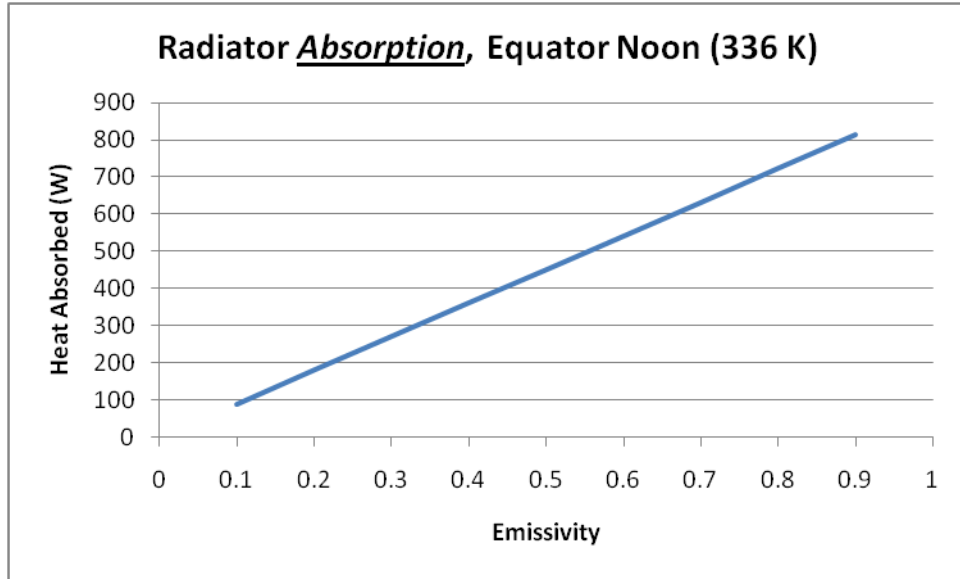
Figure 4-4: Electrochromic radiator performance in adverse conditions. During operations in hot conditions, the emissivity should be set to the lowest possible value to minimize heat absorption from the environment. This plot predicts the worst-case heat absorption for a full-suit radiator based on whatever minimum emissivity is available.

If sink temperature reaches or exceeds the radiator surface temperature (300 K), radiative cooling would no longer be possible. In the hottest condition, lunar equator at noon, the direction of heat flow is reversed, so that the radiator absorbs heat from the environment rather than rejecting heat from the suit. The goal in this case is to minimize absorbed heat by setting the electrochromic radiators to their minimum emissivity value (Figure 4-4). In adverse cases such as this, a sublimator or some other means of cooling is needed to maintain thermal equilibrium in the suit, but the electrochromic surface properties can still be used to gain advantage by reducing the net positive environmental heat load on the cooling system. (Note: Both Ashwin-Ushas and Eclipse Thin Films offer solar-reflective coatings for their electrochromic materials; the coatings should further reduce heat absorption in hot environments. However, these coatings are not factored into the present analysis due to insufficient data.)

As the primary goal of the electrochromic radiator is to reduce or eliminate water consumption, it is useful to calculate the fraction of heat load that must still be rejected by sublimation (or some other means) as a supplement to radiator capacity. Eq. (4-3) shows a percentage-based representation of that fraction.

$$\%_{sub} = \frac{Q'_{load} - Q'_{rad}}{Q'_{load}} \times 100\%$$

Equation 4-3

A result of >100% simply means that the sublimator must reject the entire internal heat load as well as absorbed flux from the hot environment, the latter being computed as negative emissive power by Eq. 4-2.
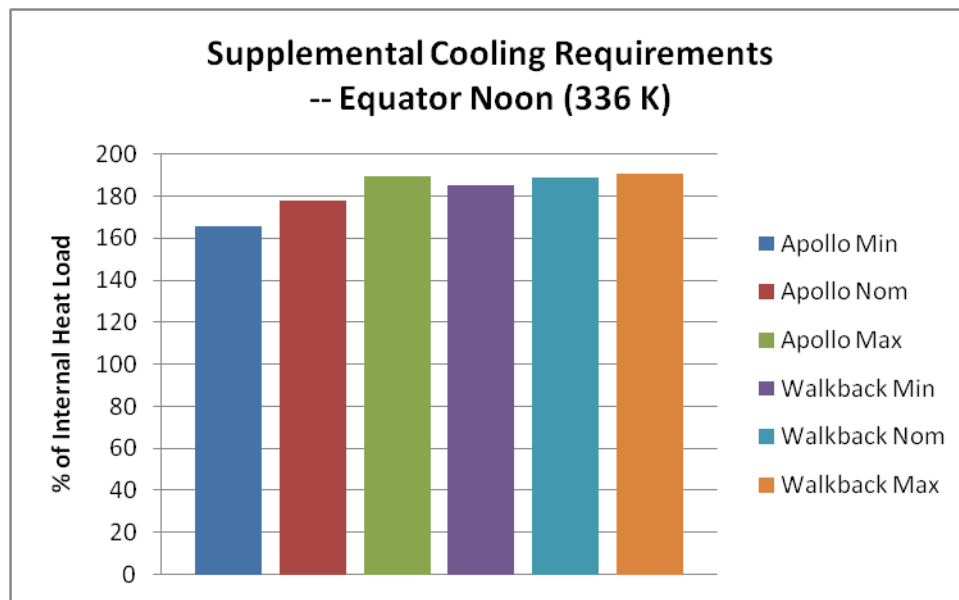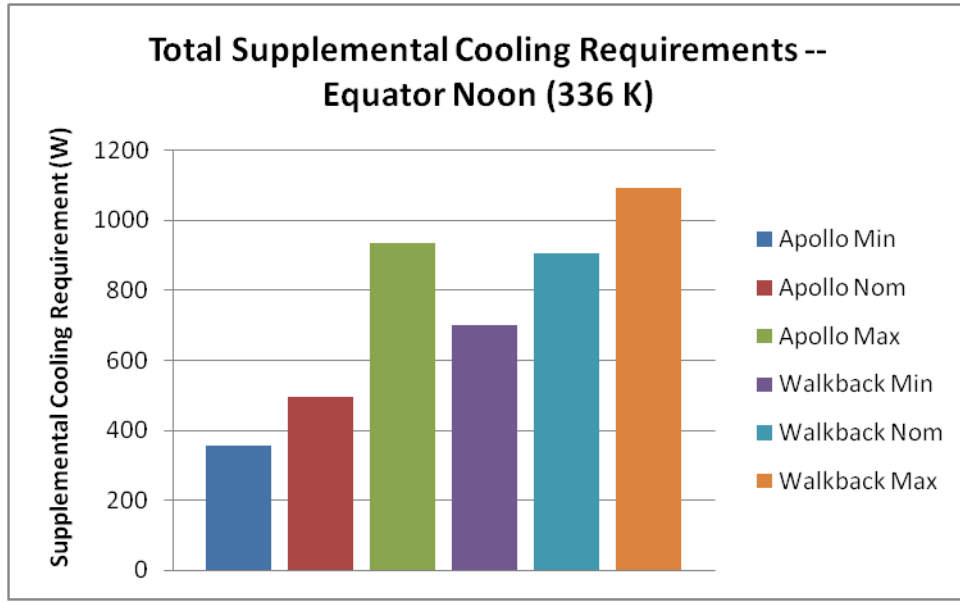
Figure 4-5: Supplemental cooling required in adverse conditions. Cooling requirement is represented as % of internal heat load as well as total heat in Watts. The heat to be rejected includes both internal heat load and minimal ($\varepsilon = 0.1$) absorbed flux from the environment.

Figure 4-5 depicts the supplemental cooling requirement in the worst-case lunar condition (Equator Noon at 336 K). In this adverse thermal condition, radiative cooling is not possible, so some other means of thermal control, such as a sublimator or evaporator, must be used to reject all of the internal heat load as well as the absorbed flux. The combined internal heat load and absorbed flux can be nearly 1100 W in the absolute worst case (Lunar Walkback maximum), so the supplemental cooling system should be sized accordingly. Note that in this scenario, the electrochromic radiator is still acting to minimize emissivity, thus reducing absorbed flux from the hot environment. The actual Apollo missions, which landed at equatorial sites, were timed to avoid the lunar noon timeframe, partly to avoid these high temperatures. Solar-reflective radiator coatings (not included in this analysis due to insufficient data) may reduce absorbed flux in hot environments, but much of the absorbed energy will

have been re-radiated from the lunar surface as infrared radiation and thus would not be mitigated by such coatings.

Assuming there is never a case where more than 100% of the internal heat load needs to be rejected, an optimal emissivity setting can be determined for each combination of internal heat load and environmental condition. A range of values from Equation 4-2 for various operational scenarios is summarized in Tables 4-3 and 4-4. Negative results indicate that heat is absorbed from the environment at lunar equatorial noon; since the radiator cannot reject heat in this hot case, supplemental cooling is required to reject both the internal heat load and absorbed flux.

Table 4-3: Optimal Emissivity Settings and % of Internal Heat Loads Rejected for Apollo Metabolic Rates

Environment	ε for Min Q	% of Min Q	ε for Nom Q	% of Nom Q	ε for Max Q	% of Max Q
Polar Shadowed Crater	0.17	100%	0.26	100%	0.54	100%
Polar Illuminated	0.20	100%	0.30	100%	0.63	100%
Equator Night	0.19	100%	0.29	100%	0.61	100%
Equator Noon	0.1	-34.2%	0.1	-22.3%	0.1	-10.7%

Table 4-4: Optimal Emissivity Settings and % of Internal Heat Loads Rejected for Lunar Walkback

Metabolic Rates

Environment	ε for Min Q	% of Min Q	ε for Nom Q	% of Nom Q	ε for Max Q	% of Max Q
Polar Shadowed Crater	0.39	100%	0.52	100%	0.64	100%
Polar Illuminated	0.46	100%	0.61	100%	0.75	100%
Equator Night	0.44	100%	0.59	100%	0.72	100%
Equator Noon	0.1	-14.8%	0.1	-11.1%	0.1	-9.0%

Based on these results, the optimal emissivity setting for these particular scenarios is within range of 0.1 < ε < 0.75 for both the Apollo and Lunar Walkback case studies. Extremely low emissivity values are only desirable to minimize heat absorption in the hottest environments. For polar missions, or equatorial night missions, the desired emissivity range is 0.17 < ε < 0.63 at Apollo-like metabolic activity, with no supplemental cooling required (though it may still be desirable as a back-up system). The desired range is 0.39 < ε < 0.75 at worst-case (Lunar Walkback) conditions, with no supplemental cooling required, if hot environments are avoided. These desired emissivity ranges are similar to the specifications already provided by Ashwin-Ushas Corp. and Eclipse Energy Systems. If low emissivities are difficult to achieve with currently available electrochromic devices, the required emissivity range can be shifted higher by reducing radiator surface area.

Turndown ratio, a comparative analysis metric commonly used for radiator performance, is usually defined as the ratio of maximum to minimum heat rejection in a given environment and involves not only surface properties but also design characteristics of the coolant loop used to transport heat to the radiator. However, this definition is reductive in the case of electrochromic radiators, and furthermore, the present study is agnostic to coolant loop design. Therefore, an alternative definition of turndown ratio is suggested for the special case of electrochromic radiators as follows:

$$Electrochromic\ Turndown\ Ratio = \frac{Maximum\ Heat\ Rejection}{Minimum\ Heat\ Load}$$

Equation 4-4

Results of this turndown ratio analysis are presented in Table 4-5, calculated for each lunar environment in the study and for Apollo historical and Lunar Walkback Test metabolic rates. The maximum heat rejection in Equation 4-4 is usually calculated from ε_{max} = 0.9, while the minimum heat load is simply the minimum metabolic rate from Table 2 combined with a constant PLSS electronics heat of 120 W. In the lunar equatorial noon case, the maximum heat rejection actually corresponds to the

minimum heat absorption, which occurs for ε_{min} = 0.1, and the ratio is negative due to the heat flux sign convention.

Table 4-5: Electrochromic Turndown Ratios

Environment	Apollo	Walkback
Polar Shadowed Crater (ε=0.9)	5.32	2.30
Polar Illuminated (ε=0.9)	4.56	1.97
Equator Night (ε=0.9)	4.75	2.05
Equator Noon (ε=0.1)	-0.34	-0.14

Conclusions

Using fundamental thermodynamic analyses based on actual metabolic and environmental parameters, and technology performance assumptions based on vendor-provided specifications, it is shown that a variable-emissivity electrochromic radiator distributed throughout the outer surface area of a space suit is theoretically capable of removing most or all of the heat load incurred during a lunar EVA, depending on specified conditions.

Specific outcomes vary by lunar region, time within the lunar day, and overall metabolic profile of the crew member; the latter being a function of space suit design, concept of operations, and individual physiology. Because of these uncertainties in the net heat load and the possibility of encountering conditions exceeding the radiator's capacity, a suit-based, electrochromic radiator design will likely require a back-up cooling system, perhaps one similar to legacy systems, or be operationally constrained to specified activities, locations and/or portions of the lunar day. Nevertheless, this analysis suggests the potential of incorporating electrochromic radiators to significantly reduce or eliminate water consumption needed for space suit heat rejection.

Beyond these steady-state analytical evaluations, test data on electrochromic devices under thermal vacuum conditions are needed to verify their actual performance capabilities in a simulated relevant environment, and detailed design solutions are needed to effectively integrate them with the suit material layup and into the heat transfer pathway. Additional implementation challenges include design of the electronic circuitry required for electrochromic modulation; development of control logic for maintaining thermal equilibrium under the highly dynamic conditions experienced during EVA; and ultimately, a system-level, cost-benefit analysis of the proposed integrated design.

Resulting Publications and Presentations:

Metts, Jonathan G., Nabity, James A., and Klaus, David M., "Theoretical Feasibility of Integrated Electrochromic Radiators for Space Suit Thermal Control", accepted for publication by *Advances in Space Research*, November 2010.

"Application of Electrochromic Materials for Active Space Suit Thermal Control", poster presentation at the 38th International Conference on Environmental Systems (ICES), San Francisco, CA, 30 June 2008 (received 4th place in the student poster competition).

Chapter 5 – Sublimator Water Consumption and Radiator Impact Case Studies

First-order feasibility analysis of a space suit radiator concept based on estimation of water mass sublimation from Apollo mission data

Abstract

Thermal control of a space suit during Extravehicular Activity (EVA) is typically accomplished by sublimating water to provide system cooling. Spacecraft, on the other hand, primarily rely on radiators to dissipate heat. Integrating a radiator into a space suit has been proposed as an alternative design that does not require mass consumption for heat transfer. While providing cooling without water loss offers potential benefits for EVA application, it is not currently practical to rely on a directional, fixed-emissivity radiator to maintain thermal equilibrium of a spacesuit where the radiator orientation, environmental temperature, and crew member metabolic heat load fluctuate unpredictably. One approach that might make this feasible, however, is the use of electrochromic devices that are capable of infrared emissivity modulation and can be actively controlled across the entire suit surface to regulate net heat flux for the system. Integrating these devices onto the irregular, compliant space suit material requires that they be fabricated on a flexible substrate, such as Kapton film. An initial assessment of whether or not this candidate technology presents a feasible design option was conducted by first characterizing the mass of water loss from sublimation that could theoretically be saved if an electrochromic suit radiator was employed for thermal control. This is particularly important for lunar surface exploration, where the expense of transporting water from Earth is excessive, but the technology is potentially beneficial for other space missions as well. In order to define a baseline for this analysis by comparison to actual data, historical documents from the Apollo missions were mined for comprehensive, detailed metabolic data

from each lunar surface outing, and related data from NASA's more recent "Advanced Lunar Walkback" tests were also analyzed. This metabolic database was then used to validate estimates for sublimator water consumption during surface EVAs, and solar elevation angles were added to predict the performance of an electrochromic space suit radiator under Apollo conditions. Then, using these actual data sets, the hypothetical water mass savings that would be expected had this technology been employed were calculated. The results indicate that electrochromic suit radiators would have reduced sublimator water consumption by 69% across the entire Apollo program, for a total mass savings of 68.5 kg to the lunar surface. Further analysis is needed to determine the net impact as a function of the complete system, taking into account both suit components and consumable mass, but the water mass reduction found in this study suggests a favorable system trade is likely.

Introduction

During extravehicular activity (EVA), space suits must collect and remove metabolic heat generated from within the suit by the crew member, waste heat from the suit's electronics, and absorbed heat from the environment. Since the net sum of these heat sources can vary considerably, the space suit thermal control subsystem must be capable of maintaining a reasonably narrow band of internal temperature over a wide range of heat inputs and outputs in order to provide thermal equilibrium for the crew member. Both the U.S. and Russian space suits currently employ a water sublimation process to provide cooling when operating without umbilical attachment to the supporting vehicle. This solution involves exposing consumable (feed) water through a porous metal surface to the cold vacuum of space, where it freezes into a thin layer over the sublimator plate (Tongue & Dingell, 1999). As heat rejection is needed, waste heat is transferred to the sublimator through a heat exchanger, causing the ice to sublimate directly to water vapor and vent away from the suit,

44

transporting the waste energy as latent heat of vaporization. Therefore, the sublimator is an "open-loop" technology, meaning that it expends mass that is not recovered.

Both manned and unmanned spacecraft, on the other hand, typically use radiators for heat rejection. Radiators emit waste heat to the environment via electromagnetic radiation by transferring heat to an exposed surface with high infrared emissivity and, therefore, are considered "closed-loop" with respect to mass. Radiators typically provide a steady level of cooling performance, as the amount of heat rejected depends primarily on the environment (sink) temperature, which is predictable in orbit or transit (Gilmore, 2002). For space suit applications, however, the heat load and radiation view factor change almost continuously, making adequate control of radiator cooling a challenging prospect. Common methods of turning down or turning off radiator cooling, including actuated surface orientation, mechanical louvers, and freezable fluid lines, would be less effective and/or likely excessively cumbersome for space suit applications. Also, there is limited surface area for mounting a flat, metallic radiator array on a suit, and previous studies that have focused on the Portable Life Support System (PLSS) backpack as a structural basis for a radiator have found it to offer inadequate surface area for effective cooling (Sompayrac et al., 2009).

Electrochromic materials have properties that can potentially solve both the turn-down and surface area problems that have so far prevented successful application of space suit radiators. By definition, electrochromic materials provide variable optical properties that can be controlled electrically (Granqvist, 1995). In recent years, this technology has also come to include thin-film devices with variable infrared emissivity that can be built onto flexible substrates, such as Kapton film (Bessiere et al., 2002; Kislov et al., 2003). The thinness and flexibility of electrochromics means that they can potentially be integrated with space suit fabric, covering nearly the entire suit, not just the flat PLSS backpack surface. Their variable emissivity control enables electrochromic devices to be used like solid-

state thermal flux modulators, with heat emission controlled electronically as a function of the emissivity setting, which is itself a function of the applied voltage (Hodgson et al., 2004).

Due to the expense of delivering mass to the lunar surface, as well as achieving programmatic goals of increasing EVA duration and frequency upon returning to the moon, a reduction or elimination of water consumption for space suit cooling is particularly desirable for lunar missions (Jones, 2009; Nabity et al., 2008). The primary goal of this study was to conduct a first-order analysis of whether electrochromic space suit radiators offer a feasible alternative and/or supplement to water sublimation. As the basic purpose of using such radiators is to reduce water consumption for heat rejection, our initial assessment of the radiators' feasibility was to analyze potential consumable mass savings if they were incorporated into the suit. This was done by using the best available actual surface EVA operational data, namely that of the Apollo lunar missions.

Background

The concept of using electrochromics for thermal control was introduced as part of a futuristic design called the Chameleon Suit (Hodgson et al., 2004). The study, however, did not analyze the performance of this technology in specific environments, nor did it quantify the expected water consumable mass savings. From this starting point, we began a series of research tasks aimed at more thoroughly examining the feasibility of this proposed novel application.

Initial approaches for physically integrating electrochromic radiators into existing and future space suits have already been conceptually outlined, with preliminary thermal analysis conducted and emissivity control functions defined (Metts & Klaus, 2009). Theoretical assessment of this concept using assumed environmental boundary conditions and manufacturer product specifications suggested that electrochromic technology would be capable of meeting the heat rejection requirements for lunar

missions, pending demonstration of the required electrochromic material performance (Metts et al.,

2010). Testing of electrochromic materials for space applications is an ongoing effort, with empirical

results and methodologies published for both steady-state, thermal vacuum testing (Bannon et al.,

2010) and transient, bench-top testing (Metts & Klaus, 2010). The next step was to examine more

practical considerations for assessing the electrochromic technology application for space suits,

including potential sublimator water use reduction during operational environmental interactions.

To perform a more detailed thermal analysis of electrochromic radiator performance, realistic

metabolic heat load data and lunar surface environmental parameters were needed, ideally coming

from the Apollo missions. NASA documents define "average" EVA metabolic rates for mission planning,

classified as minimum/nominal/maximum values (Hanford, 2004). These values, however, were not of

sufficient resolution to accurately determine the dynamic heat rejection needs over the course of a real

EVA. Fortunately, additional unpublished Apollo medical data, recorded by James M. Waligora at the

NASA Johnson Space Center between 1972 and 1975, had been compiled and correlated to specific EVA

operations by Carr & Newman (2007). This historical dataset includes detailed, minute-by-minute

metabolic rates for each individual Apollo surface EVA, allowing for comparison among the various

astronauts and even individual excursions within a particular mission, although primary documentation

was missing for the Apollo 16 Lunar Module Pilot, EVA-3. To address this shortcoming, the omitted data

was reconstructed in a similar format, though from different sources (Waligora, 1975), by correlating

timestamps to the Apollo Lunar Surface Journal (Jones & Glover, 1995) and assigning one of three

associated metabolic rates based on a description of the LMP's activities.

For the detailed radiator performance analysis conducted in this study, correlated lunar sink

temperatures were also required for each specific Apollo surface EVA. On the lunar surface,

environmental sink temperature is a function of topography and solar elevation angle. All Apollo landing

sites were in the equatorial plains region. Astronauts walked and drove the lunar rover near crater rims,

but did not actually enter any craters (due in part to thermal concerns). Solar elevation angles are catalogued in various mission documents found within the Apollo Lunar Surface Journal (Jones & Glover, 1995). These angles can be correlated with environmental sink temperature according to the results of a "flux cube radiation" analysis by Sompayrac et al. (2009).

In this case, the suit's thermal environment is dominated by the lunar surface, not the sun. The methodology to calculate sink temperatures in Sompayrac et al. (2009) already includes considerations such as view factor to the surface and lunar dust properties, so these are not explicitly included in our analysis.

Analysis

Previous work already suggested that electrochromic suit radiators are theoretically capable of supplementing or replacing the cooling function of a sublimator under certain lunar thermal conditions based on heat transfer capacity under the given temperature gradients (Metts et al., 2010). This study takes the next detailed step toward estimating the amount of consumable mass that could hypothetically be saved using a radiator to remove heat without ejecting water vapor via sublimation. To represent the range of actual EVAs performed during Apollo, individual metabolic profiles and corresponding environmental data were used for each case study in this analysis. Additional heat from the PLSS is included as the constant value q_{PLSS} = 120 W per a previous NASA study (Sompayrac et al., 2009). Total thermal energy was integrated from the metabolic profile, and as shown in Eq. 5-1, sublimator water usage is a function of the thermal load, duration, and the heat of vaporization for water, h_{vapor} = 2260 kJ/kg (adapted from Leimkeuhler et al., 2009). This formula assumes thermal equilibrium is maintained, i.e. no heat storage or deficit (hyperthermia or hypothermia) is accrued by

the crew member. Since direct data on sublimated water is not available from the Apollo lunar EVAs, we are estimating the water mass based on ideal sublimator performance.

$$m_{H2O} = \frac{\int (q_{met} + q_{PLSS})\, dt}{h_{vapor}}$$

<div align="right">Equation 5-1</div>

Radiator performance is characterized by the Stefan-Boltzmann equation (Gilmore, 2002):

$$q_{rad} = \sigma A \varepsilon \, (T_s^4 - T_e^4)$$

<div align="right">Equation 5-2</div>

The radiator surface area (A) is assumed to be 3.43 m^2 based on a conservative interpretation of available radiative surfaces on the entire Extravehicular Mobility Unit (EMU) space suit, which totals 3.90 m^2 including occluded surfaces such as armpits and inner thighs. (Tepper, 1991) Our estimate is based on multiplying the total suit area by a ratio of 88% for an average nude male, based on a study by Guibert & Taylor (1952) on the concept of radiation area, which found that this ratio of exposed area to total surface area is not sensitive to clothing. We also assume the radiation area ratio scales from a nude/clothed male to the much larger space suit. The assumed emissivity range of the electrochromic material is $0.1 \le \varepsilon \le 0.9$, with maximum heat rejection occurring at $\varepsilon = 0.9$, and the radiator surface temperature is assumed to be T_s = 300 K, as explained in the prior theoretical study (Metts et al., 2010). Maximum environmental sink temperature (T_e) for each Apollo surface EVA is given in Table 5-1, which includes solar angle data from the Apollo Lunar Surface Journal (Jones & Glover, 1995) and temperatures interpolated from Sompayrac et al. (2009). "Heat leak" (passive radiation into or out of the suit) is typically accounted for in EVA heat rejection studies. In this analysis, the standard operating

49

mode of the radiator is essentially harnessing and controlling this "heat leak" for rejecting heat from the suit. In hot cases (when $T_e > T_s$), the direction of "heat leak" is reversed, because the radiator absorbs heat from the environment; this net effect is accounted for in the results.

Table 5-1: Summary of Apollo EVA Solar Angles (Jones & Glover, 1995) and Correlated Sink Temperatures Adapted from Sompayrac et al. (2009)

Apollo ID	Solar Angle (°)	Sink T. (K)
11	10.5 - 13.5	243 *
12-1	5	205
12-2	13	246
14	23	275 **
15-1	19	265
15-2	28	286
15-3	39	305 ^
16-1	14	249
16-2	25	280
16-3	37	302 ^
17-1	14.5	251
17-2	25	280
17-3	36.5	301 ^

* Apollo 11 solar angle is given as a range, so mean temperature is used.

** Only a single solar elevation angle is documented for Apollo 14.

^ The radiator absorbs heat at temperatures > 300 K.

To assess the hypothetical impact of the integrated, electrochromic radiator on these missions, a mass savings term is defined as the difference between sublimator water usage and the equivalent water mass when radiator heat rejection is included, per Eq. 5-3. Note that when q_{rad} is negative, due to heat absorption in adversely hot conditions, $m_{savings}$ will also be negative, meaning the supplemental cooling requirement is higher than if no radiator was present. This undesirable effect may ultimately be

offset by incorporating reflective materials into the outer surface of the suit, but for this first-order analysis, the more conservative "worst-case" absorption values were used.

$$m_{savings} = m_{H2O} - \frac{1}{h_{vapor}} \int (q_{met} + q_{PLSS} - q_{rad}) \, dt$$

<div align="right">Equation 5-3</div>

A worksheet for each EVA was formulated to compile the metabolic profile data, convert it into standard metric units, and perform water consumption and radiator analyses on the data. Table 5-2 shows an example worksheet for the first lunar surface EVA by Apollo 11 Commander (CDR), Neil Armstrong. According to Equation 5-2, with the estimated solar elevation angle of 12.0 degrees, the maximum radiator capacity for this EVA is 706 W. Since the combined metabolic rate and PLSS heat load never exceeded this rejection capacity in this case (except perhaps during a short transient, which would not be captured by the documentation), use of the proposed electrochromic radiator would have been theoretically adequate to reject all of the heat. Sublimator water consumption analysis shows that this hypothetical scenario would have saved 1.48 kg of consumable water during Armstrong's famous excursion. Note also that whenever the heat load is less than the maximum radiator capacity, the electrochromic radiator could be set to a lower-than-maximum emissivity to maintain thermal balance and avoid overcooling.

Table 5-2: Apollo 11 Commander, EVA-1 Thermodynamic Analysis. Total Heat Load includes 120 W for PLSS. Shortfall is the positive difference between total heat load and maximum radiator capacity.

Historical Apollo Data			Predicted Radiator Impact		
Total Heat Load (W)	Activity Duration (min)	Estimated H2O for Sublimation (kg)	Radiator Capacity (W)	Radiator Shortfall (W)	H2O Savings (kg)
383.70	11	0.11	807.00	0.00	0.11
354.40	3	0.03	807.00	0.00	0.03
376.38	7	0.07	807.00	0.00	0.07
317.78	5	0.04	807.00	0.00	0.04
369.05	4	0.04	807.00	0.00	0.04
339.75	23	0.21	807.00	0.00	0.21
361.73	12	0.12	807.00	0.00	0.12
369.05	23	0.23	807.00	0.00	0.23
317.78	18	0.15	807.00	0.00	0.15
347.08	12	0.11	807.00	0.00	0.11
486.25	19	0.25	807.00	0.00	0.25
544.85	7	0.10	807.00	0.00	0.10
530.20	2	0.03	807.00	0.00	0.03
Totals:	146	1.48			1.48

For contrast, Table 5-3 shows the worksheet for the second surface EVA of Apollo 17 Lunar Module Pilot (LMP), Harrison "Jack" Schmitt. This mission employed an upgraded A7LB suit with additional consumables for longer EVA operations. Apollo 15 through 17 also utilized a Lunar Roving Vehicle that impacted metabolic expenditures, as astronauts worked hard to prepare the vehicle and then rested during long drives between geological stations (Jones & Glover, 1995). For this EVA, the maximum radiator capacity is 342 W, meaning the sublimator would sometimes be needed for supplemental heat rejection. The estimate of actual sublimator consumption is 4.42 kg, but the hypothetical radiator usage could have reduced that amount to 0.81 kg, saving 82% of the cooling water consumed for this EVA.   Altered view factors may have to be taken into account for the suited

crewmember while sitting in the rover to refine this estimate. Figure 5-1 presents a graphical

comparison of Schmitt's heat load and the projected radiator capacity (cooling performance); the

margin between the two lines represents heat that must be removed by sublimation when the radiator

capacity is exceeded.

Table 5-3: Apollo 17 Lunar Module Pilot, EVA-2 Thermodynamic Analysis. Total Heat Load includes 120

W for PLSS. Shortfall is the positive difference between total heat load and maximum radiator capacity.

Historical Apollo Data			Predicted Radiator Impact		
Total Heat Load (W)	Activity Duration (min)	Estimated H2O for Sublimation (kg)	Radiator Capacity (W)	Radiator Shortfall (W)	H2O Savings (kg)
328.91	11	0.10	342.00	0.00	0.10
415.64	33	0.36	342.00	73.64	0.30
578.55	2	0.03	342.00	236.55	0.02
513.50	9	0.12	342.00	171.50	0.08
189.44	74	0.37	342.00	0.00	0.37
438.49	64	0.75	342.00	96.49	0.58
246.87	6	0.04	342.00	0.00	0.04
604.92	11	0.18	342.00	262.92	0.10
214.05	24	0.14	342.00	0.00	0.14
418.86	36	0.40	342.00	76.86	0.33
201.75	18	0.10	342.00	0.00	0.10
567.70	34	0.51	342.00	225.70	0.31
297.56	9	0.07	342.00	0.00	0.07
340.92	4	0.04	342.00	0.00	0.04
265.04	6	0.04	342.00	0.00	0.04
286.72	3	0.02	342.00	0.00	0.02
319.24	7	0.06	342.00	0.00	0.06
371.10	28	0.28	342.00	29.10	0.25
251.85	14	0.09	342.00	0.00	0.09
371.10	6	0.06	342.00	29.10	0.05
316.90	3	0.03	342.00	0.00	0.03
441.42	55	0.64	342.00	99.42	0.50
Totals:	457	4.42			3.62
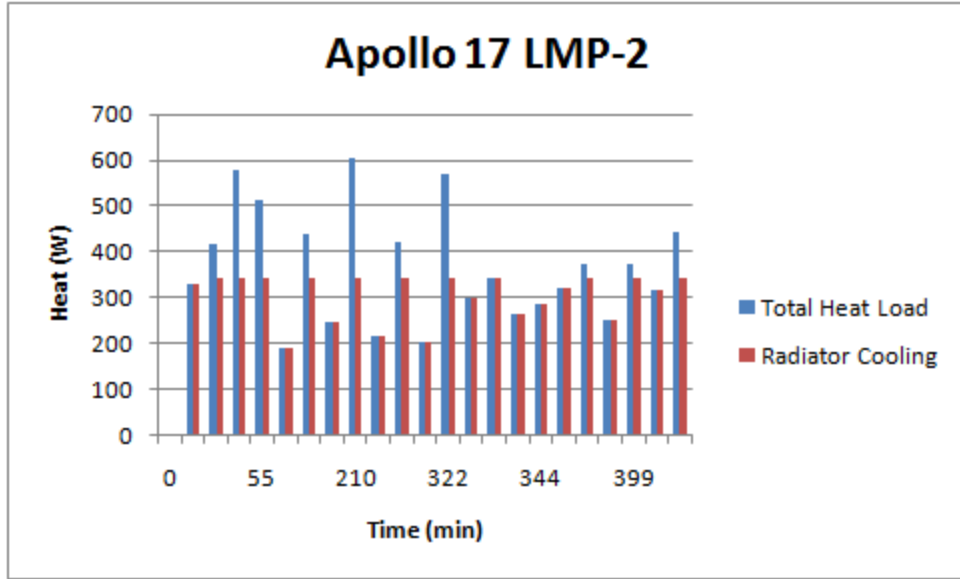
Figure 5-1: Graphical Comparison of Harrison Schmitt's Second Lunar EVA Heat Load Profile to Predicted

Electrochromic Radiator Performance (Max. Radiator Capacity = 342 W)

Similar analyses using actual metabolic and environmental data were conducted for each Apollo

surface EVA. The program-wide results with associated totals and averages are summarized in Table 5-4.

The overall result shows that a total 99.3 kg of water was sublimated during Apollo EVAs. Using the

above calculations, it was determined that incorporating the suit radiator concept could have

hypothetically reduced water sublimation to 30.8 kg (inclusive of the additional water mass sublimation

required to offset radiator heat absorption in the hot cases), for consumable mass savings of 69%

compared to the sublimator-only analysis. These results do not include lunar module (non-EVA)

sublimation. Operationally, the electrochromic radiator would be set to the lowest emissivity value in

hot environments to minimize infrared absorption from the environment (primarily solar flux re-

radiated by lunar soil), while a solar-reflective coating would minimize direct absorption from the sun.

Table 5-4: Summary of Apollo Program Thermodynamic Analysis. H2O is equivalent sublimator water usage, including 120 W for PLSS heat. Apollo 16, LMP-3 data was calculated from a different source (Waligora, 1975). Total radiator savings are based on estimated water sublimation and hypothetical mass savings over the entire Apollo program (percentages are not summed).

EVA ID	Historical Data			Radiator Projection	
	Dur. (hr)	H2O (kg)	Sink T. (K)	Savings (kg)	Savings (%)
11/CDR-1	2.43	1.48	243	1.48	100.00
11/LMP-1	2.43	1.86	243	1.86	100.00
12/CDR-1	3.90	2.52	205	2.52	100.00
12/LMP-1	3.90	2.55	205	2.55	100.00
12/CDR-2	3.80	2.27	246	2.27	100.00
12/LMP-2	3.80	2.51	246	2.51	100.00
14/CDR-1	4.67	2.66	275	2.55	95.93
14/LMP-1	4.67	2.91	275	2.83	97.12
14/CDR-2	4.58	2.83	275	2.62	92.77
14/LMP-2	4.58	3.02	275	2.76	91.56
15/CDR-1	6.53	4.59	265	4.54	98.88
15/LMP-1	6.53	4.23	265	4.21	99.62
15/CDR-2	7.22	4.75	286	2.84	59.65
15/LMP-2	7.22	4.10	286	2.79	67.94
15/CDR-3	4.83	3.25	305	-0.75	-22.96
15/LMP-3	4.83	2.75	305	-0.75	-27.12
16/CDR-1	6.10	3.62	249	3.62	100.00
16/LMP-1	6.40	4.29	249	4.29	100.00
16/CDR-2	7.25	4.06	280	3.71	91.30
16/LMP-2	7.22	4.22	280	3.67	87.02
16/CDR-3	5.53	3.14	302	-0.34	-10.71
16/LMP-3	5.63	3.35	302	-0.34	-10.23
17/CDR-1	7.20	5.09	251	5.09	100.00
17/LMP-1	7.20	5.03	251	5.03	100.00
17/CDR-2	7.62	4.41	280	3.75	84.90
17/LMP-2	7.62	4.42	280	3.61	81.73
17/CDR-3	7.25	4.58	301	-0.22	-4.79
17/LMP-3	7.25	4.80	301	-0.22	-4.57
Totals:	158.20	99.28		68.47	68.97
Averages:	5.65	3.55		2.45	70.29

While the Apollo landings provide the only source of actual lunar surface EVA metabolic or heat rejection data to date, NASA has devised a relevant terrestrial simulation, termed the Advanced Walkback Test, to help establish worst-case limits for designing next-generation lunar EVA technology. These tests, performed in NASA's "Mark III" lunar suit prototype using a Partial Gravity Simulator (POGO) harness to simulate lunar gravity, required test subjects to walk/jog for 10 km on a treadmill to simulate an emergency return by foot from a broken-down rover (at its maximum range) back to the lander/habitat (Norcross et al., 2009 and 2010). Subjects were asked to complete the trek within 2 hours and were given varying treadmill elevation patterns to represent different paths over uneven lunar terrain. Although sublimation was not used since umbilical connections provided the necessary cooling, projected water mass loss can still be estimated with similar metabolic data and analytical methods as were used for the Apollo data. Our analysis also assumed the same PLSS heat load of 120 W as in the Apollo analysis for a common basis of comparison. Also, since radiator performance analysis requires knowledge of the environment (sink) temperature, the test data have been correlated to four example temperatures from the Apollo data.

Table 5-5: Example of Advanced Walkback Test Thermodynamic Analysis. Total Heat Load includes 120 W for PLSS. Sublimated water savings due to the radiator impact are calculated for each of the representative Apollo sink temperatures.

	Advanced Walkback Test Data		Radiator H2O Savings (kg) at Each Sink Temp.			
Time Stamp (min)	Total Heat Load (W)	Estimated H2O for Sublimation (kg)	205 K	246 K	286 K	305 K
4	531.70	0.06	0.06	0.06	0.03	-0.01
9	692.20	0.09	0.09	0.09	0.03	-0.01
12	761.98	0.06	0.06	0.06	0.02	-0.01
16	821.29	0.09	0.09	0.08	0.03	-0.01
21	674.75	0.09	0.09	0.09	0.03	-0.01
26	779.42	0.10	0.10	0.10	0.03	-0.01
31	706.15	0.09	0.09	0.09	0.03	-0.01
32	597.99	0.02	0.02	0.02	0.01	0.00
37	671.26	0.09	0.09	0.09	0.03	-0.01
40	751.51	0.06	0.06	0.06	0.02	-0.01
45	615.44	0.08	0.08	0.08	0.03	-0.01
48	674.75	0.05	0.05	0.05	0.02	-0.01
53	660.80	0.09	0.09	0.09	0.03	-0.01
58	552.64	0.07	0.07	0.07	0.03	-0.01
63	667.77	0.09	0.09	0.09	0.03	-0.01
68	810.82	0.11	0.11	0.10	0.03	-0.01
73	653.82	0.09	0.09	0.09	0.03	-0.01
74	549.15	0.01	0.01	0.01	0.01	0.00
79	709.64	0.09	0.09	0.09	0.03	-0.01
84	814.31	0.11	0.11	0.10	0.03	-0.01
89	646.84	0.09	0.09	0.09	0.03	-0.01
92	563.10	0.04	0.04	0.04	0.02	-0.01
97	706.15	0.09	0.09	0.09	0.03	-0.01
100	775.93	0.06	0.06	0.06	0.02	-0.01
105	639.86	0.08	0.08	0.08	0.03	-0.01
110	681.73	0.09	0.09	0.09	0.03	-0.01
115	594.50	0.08	0.08	0.08	0.03	-0.01
118	636.37	0.05	0.05	0.05	0.02	-0.01
Totals:		2.14	2.14	2.12	0.77	-0.30

The Advanced Walkback Test analysis for all six subjects is summarized in Table 5-6, with results including the assumed PLSS heat load of 120 W. Some Apollo temperatures were greater than 300 K, the assumed radiator surface temperature, in which case the electrochromic radiator would absorb heat flux (consequently, the shortfall is greater than the full-sublimator water consumption). As with the Apollo analysis, the electrochromic radiator can be set to an interim emissivity for thermal balance in cases where the maximum (ε = 0.9) radiator capacity exceeds the heat rejection requirement. The hypothetical reduction in water consumption is 100%, 92.5%, 30.2%, and -12.3% for the four respective environment temperatures included in the analysis.

Table 5-6: Summary of Advanced Walkback Test Thermodynamic Analysis. Equivalent H2O is estimated sublimator water usage, including 120 W for PLSS heat. Sublimated water savings due to the radiator impact are calculated for each of the representative Apollo sink temperatures.

Advanced Walkback Test Data			Radiator H2O Savings (kg) at Each Sink Temp.			
Subject ID	Time (min)	Estimated H2O for Sublimation (kg)	205 K	246 K	286 K	305 K
1	118	2.14	2.14	2.12	0.77	-0.30
2	86	2.05	2.05	1.77	0.56	-0.22
3	110	2.58	2.58	2.27	0.72	-0.28
4	100	2.07	2.07	2.03	0.65	-0.26
5	92	1.90	1.90	1.85	0.60	-0.24
6	84	2.01	2.01	1.73	0.55	-0.22
Average	98.33	2.12	2.12	1.96	0.64	-0.25

Additionally, a related study at Johnson Space Center found that the maximum Walkback metabolic rate exceeded the heat rejection capacity of the Apollo-style sublimator (which is cited as ~2000 BTU/hr, equivalent to 586 W); this situation would result in heat storage in the crew member,

which can lead to debilitating conditions such as heat stroke (Vos, 2007; NASA, 2006). An examination of the data with assumptions used in our analysis confirms this finding. With the 120 W PLSS heat included, five of six test subjects never produced heat loads below 586 W, which is the Apollo sublimator limit of performance (Vos, 2007). The remaining test subject also exceeded 586 W for 105 minutes out of 118 minutes total. Adding an electrochromic radiator, therefore, may be one solution to providing adequate heat rejection capacity for the worst-case scenario, although there are certainly other options, including an increase in the sublimator plate surface area and consumable water use. Ultimately, the final comparison must also take into account the influence of location and lunar cycle on the effectiveness of a radiator, since in the hottest environmental conditions, a radiator could actually further stress the sublimator with the addition of absorbed heat.

Conclusions

Thermal analysis of actual Apollo surface EVA metabolic and lunar environmental data suggests that electrochromic radiator technology, had it been available at the time, could have reduced program-wide sublimator water use by 69%, a mass savings of 68.5 kg. Furthermore, the addition of an electrochromic suit radiator may increase total heat rejection capacity enough to prevent excess heat storage in crew members under duress, as suggested by the Advanced Walkback Test analysis.

Whether this technology can provide similar theoretical benefits for future lunar space suits will depend on factors such as landing site selection and mission timing. A complete system analysis is also required to determine the net mass trade-off between the sublimator water savings and additional components needed to implement a full-suit electrochromic radiator. More detailed integrated design information and radiator performance testing under relevant conditions will be necessary to verify

system mass comparisons. Risk and reliability analyses will ultimately be needed to determine operational feasibility.

Resulting Publications and Presentations:

Metts, Jonathan G. and Klaus, David M., "First-order feasibility analysis of a space suit radiator concept based on estimation of water mass sublimation using Apollo mission data", in peer review.

"Electrochromic Radiator Impact on Apollo Sublimator Water Consumption", poster presentation at the 40th International Conference on Environmental Systems (ICES), Barcelona, Spain, 12 July 2010 (received 1st place in the student poster competition).

Chapter 6 – Conceptual Analysis of Electrochromic Radiators for Space Suits

Abstract

Electrochromic devices offer potential benefit as variable emissivity radiators for advanced extravehicular activity (EVA) suits. Supplementing (or even replacing) the water sublimator with radiators will result in reduced mass consumption for heat rejection, and radiators can be effective in environments where sublimation is not possible. The exotic properties of electrochromic devices (ECDs) may also lead to radiators that are capable of adapting, without mechanical actuation, to changing EVA operations and environments. Three concepts for the implementation of flexible electrochromic radiators are presented, along with a preliminary thermal analysis for each configuration.

Introduction

Since the Apollo Program, non-umbilical EVA suits have used sublimators to reject heat generated by metabolic activity, from the portable life support system (PLSS) electronics, and absorbed from the environment. The sublimator expends water from a consumable supply, which will be costly to sustain on long-term missions without frequent resupply (Nabity et al., 2008). Furthermore, the current sublimator technology's performance would be impeded in the thin Martian atmosphere, where the phase change would be limited to evaporation with reduced heat rejection potential.

Multiple studies have considered concepts for EVA suit radiators to mitigate the water mass consumption of sublimator heat rejection (Nabity et al., 2007; Izenson et al., 2008; Ochoa et al., 2008). Certain factors complicate the feasibility of using suit radiators, however, such as available surface area, operational variability, flexibility, surface contamination, freezability, etc. Electrochromic devices may provide a solution to some of these issues by virtue of their dynamic optical properties, fast response times, mechanical simplicity, and modulation of effective surface area (Hale & Woollam, 1999; Hodgson

et al., 2004). ECDs with variable emissivity in the infrared wavelengths are becoming commercially available at the prototype level, with some offering reflective coatings like those typically applied to spacecraft radiators (Demiryont et al., 2006; Paris et al., 2005). Studies have shown that ECDs can also be applied to flexible substrates with a minimal decrease in performance (Bessiere et al., 2002; Kislov et al., 2003). Thus, flexible infrared ECD radiators may be considered for integration into the outer fabric layers of an EVA suit, as shown in Figure 6-1, to maximize the available surface area. This proposed solution introduces the questions of how heat would be transported to the radiators for rejection; how integrated radiators will respond to hostile environments (including lunar surface dust); how a relatively large and multi-surface radiator array will respond to highly variable orientation during EVA; and how/whether to integrate the radiators with current suit thermal control system.
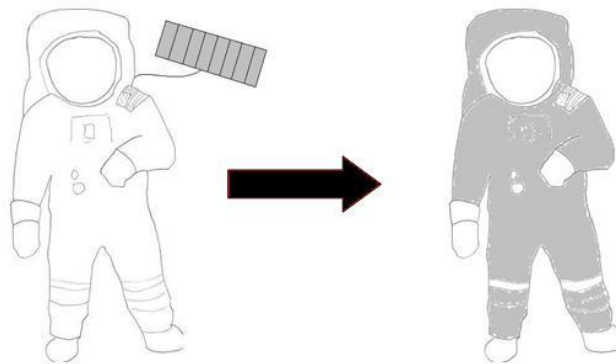
Figure 6-1: Integration of Radiators into Suit Fabric

Background

The current US Extravehicular Mobility Unit (EMU) and Russian Orlan suits have similar thermal control subsystems, consisting of a liquid cooling and ventilation garment (LCVG), multi-layer insulation (MLI) and thermal micrometeoroid garment (TMG) to minimize heat leakage and/or environmental heat flux absorption, a heat exchanger with both liquid water and oxygen gas loops interfaced with an ice

62

sublimator connected to a separate feed water tank. These components are conceptually illustrated in Figure 6-2, along with the metabolic load and the various mechanisms of heat flux through the suit to the environmental heat sink. (Note: The heat generated by PLSS components is not included in this and subsequent illustrations, for the sake of simplicity.) Most of the metabolic heat is conducted to water-filled Tygon tubing laced throughout the LCVG or convected/exhaled/perspired into the oxygen stream. The remainder is radiated from the skin or LCVG toward the MLI, which transmits only a small percentage of that heat out to the environment. Internal heat reflected by the MLI is eventually absorbed by the skin or LCVG. In steady-state operation, nearly all metabolic heat is ultimately rejected by the sublimator, while radiative heat leakage is a minor factor by design. Likewise, heat absorbed from the environment (e.g., solar flux, albedo from planetary bodies, and thermal radiation from nearby spacecraft) is low, due to the high reflectivity of the MLI and other materials in the outermost layers of the suit.

Figure 6-2: Metabolic and Environmental Heat Transfer Paths in Traditional EVA Thermal Control

Electrochromic materials have a number of unique properties that offer potential for use as radiators. By definition, ECDs can be optically modulated by applying a voltage differential (Granqvist, 1995). The actual electrochromic material consists of a thin film that is sandwiched between supporting layers, enabling ion transport to take place; this assembly is collectively what is known as the electrochromic device, shown in Figure 6-3. Certain types of ECDs, particularly those incorporating tungsten trioxide (WO_3) as the electrochromic layer, exhibit electrochromism in the infrared

64

wavelengths where thermal radiation is active. These infrared ECDs typically have $\Delta\varepsilon > 0.5$, and the effect is both continuous and reversible (Granqvist, 2000). Two commercial fabricators have been identified as possible suppliers: Ashwin-Ushas Corp. in Lakewood, NJ and Eclipse Energy Systems, Inc., based in St. Petersburg, FL. Both of these companies produce custom infrared ECDs in small batches, and both offer solar reflective coatings of the kind used on typical spacecraft radiators. The infrared electrochromic capability of an Eclipse ECD is shown in Figure 6-4. Electrochromic radiators promise certain advantages over traditional spacecraft radiators. The emissive power of ECDs can be adjusted quickly as mission operations and environmental conditions change, and the effective surface area can also be varied if the radiator panels are controlled in parallel. Furthermore, these changes do not involve any physical mechanisms, which may translate to reduced mass and improved reliability compared to mechanical louvers and/or gimbals as typically used on traditional radiators. These properties suggest that ECDs may be particularly appropriate for EVA, in which heat loads, orientation, and environmental conditions change frequently and abruptly, and since relative attitude stability, system mass and surface area constraints differ from those of a larger spacecraft. A preliminary trade analysis based on the Equivalent System Mass (ESM) metric to weigh overall costs and benefits is presented later in this chapter.
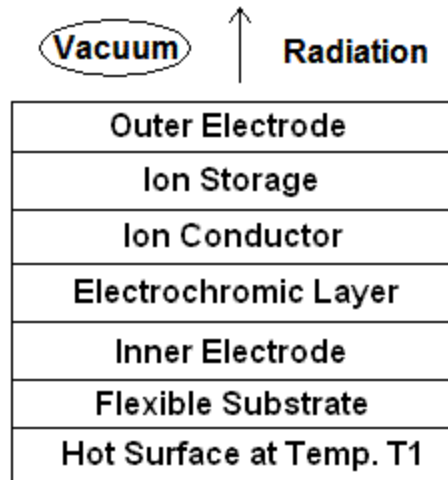
Figure 6-3: Diagram of Infrared ECD Radiator (adapted from Kislov et al., 2003).
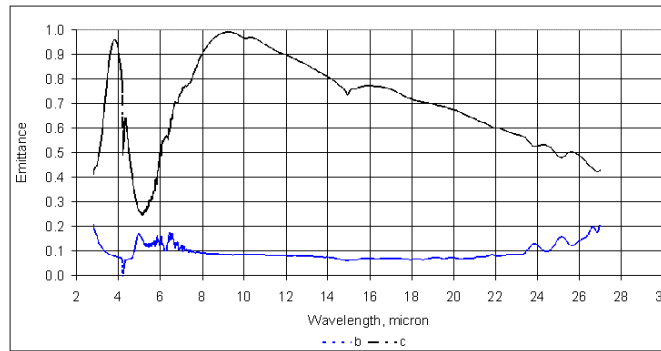
Figure 6-4: Infrared Performance of Eclipse ECD in Bleached (Low ε) and Colored (High ε) Modes (Image

courtesy of Eclipse Energy Systems, Inc., with permission.)

Proposed Configurations

Depending on the design configuration, performance capacity, available surface area,

operations, and environmental conditions, radiators alone may or may not be capable of rejecting all

metabolic heat from the suit. (For this paper, heat from PLSS hardware is neglected, both in the

conceptual designs and supporting thermodynamic analyses.) We have identified three configuration

concepts for integrating electrochromic radiators into the EVA suit thermal control system:

Concept #1

The radiators are embedded in the outermost layers of suit material, external to the MLI, as

shown in Figure 6-5. All legacy components are retained. A bypass feature is added to the heat

exchanger, allowing some or all of the heat to be diverted from the sublimator to the radiators. A

separate, closed fluid loop (not necessarily water) transports the bypassed heat to a network of

electrochromic radiator panels.
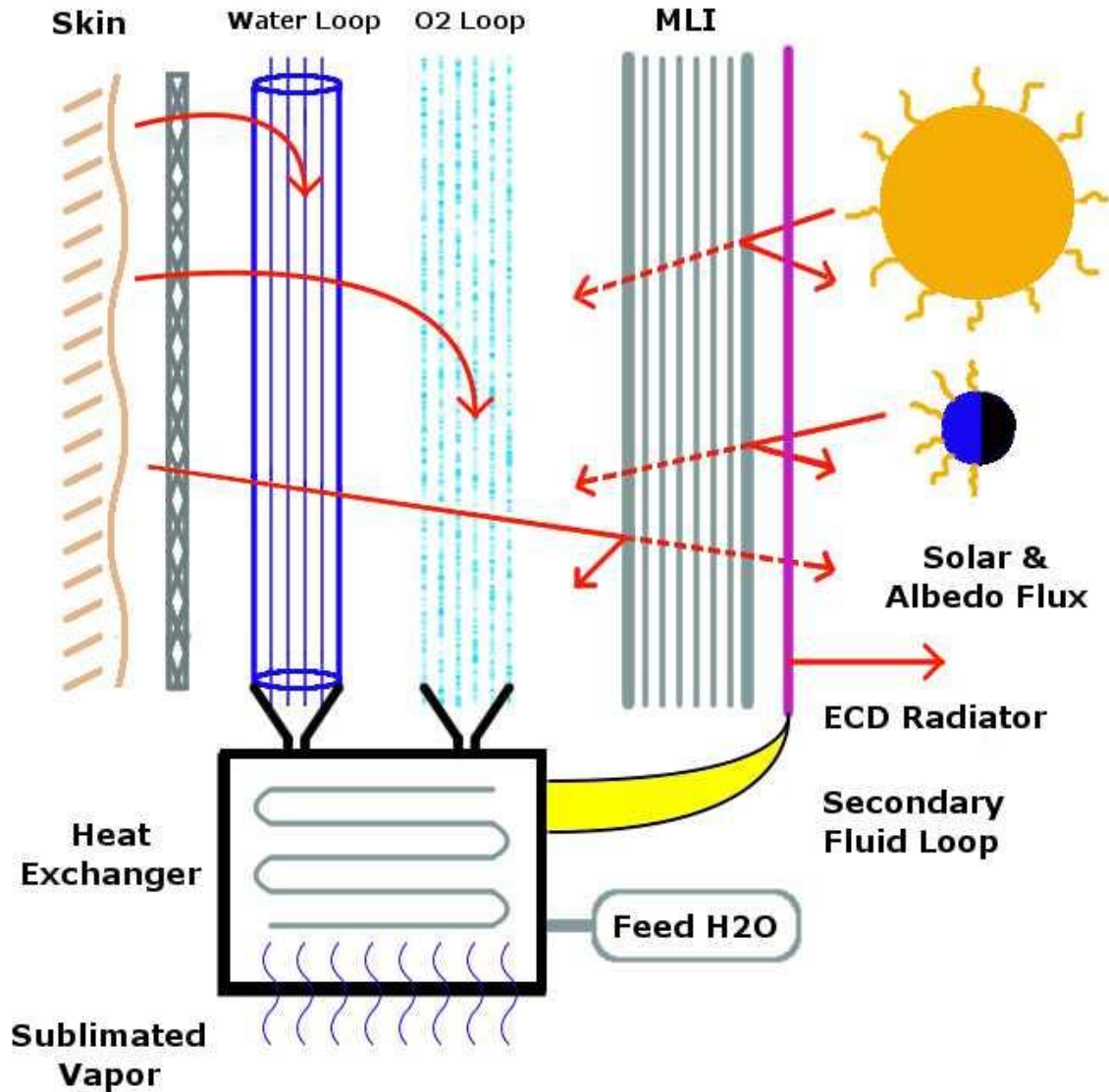
Figure 6-5: Concept 1 – ECD Radiators with Heat Exchanger Bypass Loop

Concept #2

The MLI is replaced by electrochromic radiators as shown in Figure 6-6. Non-thermal functions

of the external suit materials, such as micrometeoroid protection, must be provided by other thermally

transparent materials that will not interfere with radiator performance. Although some heat is radiated

from the skin, absorbed, and re-radiated by the ECD radiators, most heat transport to the radiators is via

convection from the ventilation loop. The LCVG and sublimator are still active, so this radiator concept

is a passive bypass system. It does not require any new heat exchanger functionality or an additional

fluid loop.
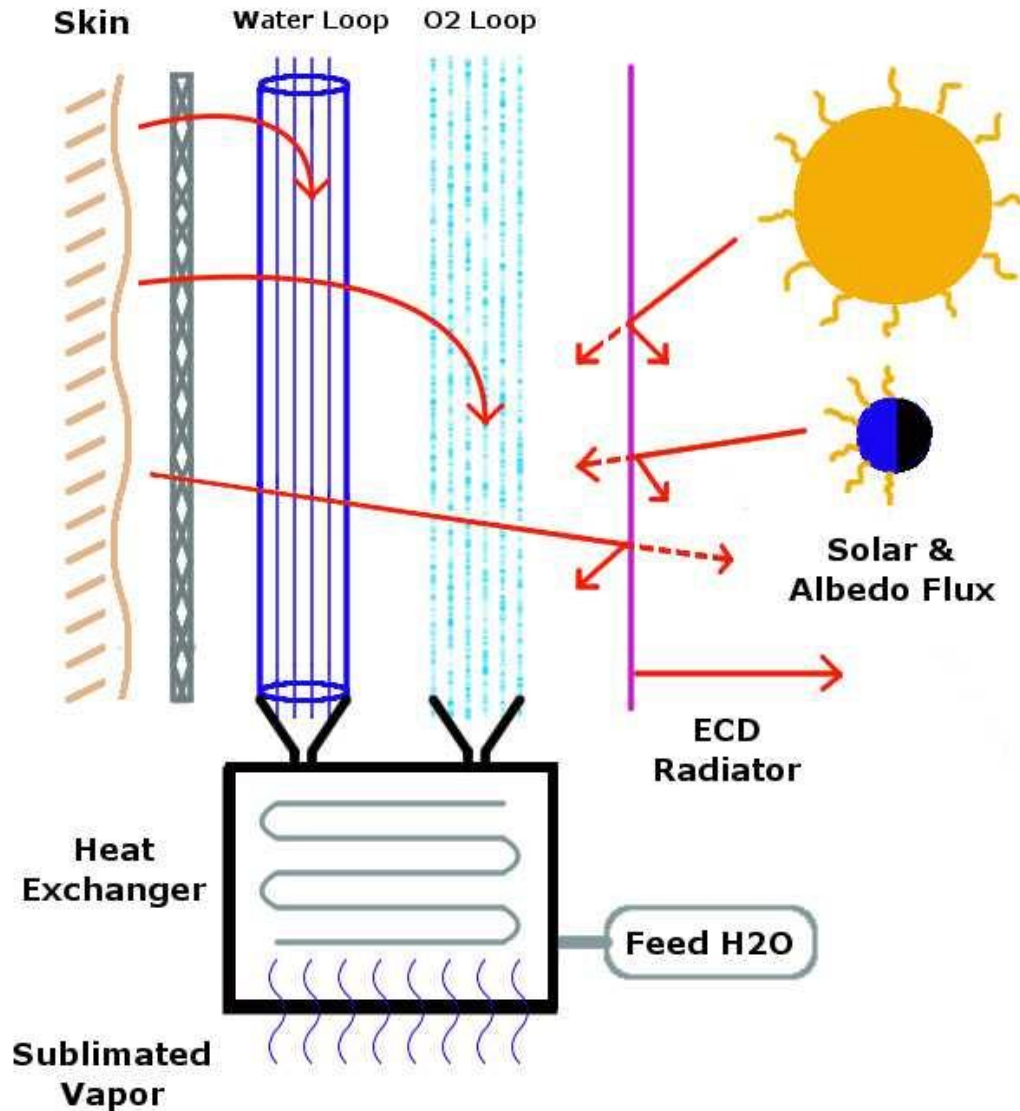
Figure 6-6: Concept 2 – ECD Radiators Replacing MLI

Concept #3

The ECD radiators are located near the skin level with conductive pathways from the skin to radiators (Figure 6-7). There is no LCVG, MLI, heat exchanger, or sublimator. All heat rejection is governed by the radiators. This concept very likely requires the use of mechanical counter-pressure (MCP) or a similar technology to replace the physical benefits of gas pressurization associated with the LCVG and its pure oxygen loop (Pitts et al., 2001). Gas ventilation is still required in the helmet and upper torso to facilitate respiration, so the metabolic heat released via respiration would still need to be conducted to the ECD radiators or rejected from the suit by some other method.
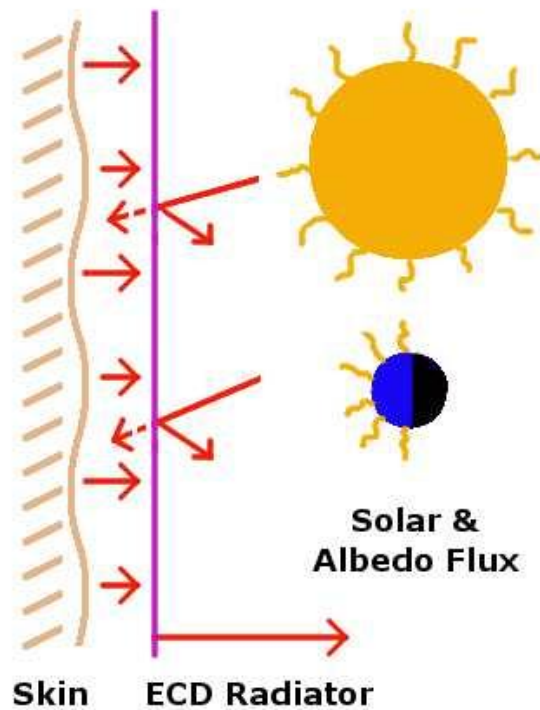
Figure 6-7: Concept 3 – ECD Radiators Replacing LCVG, MLI, and Sublimator

Methods

In order to compare and evaluate these three configuration concepts, a simplified thermodynamic model was used. The analysis assumes a steady state heat balance among metabolic heat generation, solar flux absorption, and radiator heat rejection. For concepts that include a sublimator, it is assumed that the sublimator can reject all heat not bypassed to the radiators. The emissive power of a radiator is governed by the Stefan-Boltzmann equation (Çengel, 1997):

$$Q_{emit} = \sigma A \varepsilon (T_s^4 - T_e^4)$$

Equation 6-1

This fourth-order equation includes radiator surface area, A, the surface emissivity ε (which is variable for ECDs), and the Stefan-Boltzmann constant, σ. Also, T_s refers to the radiator surface temperature, and T_e is the environment sink temperature. If the environment is hotter than the radiator, Q_{emit} will be negative, meaning the radiator is absorbing more heat from outside than it can reject. The steady-state heat balance of the EVA suit (again, neglecting PLSS heat loads) with radiators, adapted from (Trevino & Orndoff, 2000), can be expressed as:

$$Q_{met} + Q_{env} - Q_{emit} - Q_{sub} = 0$$

Equation 6-2

Note that, in general, some heat is always absorbed from the environment since the suit insulation is neither perfectly reflective nor perfectly opaque at infrared wavelengths. However, the MLI is designed to minimize this flux.

Performance predictions for each concept were calculated for lunar surface EVA operations. The metabolic loads are based on Apollo data (Table 6-1). Environment temperatures are based on lunar polar conditions, with the maximum being in sunlight (230 K) and the minimum being in a permanently

71

shadowed crater (40 K) (Heiken et al., 1991). Surface area is approximated to 2.0 m^2 based on an adult

human's skin surface area (Farabee, 2001). (Note: Analyses conducted later revised this estimate to A =

3.43 m^2 for reasons explained in those sections.) For each concept, the radiator surface temperature is

assumed to be equal to the typical mean skin temperature (306 K) (Nunneley, 1970). Spectral emissivity

(tuned to infrared wavelengths, 3-30 μ) is an independent variable between 0.1 and 0.9, the best range

available in current electrochromic technology. Finally, the radiation emitted at wavelengths other than

infrared is factored out of these calculations by applying Planck's blackbody radiation functions,

evaluated at the wavelength boundaries (3-30 μ) and radiator temperature (Moran et al., 2003). View

factors will vary and are not included in this first-order analysis.

Table 6-1: Standard EVA Metabolic Rates (Adapted from NASA, 2006)

	Metabolic Rates (W)		
Operational Environment	Minimum	Nominal	Maximum
μ Gravity (ISS and STS)	169	264	644
Apollo Lunar Surface EVA	144	286	724
Lunar Walkback Test	491	696	880

Preliminary Results

Results from the analyses are presented in accordance with unique considerations for each

concept. For Concept #1, results are presented in terms of what percentage of metabolic heat can be

rejected by the ECD radiators, because this concept includes the bypass option from the main heat

exchanger (Figure 6-8). If radiator capability exceeds 100% of the metabolic input, emissivity should be

reduced to prevent excess heat rejection, which would make the astronaut cold. For radiator capability

less than 100%, the remaining metabolic heat must be bypassed to the sublimator to prevent heat

buildup in the suit. The two environmental extremes being considered represent boundary conditions

72

for the moon's polar regions, but given the consistent solar conditions in these regions, there is little variation in the intermediate range.

The ECD radiators in Concept #1 are generally capable of rejecting 100% of the metabolic heat, except some fraction in the case of hot sink with maximum loading. Operationally, the greater concern is that of rejecting too much heat, as this relatively large radiator surface emits more than 100% of the metabolic heat in most cases. By adjusting the emissivity of the ECD radiators, net heat rejection can be reduced until thermal balance with metabolic input is reached.

Concept #1 Heat Rejection (2 m^2, 40K)

a) Cold Sink with Full Area

Concept #1 Heat Rejection (2 m², 230K)
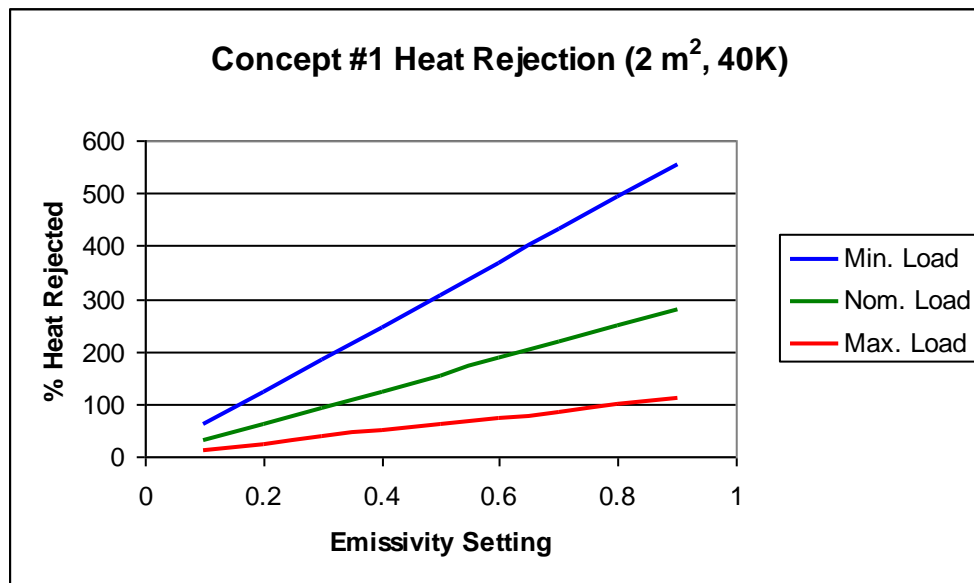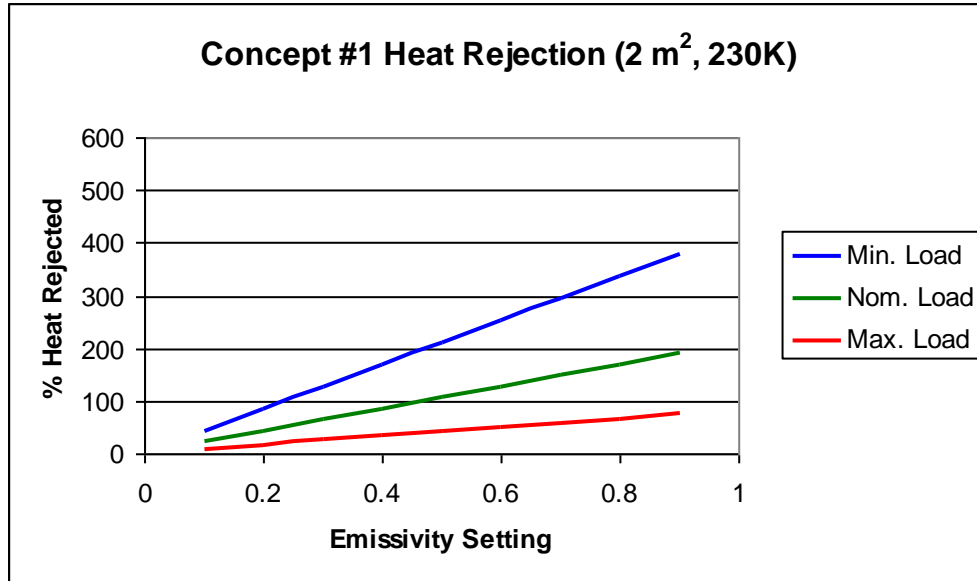
b) Hot Sink with Full Area

Figure 6-8: Results of Concept #1 Analysis

Although these results indicate that a sublimator bypass would only be used in the most adverse case, it may be worthwhile to keep the sublimator as an independent backup system for redundancy. Also note that surface area has a strong influence on these calculations. The same analysis was repeated for a more conservative surface area allowance (Figure 6-9). This reduced area configuration could represent limitations on the suit regions that could be serviced by the additional fluid loop.

With only 1 m² available for ECD radiators, the % Heat Rejected is halved for each metabolic case. Even with this reduced performance, Concept #1 is still capable of rejecting all metabolic heat at minimal and nominal loading. However, maximum loading (and some levels between nominal and maximum) will require partial bypass to the sublimator in either thermal environment, as the configuration cannot reject 100% of the metabolic heat in this case, even with ε = 0.9. When the bypass is being used, the suit is consuming feed water for sublimation, but the rate of water consumption is reduced when compared to the traditional, all-sublimation method.

74
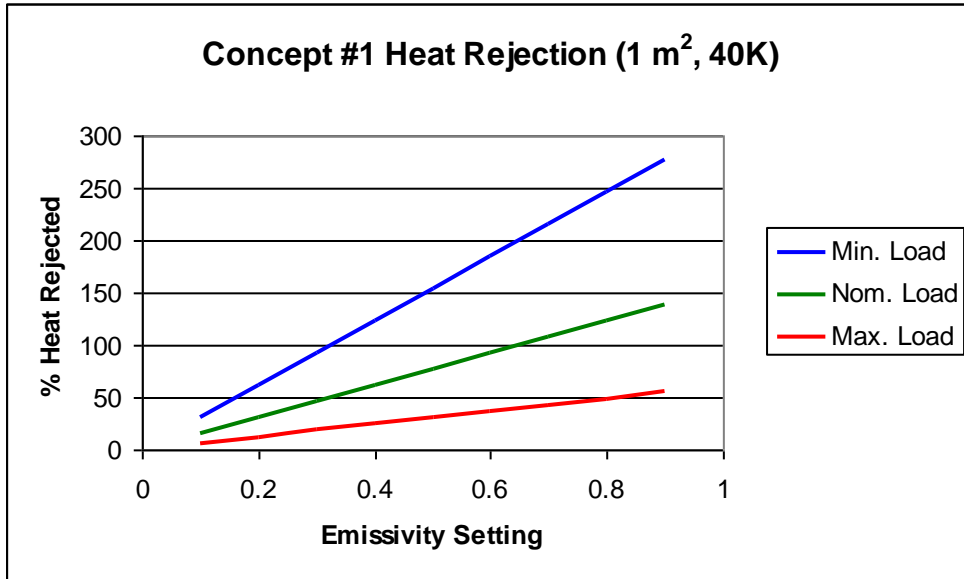
a) Cold Sink with Half Area
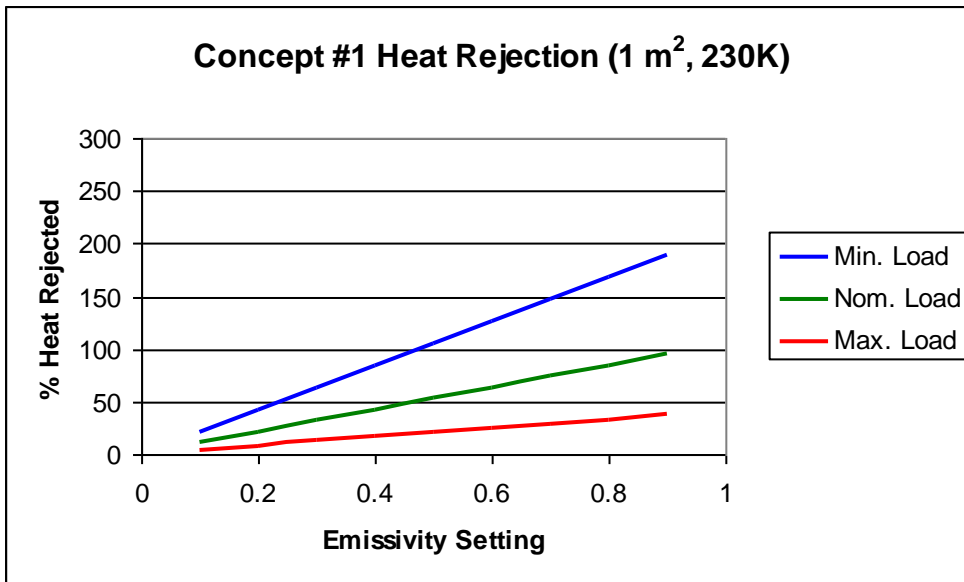
b) Hot Sink with Half Area

Figure 6-9. Reduced-Area Concept #1 Analysis

There is no active bypass to the radiators in Concept #2, so any heat transported to the ECD radiators is convected through the gas ventilation loop. A portion of the heat convection is passed to the radiators, while the remainder continues on to the humidity separators and heat exchanger.

Furthermore, the ventilation loop is only responsible for a portion of the metabolic heat load – the rest is removed by the cooled water tubes in the LCVG. Early studies on EVA suits found that air ventilation can nominally remove metabolic heat up to 176 W. Beyond that level, the effectiveness of convective heat removal tapers off towards a maximum of 234 W. (These limits led to the inclusion of liquid water cooling to increase overall heat removal of the suit, according to Nunneley, 1970.) Of the nominal convective heat transfer, the fraction that can be passed on to the internal radiator surface depends on the temperature difference and the convective coefficient, which depends on a complex array of factors including gas density, flow velocity, turbulence, and characteristic length related to the surface area exposed to the fluid (Çengel, 1997).

For this preliminary analysis, a heat transfer factor of 25% was assumed between the ventilation flow and ECD radiators; this factor is merely an estimate based on the limits of suited gas cooling (Nunneley, 1970) and convective heat transfer to the ECD material due to a relatively small temperature gradient between the skin and ECD radiators. The radiator surface temperature must be lower than skin temperature in order to facilitate any convective heat transfer to the radiators, yet it must be maintained higher than the environmental sink temperature in order to emit, rather than absorb, thermal radiation. Therefore, this analysis assumes a radiator surface temperature of 280 K for Concept #2. Given that this passive configuration can only reject a portion of the metabolic heat, the radiator sizing becomes significant; Figure 6-10 can be used for suit design to determine how much surface area should be allocated for radiators based on mission parameters (expected sink temperature) and available emissivity settings. The required surface area to reject this 25% portion of internal heat load is reduced for high emissivity settings, but with over 3 m^2 available surface area on the exterior of current space suits (Tepper et al., 1991), analytical results shown in Fig. 6-10 indicate that Concept #2 can be implemented even with much lower emissivity settings available. There is no performance-based reason

to use more surface area than is needed to reject the fraction of metabolic heat that can be passively transferred to the radiators (25% in this study).
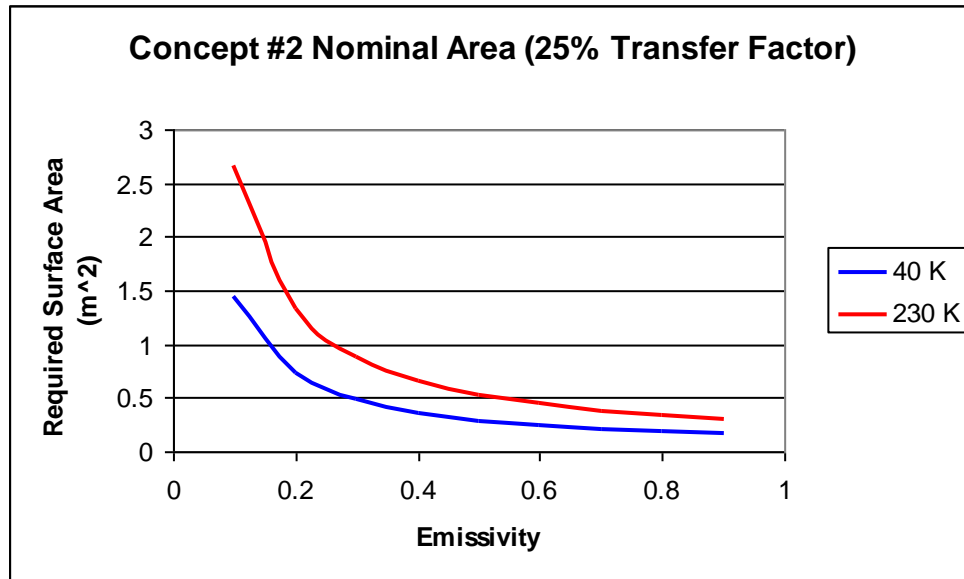
Figure 6-10: Concept #2 Radiator Area for 25% of Nominal Heat Load

The role of variable emissivity in Concept #2 is related to the required surface area curve. Because actual surface area is constant once the suit is designed and built, the ECD radiators in Concept #2 may emit too much heat when metabolic heat generation is below the nominal level. In this scenario, the emissivity can be reduced to achieve the same proportion of radiative heat rejection for a lower amount of metabolic loading.

Concept #3 does not have an LCVG or sublimator, so there is no bypass capability. Without any backup system, the entire metabolic heat load must be rejected by the ECD radiator. Therefore, at least 2 m^2 of radiator surface area is required, as shown in the Concept #1 results. Note that Concept #3 has no heat exchanger fluid loop, so the limitations on placement of ECD radiators around the suit may be less strict.

In order to maintain thermal balance of the suit, the emissivity of the ECD radiators must be carefully adjusted in real-time to ensure that heat rejection equals metabolic heat production. Figure 6-11 shows the optimal emissivity setting for a given metabolic load in two different sink temperatures; for example, an astronaut generating 400 W in the 40 K environment would need ε set to about 0.45 for thermal equilibrium. An increase in metabolic loading would require a proportional increase in emissivity, likely maintained by an automatic control system. Any deviation from these calibration curves will result in the astronaut storing or losing internal body heat, which can lead to sweating, shivering, hyperthermia, or hypothermia.

Concept #3 Performance
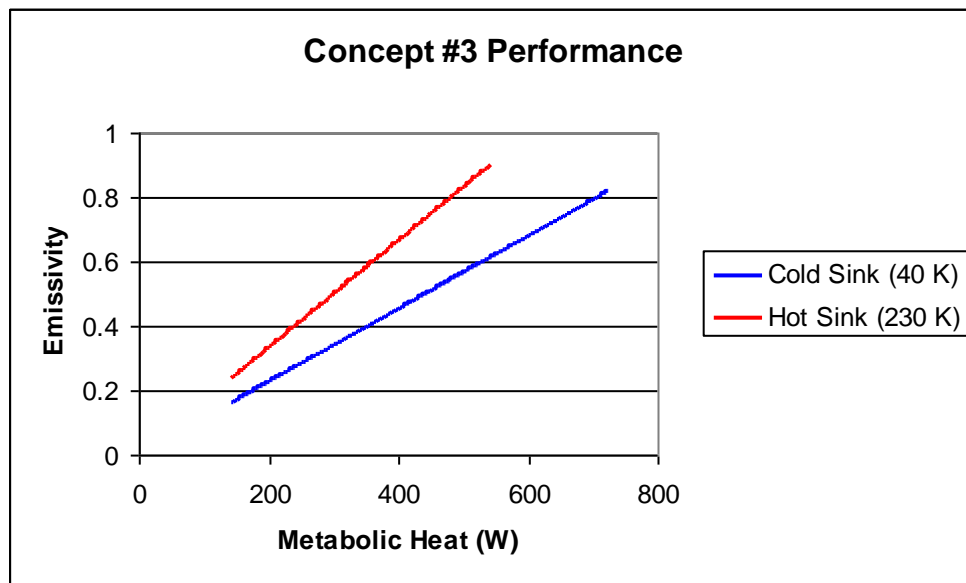
Figure 6-11: Electrochromic Radiator Calibration for Concept #3

One important note about all these results are that they assume the entire bank of ECD radiators is being tuned to the same emissivity. With parallel controllers, it is possible to fine-tune the radiators so that different surfaces on the suit are emitting different amounts of heat. Because this level

of resolution is coincident with view factors, surface contamination, and other complex considerations, it should be examined in a future study.

It should also be noted that the lunar polar regions are particularly well suited to radiator performance for the given conditions. The environment temperature never exceeds skin/radiator temperature, so the radiators are always emitting heat. This would likely be a problem with traditional radiators, leading to shut-down features, freezability concerns, etc. With ECD radiators, the "favorable" temperature gradient is more easily handled by turning down the emissivity when too much heat is being rejected.

There are many EVA environments (low Earth orbit, lunar equatorial regions, Mars) where the environmental temperatures frequently exceed 306 K. In these conditions, the ECD radiators can sometimes absorb heat from the hotter environment. Although this effect can be regulated by adjusting emissivity (and it may sometimes even be desirable), the radiators cannot reject metabolic heat in adversely hot thermal conditions. Solutions to this problem may include more complex thermal management to increase radiator temperature, using a sublimator or evaporator via bypass feature, and/or operational planning to avoid hot conditions. The aforementioned granularity of ECD radiator control may also be used to direct heat rejection towards colder parts of the environment while simultaneously minimizing heat absorption from the hotter surrounding areas.

Conclusion

Three concepts have been proposed for integrating electrochromic radiators into an EVA suit for no-consumables or reduced-consumables rejection of metabolic heat loads. These concepts offer different approaches to supplementing or replacing traditional heat removal and rejection technology. Each concept has been analyzed for heat rejection capability under specified ranges, radiator sizing needs, and/or emissivity tuning requirements. Future work will include more complex thermodynamic

analyses (including studies in less favorable environments), thermal vacuum testing with infrared ECD samples, and a system-level trade analysis comparing this solution to the traditional sublimator and other candidate technologies.

Resulting Publications and Presentations:

Metts, Jonathan G. and Klaus, David M., "Conceptual Analysis of Electrochromic Radiators for Space Suits", SAE Paper No. 2009-01-2570, 39th International Conference on Environmental Systems, Savannah, GA, July 2009.

"Conceptual Analysis of Electrochromic Radiators for Space Suits", presentation at 39th International Conference on Environmental Systems, Savannah, GA, 16 July 2009.

Chapter 7 – Equivalent System Mass Analysis for Space Suit Thermal Control

Introduction

Engineering and system design often require selecting a technology solution from an array of candidates. Even an objective selection process can be complex in the case of integrated systems like those in human spacecraft. This study presents a systems-level trade study to compare competing technologies for space suit heat rejection. The field of candidates includes diverse technologies that cannot be directly compared due to having highly varied approaches to solving the problem. In order to compare performance, costs, and other selection criteria, a methodology termed Equivalent System Mass (ESM) can be applied; however, there are limitations and special considerations for this approach, and these will be noted (Drysdale, 2003).

Extravehicular activity (EVA) suits must reject heat to the outside environment in order to maintain thermal equilibrium and a safe internal temperature for the crew member. Heat sources include the crew member's metabolic activity, electronic/mechanical/chemical systems in the suit, and absorbed external heat. Since the Apollo program, both American and Russian space suits have rejected heat from these combined sources via water sublimation. Heat is collected by the Liquid Cooling & Ventilation Garment (LCVG) and transported to a heat exchanger in the Portable Life Support System (PLSS) backpack. Water from a separate feed water tank is supplied to a porous metal plate that is exposed to the cold vacuum of space, where it forms a thin sheet of ice. Collected heat is transferred from the heat exchanger to this plate, causing the ice sheet to sublimate directly to vapor and drift away from the suit. The unwanted heat is carried with the water as latent heat of vaporization. Since this is an open-loop process, feed water for heat rejection is a limited consumable that must be recharged between missions or mid-EVA with an umbilical connection to the nearby spacecraft.

Various studies have identified problems with the sublimator approach, particularly as human exploration missions turn to longer-term lunar bases and Mars expeditions. These problems include the high launch cost for consumable water beyond low Earth orbit (Nabity et al., 2007; Nabity et al., 2008; Jones, 2009), logistical difficulty of replenishing consumable water, water vapor contamination of windows and other spacecraft surfaces, unintended torques and impulses from water vapor evacuation, sublimator contamination due to feed water impurities (Leimkuehler & Stephan, 2008), and the inability to sublimate water in the Mars atmosphere (Bue et al., 2009). A number of alternate technologies have been developed or proposed to address these problems. As NASA and private space companies develop new space suits for the next phases of human space exploration, there is a need to evaluate these competing technologies and accurately compare them to the existing baseline.

Background

As a method for comparison, Equivalent System Mass (ESM) analysis is a form of trade study in which disparate performance characteristics and specifications are converted to a unified, quantifiable metric that is easily compared among multiple candidates that may be extremely diverse and otherwise difficult to evaluate in a traditional trade study (Drysdale, 2003).

The central idea of ESM is based on the principle that spacecraft are propelled by launch vehicles with finite payload mass capability. All else being equal, reducing the mass of a spacecraft (or any of its subsystems or components) either increases total propulsion capability, opens up an overall mass margin that can be used to launch additional payload, or in some cases allows for the use of a smaller, less expensive launch vehicle. The ESM methodology involves applying "infrastructure costs" to convert volume, power, cooling, and even crew time into units of mass, which are then added to the actual system mass and any consumable mass to obtain the total ESM value for a particular candidate ().

Infrastructure costs, which are published and updated periodically in NASA's Basic Values and Assumptions Document (BVAD), depend heavily on mission destination, launch vehicle, power generation efficiency, system cooling efficiency, etc. For example, a mission to Mars utilizing solar panels would have higher infrastructure costs for power requirements than a similar mission to the Moon, because less solar power can be generated near Mars than at the Moon.

The ever-changing nature of infrastructure costs means that ESM analysis does not represent a fixed evaluation outcome, rather a thorough comparison of technologies based on the best available information at the time. Furthermore, since ESM analysis often involves advanced technologies that may not be fully tested or characterized, all assumptions must be clearly documented and referenced to the best available sources. Over time, the results of an ESM analysis may change if repeated with updated specifications, performance data, and/or infrastructure costs (Levri & Drysdale, 2003).

Analytical Methods

A set of diverse space suit cooling technologies were selected for comparison with the legacy system and each other. All of the candidates included in this analysis are being developed or have been developed in conjunction with NASA and/or with some level of funding support from NASA.

"Sublimator" is the legacy system, an on-demand ice sublimator connected directly to the PLSS heat exchanger with heat distribution provided by the LCVG (Nunneley, 1970; Kuznetz, 1975; Pisacane et al., 2006). This technology has the benefit of high reliability and hundreds of successful flight operations to prove its viability (Tongue & Dingell, 1999; Anderson et al., 2006; Leimkuehler & Stephan, 2008). Dry mass and volume are relatively low, but the sublimator consumes water proportional to the heat load rejected. The consumable mass and volume inputs are based on nominal metabolic activity over an 8-hour lunar EVA and include offsets for recovered condensate that is provided directly to the

sublimator as a supplement to the feed tank (NASA, 1998). Crew time is estimated at 0.5 hours for feed tank water to be recharged, either between or during EVAs.

"SWME" is the Space Suit Water Membrane Evaporator, NASA's state-of-the-art successor to the sublimator. Warm water from the LCVG is passed through a membrane that is exposed to cold vacuum; the membrane allows vapor but not liquid to pass through (Bue et al., 2009). SWME is also functional in higher atmospheric pressure such as that found on Mars. The evaporator unit is made of lighter materials than the sublimator, and the internal fluid lines and tankage are reduced because SWME is more tolerant to contaminated water and thus is more directly integrated with existing water loops in the suit (Sompayrac et al., 2009). However, consumption rates are higher due to the less efficient phase change (evaporation vs. sublimation). Crew time for water recharge should be similar to the sublimator.

"Ashwin ECD" and "Eclipse ECD" are two variants of an electrochromic suit radiator, with different electrochromic materials produced by Ashwin-Ushas Corp. and Eclipse Energy Systems, respectively, and both are assumed to be attached to flexible Kapton substrates (Bessiere et al., 2002; Kislov et al., 2003). Based on previous studies (Metts & Klaus, 2009; Metts et al., 2010), we assume that electrochromic radiators will span virtually the entire available surface area of the space suit in order to provide optimal heat rejection performance. This approach is entirely closed-loop because radiators reject heat without mass consumables. Although both electrochromic technologies are relatively thin and lightweight (Demiryont et al., 2009; Ashwin-Ushas, 2010; Eclipse Energy, 2010), they must be supported by some method of distributing heat to the radiator surfaces. There are multiple concepts for addressing this problem (Metts & Klaus, 2009), but for the sake of the ESM analysis, we assume there will be an additional fluid loop similar in size and weight to the existing LCVG to transport the internal heat load from the PLSS heat exchanger to the electrochromic radiator panels. If the LCVG is like a network of veins, collecting heat and transporting it to the centralized PLSS heat exchanger, the radiator

fluid loop is analogous to a network of arteries, transporting heat back out of the PLSS heat exchanger and distributing it to the array of electrochromic radiator surfaces across the suit.

"Combined ECD/Sub" refers to a configuration in which primary cooling is provided by one of the electrochromic technologies described above (properties averaged when different between the two manufacturers), with supplementary/backup cooling provided by a sublimator. While the dry system mass and volume is higher with this approach than for the individual technologies, performance and reliability are more robust due to the use of dissimilar redundant systems. The consumable water inputs are based on an assumption that 30% of the internal heat load will be rejected via sublimator, based on a study of hypothetical radiator impact on Apollo EVAs (Metts & Klaus, 2010). The sublimator is activated either because the radiator capacity has been exceeded or because the radiator is unable to reject heat at all due to excessively hot conditions (environmental sink temperature is greater than radiator surface temperature). This combined approach is more practical in a larger range of EVA environments than electrochromics alone, and it consumes significantly less water than the sublimator alone. Estimated crew time of 0.15 hours to recharge the feed tank is proportional to the reduced water consumption as compared to the standalone sublimator.

"Sub-Cooled PCM" is a phase-change material concept utilizing fixed-mass packs of ice, cooled below the freezing point of water. When connected to the PLSS heat exchanger, the internal heat load is absorbed by the ice, first as sensible heat (to raise the temperature to the freezing point) and then as latent heat of fusion as the ice becomes liquid water (Leimkuehler et al., 2009). Because no water is allowed to escape the SPCM packs, the unwanted heat is effectively stored throughout the EVA. When no solid ice remains, or the EVA is complete, the crew member detaches the portable SPCM unit and places it in an exterior radiator unit to regenerate (refreeze) the ice packs between EVAs. While this process consumes no mass, the system mass and volume are relatively high due to the amount of water/ice required to enable an 8-hour EVA. The baseline design calls for SPCM packs to be sized for 4

hours per pack in order to reduce on-back mass and volume, with mid-EVA switching to allow for extension up to the full 8 hours. In the current analysis, the mass and volume of the regeneration equipment is excluded on the assumption that the SPCM packs will interface with existing vehicle (lander, habitat, or rover) radiators. If the vehicle uses sublimation/evaporation instead of radiators, there would be an associated consumable mass and volume cost added to the ESM inputs for this technology. Crew time of 0.5 hours is estimated for switching ice packs and connecting used packs to the regeneration equipment.

"Absorber/Radiator" refers to a closed-loop EVA cooling concept by Creare, Inc. that includes an evaporative cooling garment (ECG, replacing the LCVG), a bed of vapor-absorption material, and a backpack-mounted radiator panel (Izenson et al, 2009). Cool water is pumped through the ECG and across the crew member's skin, where the metabolic heat load causes the water to evaporate through the porous ECG material and be collected in the PLSS. A heat exchanger and vapor pump supply the hot water vapor to a bed of anhydrous LiCl that is capable of absorbing and storing the vapor. During the EVA, an adjacent radiator panel mounted on the PLSS backpack continuously rejects a portion of the stored heat, causing some (though not all) of the absorbed vapor to cool and return to the ECG liquid water loop. This process allows for a relatively high radiator surface temperature (compared to the electrochromic radiators), which results in better cooling performance for a smaller radiator surface (Sompayrac et al., 2009). However, the radiator performance is still less than the nominal heat load, so the absorption bed eventually becomes saturated with water vapor over the course of an EVA. The system is regenerated between EVAs by storing the absorber/radiator apparatus (if not the entire PLSS) outside the crew vehicle, thus allowing stored heat to radiate over time and returning the water vapor to its liquid phase.

Equivalent System Mass analysis provides a method to compare these diverse technologies. The formulation of ESM is given in Eq. 7-1, adapted from Levri et al. (2000), which gives results in units of mass.

$$ESM = M_s + \gamma_V V_s + (M_c + \gamma_V V_c + \gamma_P P + \gamma_t t) * N$$

<div align="right">Equation 7-1</div>

M_s and V_s are the system mass and volume, also known as dry mass/volume, which are not consumed per use of the system. M_c and V_c are the mass and volume of consumables required per EVA. P is the power required per EVA to operate the heat rejection system. t is the crew time required per EVA for operation and maintenance of the heat rejection system. N is the number of standard, 8-hour EVAs to be performed during the mission, which is baselined at 16 for 2-week lunar sortie missions and 160 for the lunar outpost concept (NASA, 2006). γ_x represents infrastructure cost, in units of kg/m^3, kg/kW, etc. that allows non-mass parameters to be converted into equivalent mass and then added to the actual masses. Infrastructure costs are evaluated by NASA according to current baselines for launch vehicles, spacecraft, and supporting equipment. They are also specific to location, since the relative cost to launch a unit of mass to low Earth orbit is less than to the moon, and both of those are less than to Mars. Infrastructure costs depend strongly on mission architectures and are updated in the Basic Values and Assumptions Document (BVAD) every few years. The infrastructure costs used in this study are based on NASA's current design reference missions and the Constellation vehicle architecture and are summarized in Table 7-1.

<div align="center">Table 7-1: Applicable Infrastructure Costs for Lunar Missions (BVAD, 2010; with permission)</div>

Infrastructure Costs for Lunar EVA		Units
γ_V (Volume)	80.8	(kg/m^3)
γ_P (Power)	0.136	(kg/W)
γ_t (Crew Time)	6.09	(kg/hr)

Each candidate technology described above has been sized for 100% rejection of the internal heat load for a single, typical 8-hour lunar surface EVA; internal heat load is assumed to consist of the nominal metabolic rate from Apollo data (286 W) plus a constant PLSS heat load of 120 W (Sompayrac et al., 2009). All crew times are estimates based on available information on the operation of these technologies. For candidates requiring regeneration between uses, this analysis assumes that full regeneration is possible between successive EVAs; i.e., no additional hardware units are required to maintain the nominal EVA schedule. A literature review was conducted for each candidate to determine the most accurate and up-to-date quantitative data for inclusion in the ESM formulation, and the principle investigators (or corresponding authors) of each technology were contacted for confirmation and updates to the quantitative data. The data summarized in Table 7-2 represent the most accurate and up-to-date information about these technologies as of this writing.

Table 7-2: ESM Analysis Inputs with Consumables and Crew Time per EVA

Technology	Dry Mass (kg)	Dry Volume (m^3)	Con. Mass (kg)	Con. Volume (m^3)	Power (W)	Crew Time (hr)
Sublimator	3.38	0.00203	4.57	0.00459	0	0.5
SWME	1.59	0.00205	6.35	0.00638	0	0.5
Ashwin ECD	5.669	0.003659	0	0	0.08	0
Eclipse ECD	3.626	0.003659	0	0	3.43	0
Combined ECD/Sub	9.049	0.005689	1.371	0.0006885	1.755	0.15
Sub-Cooled PCM	60	0.03186	0	0	0	0.5
Absorber/Radiator	7.1	0.0147	0	0	0	0.5

One aspect of these technologies not expressed in the ESM metric is maturity. NASA uses a standard scale called Technology Readiness Level (TRL) to define the maturity of developing technologies. Table 7-3 provides descriptions of each TRL ranking, adapted from Mankins (1995).

Technology procurement guidelines often require TRL ≥ 6 components and subsystems, due to the cost and technical difficulty of increasing TRL within the span of a given system's development.

Table 7-3: Technology Readiness Level Definitions (Mankins, 1995)

TRL 1	Basic principles observed and reported
TRL 2	Technology concept and/or application formulated
TRL 3	Analytical and experimental critical function and/or characteristic proof-of-concept
TRL 4	Component and/or breadboard validation in laboratory environment
TRL 5	Component and/or breadboard validation in relevant environment
TRL 6	System/subsystem model or prototype demonstration in a relevant environment (ground or space)
TRL 7	System prototype demonstration in a space environment
TRL 8	Actual system completed and "flight qualified" through test and demonstration (ground or space)
TRL 9	Actual system "flight proven" through successful Mission operations

Results

A summary of results from the ESM analysis is presented in Table 7-4 (candidates with lower ESM values trade better). Due to the formula's dependency on usage rate, which is tied to mission duration, a two-dimensional plot of ESM values vs. number of EVAs is presented in Figure 7-1. A "break point" between any two technologies can be defined as the intersection on this plot, representing the number of EVAs at which one technology's ESM value begins to exceed that of the other. In other words, it is the design point at which short-term and long-term costs are equal. An estimated TRL value for each candidate technology is also included in the table to provide additional information that is not a factor in the ESM calculation but must be considered in a comprehensive trade study. The ESM results do not quantifiably account for the maturity (TRL) or reliability of the various candidate technologies. Immature technologies generally require more funding and time for development and testing before they can be considered acceptable as flight hardware. Less reliable (i.e more complex or less fault-tolerant)

hardware may require additional back-up parts and systems, while any required maintenance will impact crew time.

Table 7-4: Equivalent System Mass Results for Lunar EVA Cooling Technologies. Results are for 1 EVA, a Lunar Sortie mission (16 EVAs), and a Lunar Outpost mission (160 EVAs); lower ESM values trade best.

EVA Suit Cooling Technology	TRL	ESM (kg)		
		1 EVA	16 EVAs	160 EVAs
Sublimator (Legacy)	9	11.53	131.32	1281.28
Spacesuit Water Membrane Evaporator	6	11.67	160.32	1587.44
Ashwin Electrochromic Radiator	4	5.98	5.98	5.98
Eclipse Electrochromic Radiator	4	4.39	4.39	4.39
Combined EC Radiator/Sublimator	3	11.12	47.06	392.05
Sub-Cooled Phase Change Material	4	65.62	111.29	549.77
Creare LiCl Evaporative Absorber/Radiator	5	11.33	57.01	495.49
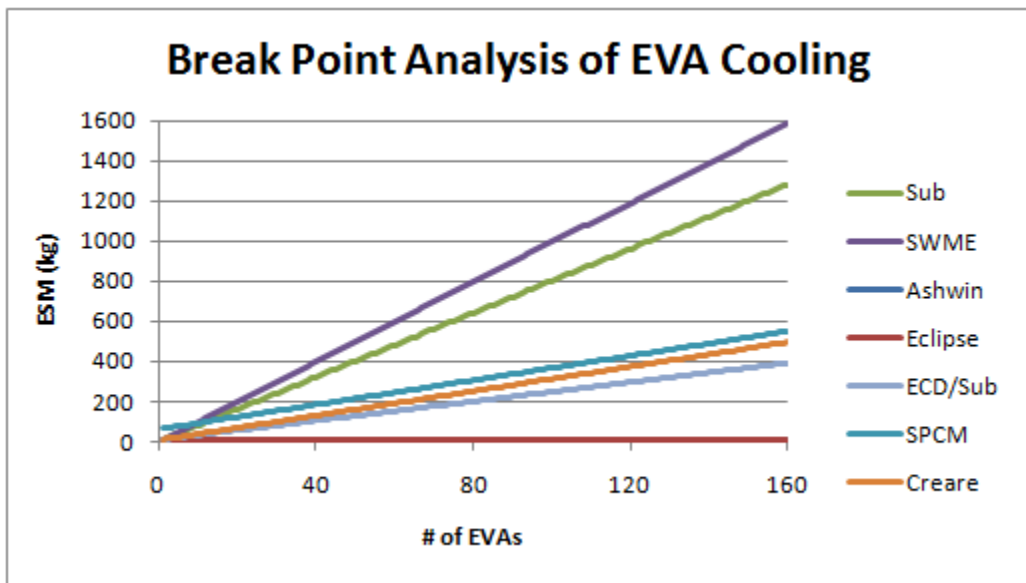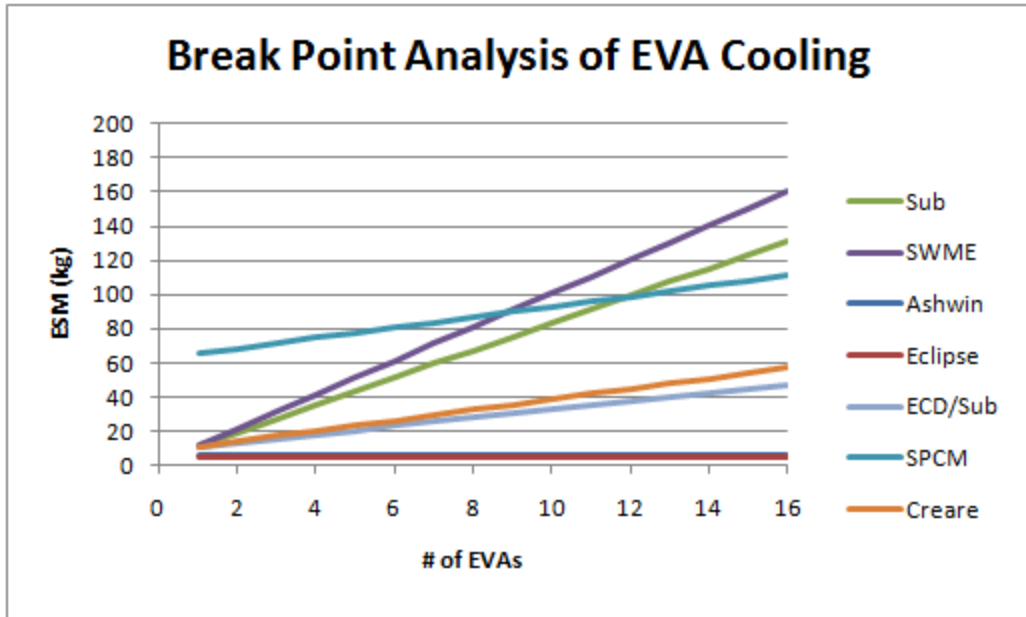
Figure 7-1: Equivalent System Mass Results for EVA Cooling Technologies. Results shown as function of

number of EVAs for a Lunar Sortie mission (top) and Lunar Outpost mission (bottom).

Based on the ESM results, the maximum break point for all of the non-venting technologies to

surpass the sublimator or SWME is 12 EVAs. This number is less than the baseline of 16 EVAs for NASA's

lunar sortie missions. Beyond this break point, non-venting technologies become more desirable as

additional EVAs are performed per mission. The Creare absorber/radiator concept and all of the electrochromic radiator options result in ESM values superior to the venting technologies within a single EVA, indicating these technologies may be more desirable regardless of how many EVAs are planned.

Note that ESM values for the Ashwin and Eclipse electrochromic radiator concepts appear to be constant with respect to the number of EVAs. This result is due to the minimal recurring costs for these technologies. Although electrochromic radiators are associated with some power consumption, the infrastructure costs for lunar EVA (Table 7-1) convert the power consumption for these radiator candidates into negligible recurring ESM relative to other factors. For a different mission, such as to the Mars surface, the capability to provide electrical power on a recurring basis may be much more difficult and expensive, which would be reflected in a different set of infrastructure costs. Also, there is no crew time anticipated for nominal operation of these electrochromic radiator concepts. This assumption may be revised to include maintenance tasks (e.g., cleaning dust from the suit exterior to prevent thermal interference and mechanical abrasion of radiator surfaces) that would be reflected in an updated ESM analysis. The unusual result above, a nearly constant ESM value, is likely to change as more realistic data replaces assumptions about the radiator options. Moreover, the thermal performance boundaries of radiator cooling (Metts et al., 2010; Metts & Klaus, 2010) mean that the approach of combining a sublimator or evaporator with one of these electrochromic radiator technologies will enable a much broader range of lunar environments for EVA. This robustness may trump lower ESM values in a comprehensive trade study.

Conclusions

By design, ESM is a reductive form of analysis. There are a number of important factors, including some qualitative, that are not captured in this type of analysis. For instance, while the

92

electrochromic-only options clearly have lower ESM in the long-term, the combination electrochromic/sublimator option is more robust and enables a broader range of mission environments. A complete trade study involves consideration of many such factors and requires far more detailed knowledge of the mission, vehicle, EVA suit, and concept of operations than is currently available. The ESM results indicate that the non-venting technologies in the study are preferable to the legacy Sublimator or SWME successor if at least 12 EVAs, in some cases fewer, are planned for the mission.

This ESM analysis represents a snapshot of various technologies as they exist today. As these candidates are further developed, the ESM input quantities may change significantly. Furthermore, infrastructure costs can and do change over time as NASA's standard mission architectures and design reference missions are redefined. Analyses similar to this one should be performed frequently so as to provide updated results and to include additional candidate technologies as necessary.

Resulting Publications and Presentations:

Metts, Jonathan G. and Klaus, David M., "Equivalent System Mass Analysis for Space Suit Thermal Control", abstract submitted to the 41st Annual International Conference on Environmental Systems, Portland, OR, July 2011.

Chapter 8 – Bench-Top Testing of Electrochromic Radiator Material Performance

Abstract

A bench-top method was devised for testing electrochromic radiator to determine cooling performance under ambient environmental conditions. Prototype electrochromic devices were evaluated with each trial differentiated by the device's emissivity setting, which was controlled by an applied voltage. Cooling time results are presented for the extreme light (minimum emissivity) and dark (maximum emissivity) states. An iterative analytical method was used to estimate emissivity of the test article based on correlation of empirical data to analytical methods. The results demonstrate the effectiveness and limitations of the bench-top radiator experiment. The methodology combines experimental and analytical techniques that are uniquely applicable to variable emissivity devices such as electrochromic materials. Future improvements in test methodology and equipment are suggested.

Introduction

Electrochromic materials are being evaluated as a potential technology for enabling flexible, adaptive radiators that can be integrated into a space suit cooling system. These materials have controllable optical properties, including emissivity, that change when a small voltage is applied. Previous work examined the theoretical feasibility and explored design concepts for implementation in current and future space suits (Metts & Klaus, 2009). Rigorous testing is needed, however, to establish practical performance data for electrochromic radiators. Thermal vacuum chambers are typically used to simulate a space environment, but these facilities are complex and expensive to operate. This current work establishes a bench-top experimental methodology for characterizing electrochromic radiator properties that produces limited, but useful performance data without the need for a strictly controlled

environment. The bench-top experiment is easy to set up and requires much less time per trial than thermal vacuum testing, with modifications readily made to the sensor arrangement and/or test samples between runs.

Background

The experiment described in this report is loosely based on a prior study conducted by Eclipse Thin Films, in which that company's electrochromic devices were exposed to the space environment aboard the MidSTAR-1 satellite (Shannon et al., 2008). Because orbital experiments are even more expensive and complex than thermal vacuum testing, an ambient bench-top analogue was developed to evaluate similar results with much simpler equipment. Also, the transient nature of the test means that strict environmental control is not required to produce useful results.

In a bench-top environment (i.e., exposed to normal atmospheric conditions), convective cooling is typically the dominant means of heat transfer, while this process is obviously not present in thermal vacuum testing or an actual space environment. However, since free convection is a function of surface area and various environmental parameters that can be held constant with thermostat-based controls, any differences observed in cooling rate (indicated by a change in radiator temperature) can be attributed to radiative emission power. Therefore, differences in cooling time are directly related to emissivity modulation, and analytical methods can be used to estimate the emissivity of each state.

Experimental Methods

Electrochromic devices (ECD) used in this study consist of a stack of variable emissivity thin films deposited on a flexible polyethylene terephthalate (PET) substrate. The optical properties are modulated by applying a small voltage across the electrochromic surface and outer substrate, which

have independent conductive layers. Changes in emissivity are persistent and reversible. The devices used in this study are commercial prototypes, so the performance data produced is intended to evaluate the test procedure and should not be considered representative of the final product capabilities.

An ECD was affixed to a plate of polished aluminum (6061 alloy), which itself has a very low emissivity rating of approximately ε = 0.1. Aluminum was chosen because it radiates very little heat, so the vast majority of any radiative cooling observed is due only to the ECD itself. A thermocouple (TC) was affixed between the plate and ECD to measure surface temperature without blocking any visible surface area of the ECD. Electrical leads were attached to the ECD to allow emissivity control without the need to physically touch the device during the experiment. A variable DC power supply was used to apply the voltage for emissivity modulation. The ECD and aluminum plate were placed on a block of melamine foam to minimize heat conduction to the countertop below. A 65 W incandescent lamp was positioned directly above the test sample as the heat supply. Finally, a second thermocouple was suspended near the center of the laboratory to measure room temperature. Temperature measurements were routed through National Instruments DAQ hardware to be monitored and recorded using LabVIEW. The experiment sample setup is shown in Fig. 8-1, and a flow chart of the general data collection scheme is shown in Fig. 8-2 (heat flux sensors were not used in this experimental setup, as they only measure conductive heat transfer). Note that these tests were performed in Boulder, Colorado at an elevation of approximately 5,400 feet (1650 meters) above sea level, and therefore at ~80% of standard atmospheric pressure.
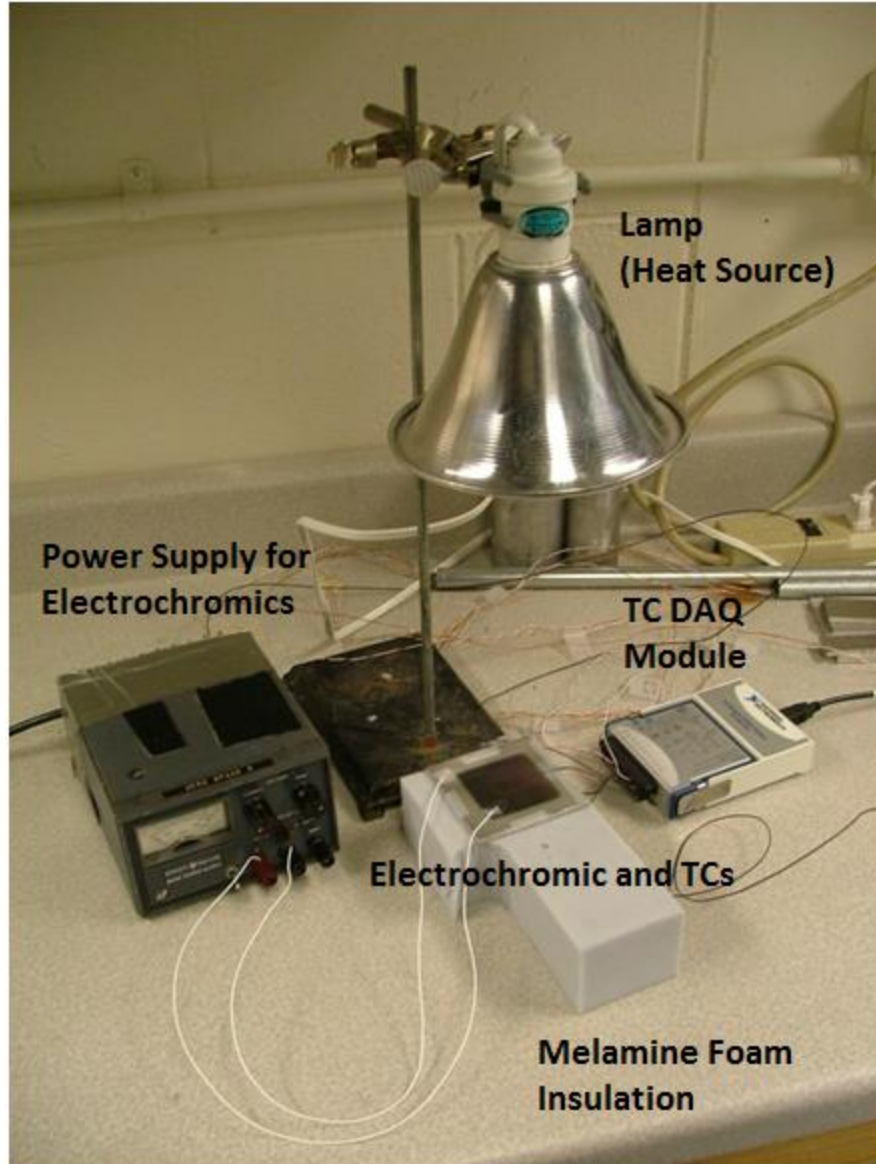
Figure 8-1: Bench-Top Cooling Experiment Setup. Components include electrochromic device, aluminum plate, melamine foam, heat lamp, power supply, and data acquisition module.
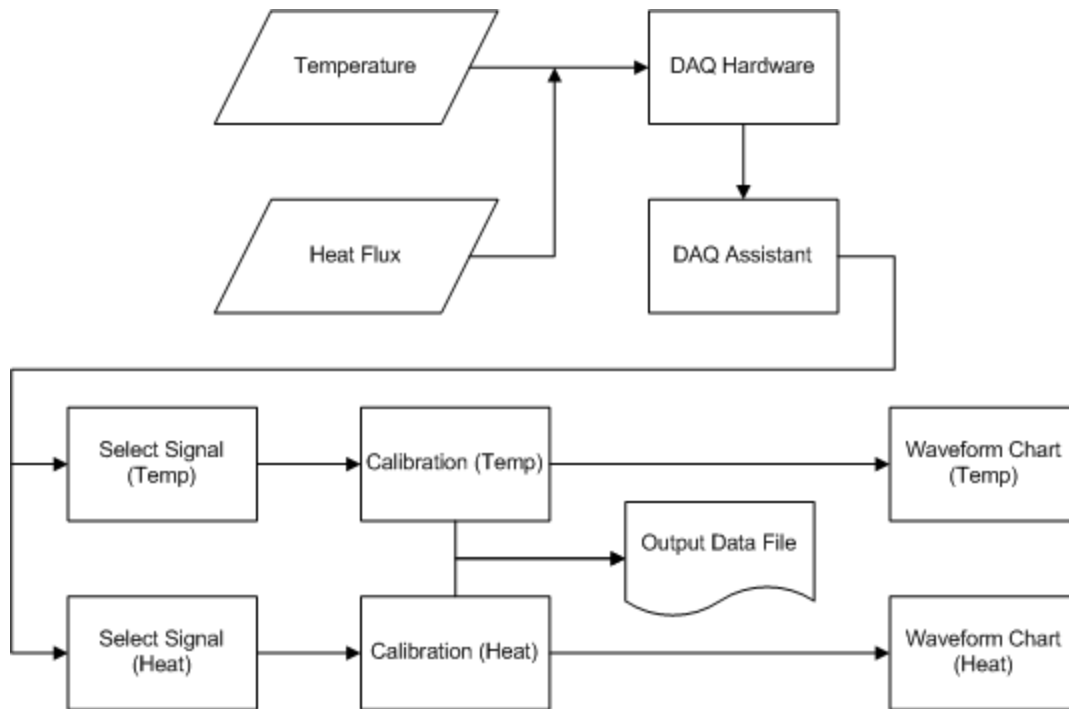
Figure 8-2: Data Acquisition Program Flow Chart

For each experiment, the ECD was powered to a specified emissivity state per the
manufacturer's instructions. After allowing 2-3 minutes for complete state transition, data recording
was begun and the heat lamp turned on. The ECD surface temperature was allowed to increase from
approximately 25 C (room temperature) to 60 C. At this point, the lamp was turned off. Data continued
to be recorded as the ECD surface cooled from 60 C to 30 C, at which point the trial was complete. The
ECD state was changed between light and dark, as shown in Figure 8-3, for each subsequent trial until at
least 3 trials in each state were completed.
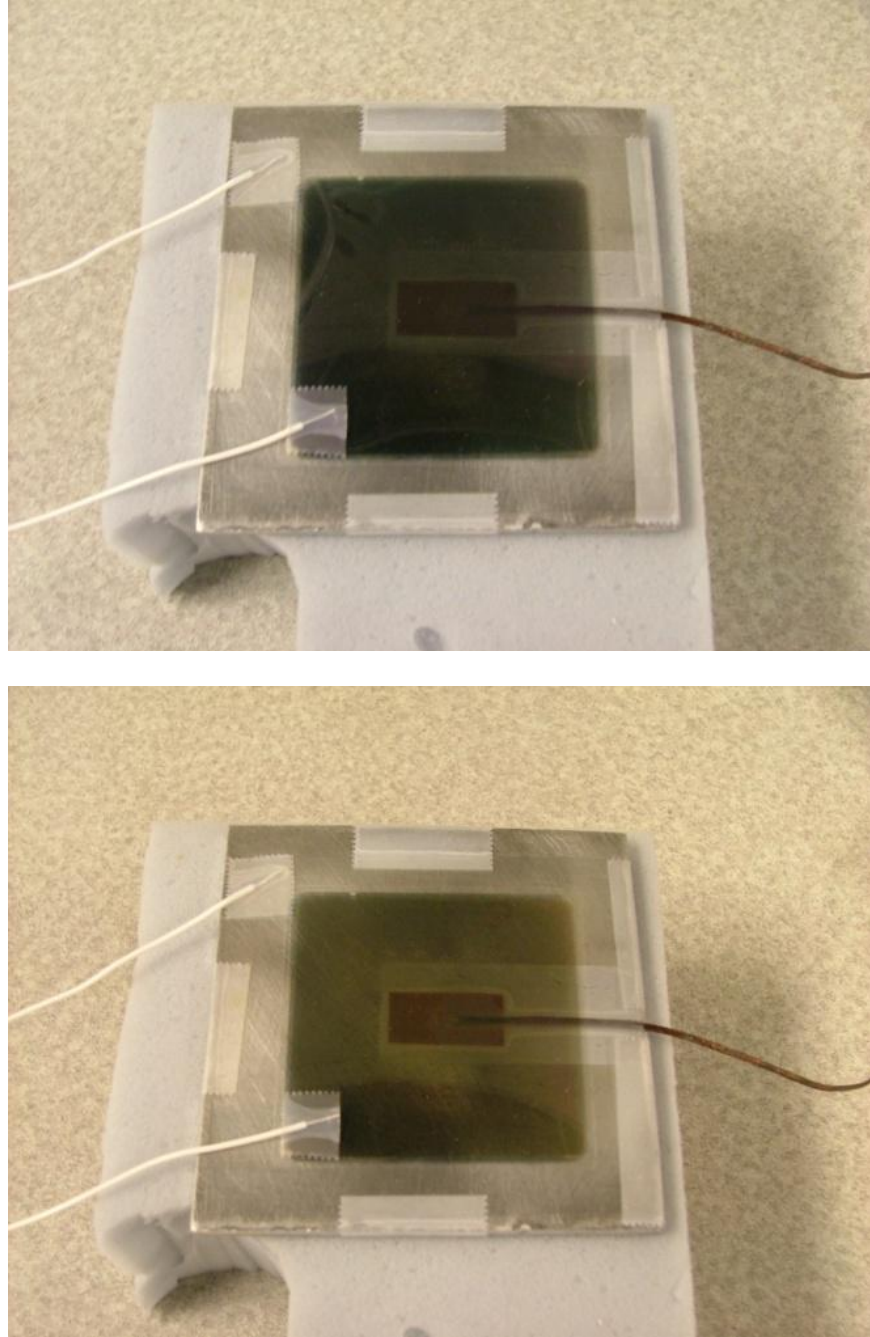
Figure 8-3: Electrochromic device in dark state (top) and light state (bottom).

Analytical Methods

  The goal of the above experiment was to demonstrate a difference in cooling time between two electrochromic states, with all other variables held constant. Cooling in the bench-top environment is

dominated by free convection, as modeled by a differential form of Newton's Law of Cooling (Incropera et al., 2007):

$$q_c = h_c A_s (T_s - T_e)$$

<div align="right">Equation 8-1</div>

$$h_c = \frac{pk Nu_L}{A_s}$$

<div align="right">Equation 8-2</div>

In Equations 8-1 and 8-2 , q_c (in Watts) is convective heat transfer, h_c is the heat transfer coefficient, A_s is total surface area of the test sample, T_s is the surface temperature, T_e is the environment (sink) temperature, p is perimeter, k is the conductivity of air, and Nu_L is the non-dimensional Nusselt number for quiescent air for the characteristic length (already included as a ratio between perimeter and surface area). Evaluation of the Nusselt number depends on the orientation of the hot surface (Incropera et al., 2007); in this case, it is calculated as:

$$Nu_L = 0.54 Ra_L^{1/4} \ \ (\text{when } 10^4 \leq Ra_L \leq 10^7)$$

<div align="right">Equation 8-3</div>

The non-dimensional Rayleigh number, Ra_L, is based on gravitational acceleration, film temperature, viscosity, and other constant environmental factors. In a sufficiently large room with environmental control, only T_s varies with time as the surface cools.

The secondary effect of thermal radiation (q_r in Watts) is relatively more pronounced at higher temperatures due to the fourth-order Stefan-Boltzmann equation (Incropera et al., 2007):

$$q_r = \sigma(\varepsilon_1 A_1 + \varepsilon_2 A_2)(T_s^4 - T_e^4)$$

<div align="right">Equation 8-4</div>

In Eq. 8-4, σ = 5.67 x 10^{-8} W/m^2/K^4 is the Stefan-Boltzmann constant. The test sample has mixed surface properties; the outer conductive layer of the ECD is transparent, so the emissivity (ε_1) for that surface is equal to that of the underlying polished aluminum (a known reference value). The electrochromic surface emissivity (ε_2) is a controlled variable that is held constant during each trial.

Conduction from the underlying aluminum to the test structure is negligible due to the use of melamine foam as an insulating support material. Other surfaces are surrounded by air, which is likewise an excellent insulator. To model transient heat transfer from convection and radiation together, instantaneous thermal energy is differentiated in the form (Incropera et al., 2007):

$$q = \frac{dE}{dt} = mC\frac{dT_s}{dt} = q_c + q_r$$

<div align="right">Equation 8-5</div>

In Eq. 8-5, total heat transfer (q in Watts) is the derivative with respect to time of total thermal energy (E in Joules), m is the mass of the test sample, and C is specific heat of the test sample, approximated by the reference value for the aluminum plate, as the electrochromic device and other materials have relatively little mass. This equation is solved for dt and numerically integrated, using the experimental temperature data as the step size. This approach makes it possible to predict the time required to cool from one temperature reading to the next, and directly compare that analytical result to the experimental cooling time. By iteratively changing the electrochromic emissivity value (ε_2) until the analytical prediction converges to experimental data, the effective emissivity of the ECD surface can be estimated. Input parameters for the bench-top electrochromic test are shown in Table 8-1.

101

Table 8-1: Bench-Top Transient Cooling Test Parameters. Some parameters are computed from others according to the above equations.

σ	5.67E-08 W/m^2/K^4
ε_1	0.100
A_1	0.0033 m^2
A_2	0.0025 m^2
T_e	293.19 K
m	49.75 g
C	0.900 J/g/K
α	2.25E-05 m^2/s
ν	1.59E-05 m^2/s
p	0.304 m
k	2.63E-02 W/m/K
g	9.81 m/s^2
B	0.003192 K^{-1}
T_f	313.2534 K
Ra	977.59
Nu	3.02
h_c	9.66 W/K

This approach was previously demonstrated with fixed-emissivity materials using reference surface properties. The fixed-emissivity demonstration results are shown, for reference, in Fig. 8-4. Three test samples of equal thermal mass and surface area were compared to demonstrate that differences in emissivity could result in observable differences in cooling time despite the dominant convection effect. The two aluminum test samples are identical, except that one has been affixed with silver-Teflon tape, a common radiator coating for spacecraft applications. The reference values for these samples are ε = 0.1 (polished aluminum-6061 alloy), ε = 0.8 (silver-Teflon radiator tape), and ε = 0.85 (industrial graphite). For the demonstration trials, "effective emissivity" was not computed by the iteration method described above, so predicted cooling times are based on reference emissivity values only.
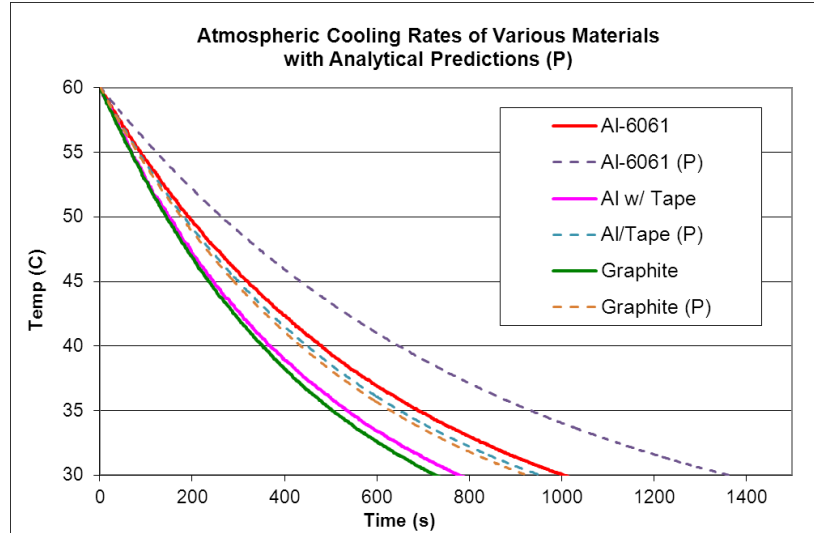
Figure 8-4: Bench-Top Cooling Demonstration with Fixed-Emissivity Materials. Predicted cooling times are based on reference emissivity values, and some atmospheric parameters are estimated.

Results

The experiment was run five times for each ECD state (light and dark). The slowest and fastest cooling profiles from each set were omitted, and the remaining three trials were averaged. The averaged data sets are plotted in Fig. 8-5 as temperature profiles with respect to time, along with the analytically predicted temperature profiles for each state that have been iterated with respect to ECD emissivity to match final cooling times.
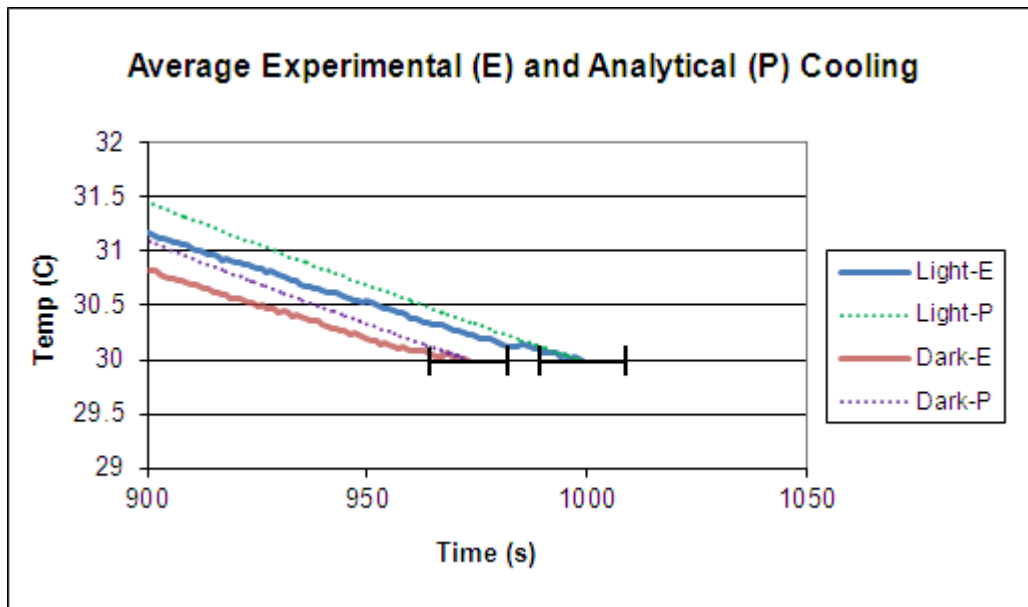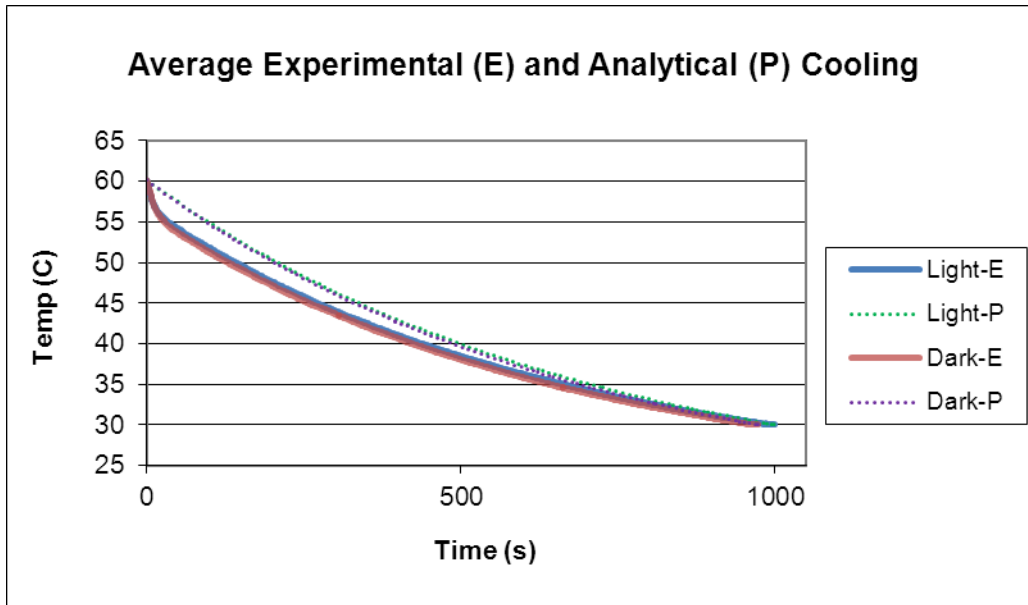
Figure 8-5: Average experimental (E) and predicted (P) cooling times. Results are shown from 60 C to 30 C radiator surface temperature. Predicted data have been matched to overall cooling time for emissivity estimation. The lower view is zoomed to show the final cooling times, with ±1 σ error bars.
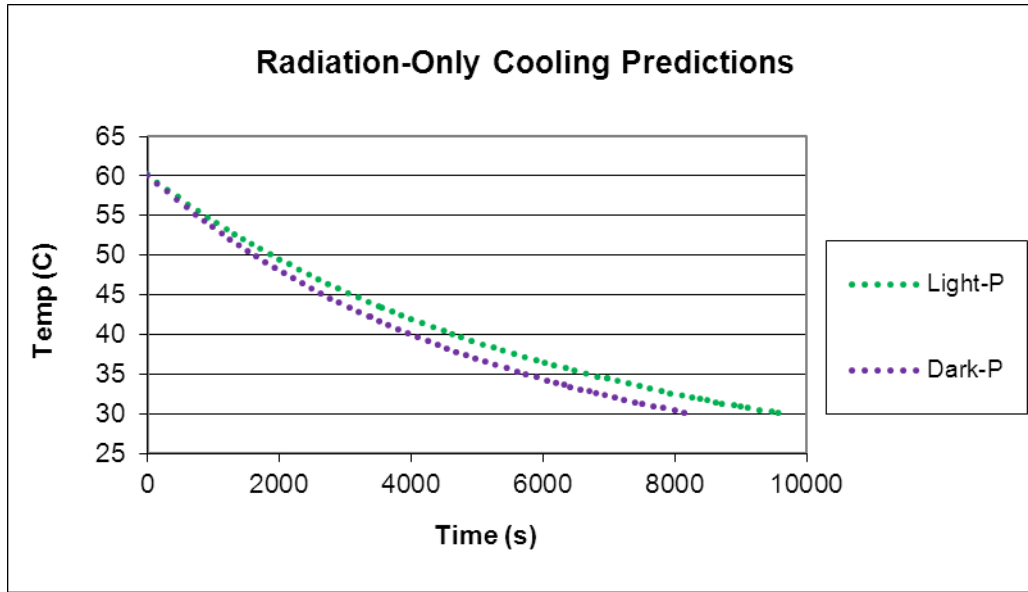
Figure 8-6: Radiation-only cooling time predictions. Light and dark cooling rates are predicted with estimated emissivity values (ε = 0.275 and ε = 0.339, respectively).

The average cooling times from 60 C to 30 C are 999 ± 9.4 seconds (light) and 973 ± 8.5 seconds (dark). The difference between these cooling times is small relative to the scale of the test duration. This result is not surprising due to the overwhelming effect of free convection, which is identical in both data sets. Iterative analysis of Eq. 8-5 provides estimated emissivity ratings of $\varepsilon_2 = 0.275$ (light) and $\varepsilon_2 = 0.339$ (dark). Using these emissivity results, "radiation-only" temperature profiles that would be expected under actual vacuum conditions can be predicted with Eq. 8-4.

The "radiation-only" analysis shown in Fig. 8-6 predicts the outcome for the same experiment as if it was conducted in a vacuum, resulting in cooling times of 9632 seconds (light) and 8247 seconds (dark). As expected, the differences in cooling rate are more pronounced in the absence of convection (15.5% change predicted compared to 2.6% change in actual bench-top data), which is one of the primary motivations for conducting thermal vacuum testing when evaluating radiators.

A notable anomaly when comparing experimental to predicted data is that the curves are shaped differently. This artifact may be at least partially due to the test sample not facing the true

105

"room temperature". Instead, the ECD was partially exposed to the still radiating heat lamp, which remains hot after being deactivated. Therefore, the actual sink temperature is changing with time as the lamp itself cools. Moreover, a portion of the test sample's "view" is occupied by the lamp, and the sample cannot radiate to the lamp due to the adverse temperature gradient of the hot lamp. The dynamics of free convection are also complicated by the hot lamp, which is facing downward and thus creating air movement that may be stronger and in opposite circulation from that caused by the test article. A simple fix for these problems for future testing would be to physically remove the lamp once the maximum temperature is reached, instead of merely turning off its power, or to replace the lamp with a conductive heater to supply thermal energy directly to the radiator. This corrective step should also increase the relative effectiveness of radiative cooling for more apparent differences between light and dark states in the experimental results.

Another way to emphasize and further isolate the contribution of thermal radiation, even in the bench-top environment, would be to increase the upper temperature limit in the experiment. In this study, 60 C was chosen for safety reasons and out of concern for damaging the ECD prototypes. Collecting data at higher temperatures will result in an increase in radiation vs. convection due to the fourth-order temperature terms in Eq. 8-4, whereas Eq. 8-1 scales linearly with temperature. Subsequent electrochromic devices may be deposited on Kapton film substrates rather than PET, which should allow for higher surface temperatures while maintaining flexibility. In the future, an emissometer device could be used to verify the emissivity values estimated by the analytical model. Such a device was not available for this study.

Conclusion

A bench-top experiment was developed to demonstrate radiator cooling performance of a prototype electrochromic device in different optical states under ambient test conditions. When

combined with analytical predictions, this experiment provides a method for estimating the effective emissivity of an electrochromic radiator at vacuum based on transient cooling data under ambient conditions, which requires much less environmental control than traditional steady-state thermal testing. This method's validity is based on the primary assumption that convective effects remain the same for each test run. This assumption is perhaps uniquely appropriate in the case of variable-emissivity devices such as electrochromics, since the same test article can be used for multiple test points, with only the emissivity being varied by an electronic, solid-state process. Thus, any change in cooling rate can be attributed entirely to the emissivity setting. Additional controls on environmental factors, especially the radiation sink, can be incorporated to increase accuracy for future testing while still preserving the accessibility, affordability, and modularity of the simple bench-top test format. While thermal vacuum testing is preferred for optimal simulation of the space environment, at least for steady-state conditions, the methodology described in this study appears to be useful for electrochromic radiator testing when thermal vacuum testing is not available. Furthermore, there is value in continuing to develop and conduct transient experiments such as these for electrochromic radiator evaluation, as proposed applications for EVA thermal control will involve highly dynamic heat loads and thermal environments. Future planned work will include repeating the experiments with the electrochromic devices flexed around aluminum cylinders in order to investigate the effect, if any, of structural flexing on the emissivity range. Flexibility and adequate performance when flexed are key requirements for enabling electrochromic radiator integration with EVA suit surfaces.

Resulting Publications and Presentations:

Metts, Jonathan G. and Klaus, David M., "Bench-Top Transient Cooling Testing of Electrochromic Radiator Material Performance", AIAA-2010-6160, 40th International Conference on Environmental

Systems, Barcelona, Spain, July 2010.

"Bench-Top Transient Cooling Testing of Electrochromic Radiator Material Performance", presentation at 40th International Conference on Environmental Systems, Barcelona, Spain, 13 July 2010.

"Electrochromic Radiators for Space Suits: Preliminary Testing Results", poster presentation at the 39th International Conference on Environmental Systems (ICES), San Francisco, CA, 13 July 2009 (received 2nd place in the student poster competition).

Chapter 9 – Electrochromic Radiator Thermal Vacuum Testing

9.1 – Steady-State Electrochromic Coupon Emissivity Verification Test Results

An electrochromic radiator coupon from Ashwin-Ushas Corp. was successfully tested in Chamber N, Building 33, Johnson Space Center. Chamber pressurization began at mid-day, August 3, 2009, and the test was completed by 11:00pm on August 5, 2009. The test requesters in the Crew and Thermal Systems Division (CTSD) were Rubik Sheth of Thermal Systems and Engineering Support (EC2) and Luis Trevino and Jonathan Metts of Space Suit and Crew Survival Systems (EC5).
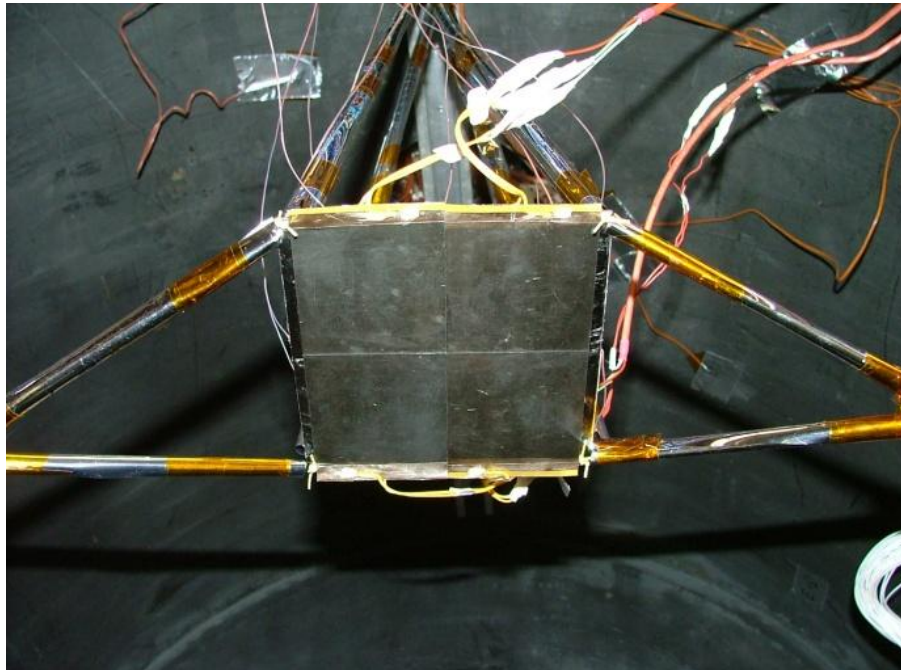
a) Electrochromic surface of test article
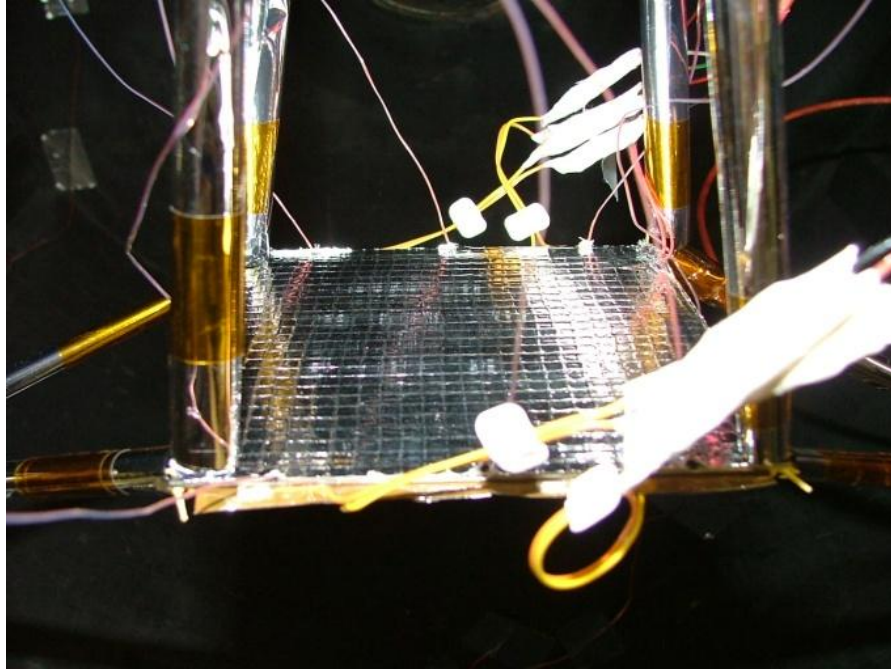
b) Aluminized Mylar (single-layer MLI) surface of test article

Figure 9-1: Installed Test Article – Electrochromic Surface (above) and Aluminized Mylar Surface (below)

Electrochromic materials are being studied for potential application in spacecraft and space suit radiators, due to their unique ability to vary optical properties in response to electrical potential. Practically speaking, the emissivity of an electrochromic surface can be adjusted by applying a small voltage. Heat rejection from a radiator surface is determined, in part, by the emissivity; modulating this property enables solid-state control of the radiator performance. Electrochromic devices for space applications, including those used in this test, typically include a solar-reflective coating.
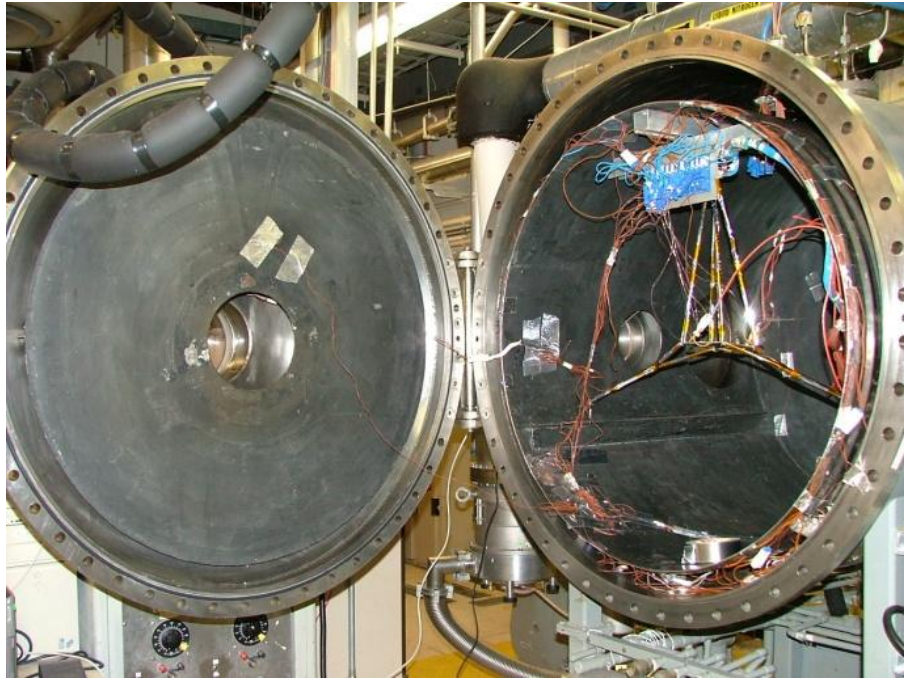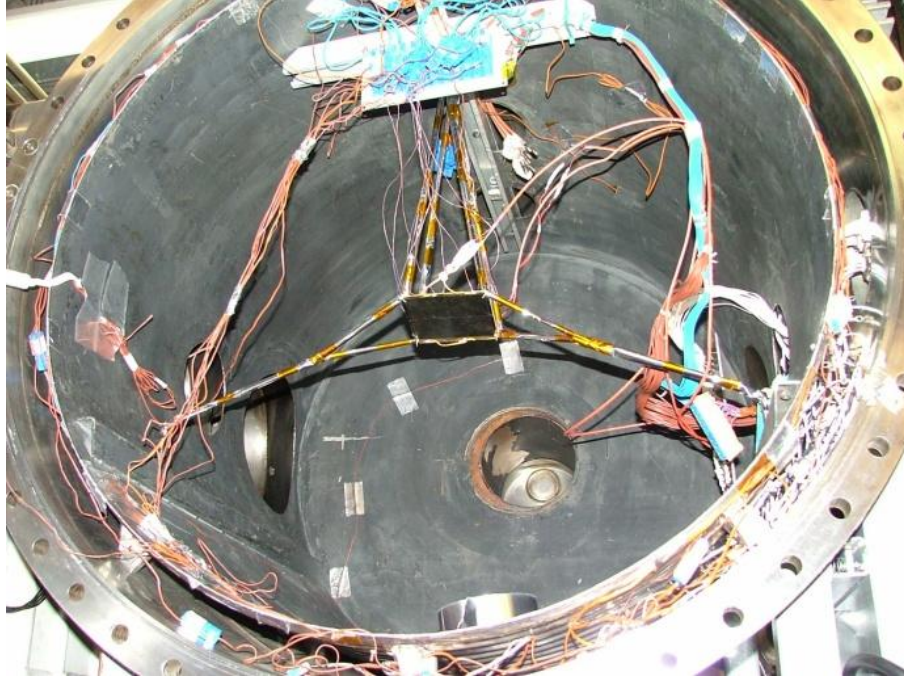
Figure 9-2: Electrochromic Thermal Vacuum Test Article, Suspended with Kevlar String Wrapped in

Mylar and Kapton Tape in Chamber N at Johnson Space Center

The test was designed to determine steady-state emissivity of the radiator coupon at various heat loads and electrochromic settings. If the heat input, radiator surface temperature, and environment temperature are known, and the heat transfer modes are sufficiently constrained, the effective emissivity can be calculated based on steady-state analysis. There are small conductive losses via the wiring and support structure, calculated by Bannon (2010) to result in a surface temperature change of 0.0051 K, well below the TC resolution. Coupon temperatures are measured below the radiating surface, and all four pixels are assumed to have identical capabilities, so this test finds an "effective" emissivity rather than directly measuring the material's optical properties. By comparing the effective emissivity results to the voltage settings, a calibration curve can be established for this particular electrochromic coupon.

The primary measured quantity was temperature, output by Type-T thermocouples (measurement resolution of 0.5 K) placed on the test article and around the shroud. The latter set was used only to verify a stable environment at 95-100 K, corresponding to "full flow" of liquid nitrogen through this thermal vacuum chamber. Thermocouple (TC) placements are shown in the figures below. Voltages across the electrochromic pixels and Kapton heater were measured manually with a multimeter. Heater output was calculated from the measured voltage input, device resistance specification, and an assumption of 100% efficiency, which is standard for electric heaters because electrical efficiency typically takes the form of heat anyway.

X – Heater Wires	
O – Thermocouple Wires	
/// – Electrochromics Wires	

Top Side (MLI cover not shown)   Bottom Side (solar reflective coating not shown)
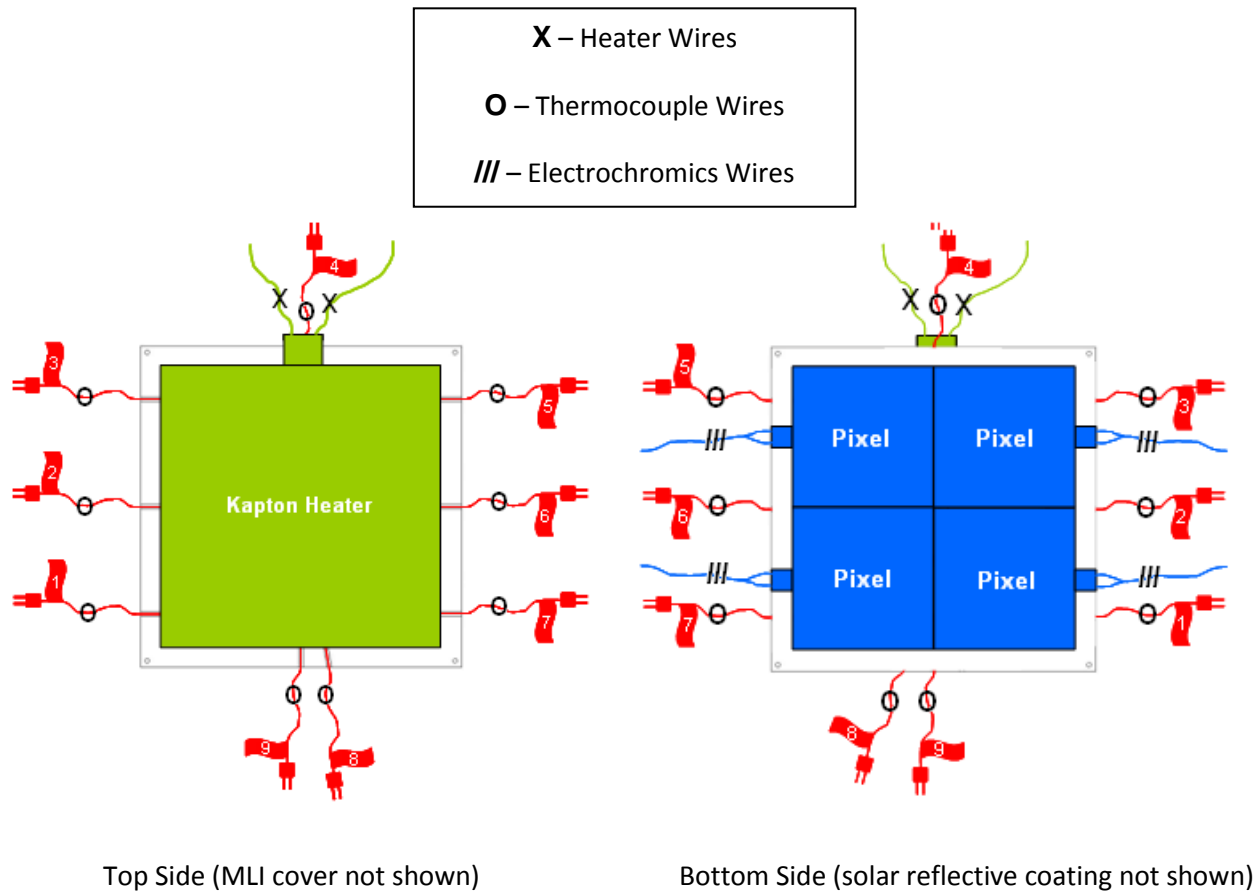
Figure 9-3: Electrochromic Test Coupon Sensor and Wiring Layout (Adapted from Sheth & Metts, 2009)

The governing relationship (Equation 9-1) is the Stefan-Boltzmann equation for steady-state thermal radiation. One side of the test article has the electrochromic coupon; the other side is covered by aluminized Mylar (single-sheet MLI) to minimize radiation not associated with the electrochromic surface. Previous testing found the effective emissivity of this Mylar sheet to be 0.081. The surface area and environmental temperature are equal for both sides; the radiated heat Q' is equal to heat input and is controlled by a thin Kapton heater with known resistance (R) and voltage (V); and σ = 5.67e-08 (W/m^2/K^4) is the Stefan-Boltzmann constant. With the lumped capacitance assumption, surface temperature of both sides is equal to the average of thermocouple readings inside the coupon. Thus,

the equation can be solved for electrochromic emissivity as a function of known and measured

quantities (Equation 9-2).

$$Q' = \frac{V^2}{R} = \sigma A \, (\varepsilon_{EC} + \varepsilon_{MLI})(T_s^4 - T_e^4)$$

<div align="right">Equation 9-1</div>

$$\varepsilon_{EC} = \frac{V^2}{R\sigma A \, (T_s^4 - T_e^4)} - \varepsilon_{MLI}$$

<div align="right">Equation 9-2</div>

An analysis of this experimental setup, performed by Bannon (2010), determined the

uncertainty of ε_{EC} to be $\pm$ 0.071. Subsequent improvements to the experiment setup resulted in a

reduction of uncertainty to $\pm$ 0.0127, but that subsequent test was canceled due to other problems.

This test was primarily a repeat of the previous electrochromic radiator test; the new coupon

from Ashwin-Ushas Corp. was expected to show a larger emissivity range based on vendor projections,

but preliminary test conclusions show that the second coupon actually had worse emissivity modulation

characteristics.

The vendor (Ashwin) predicted this coupon to have an emissivity range of 0.47 (at -1.1 V) to 0.76

(at 0.6 V), for $\Delta\varepsilon$ = 0.29 or a turn-down ratio of 1.62. Based on initial data analysis of the test results, the

actual performance of the electrochromic radiator was ε = 0.41 to 0.63 at the beginning of testing, and

these values were affected by an observed temperature dependency, such that the maximum emissivity

was observed at the hottest test point, while the lowest emissivity was observed at the coldest test

point. At a single, moderate surface temperature of 298 K, the emissivity range was found to be ε = 0.42

to 0.53. Additionally, performance degradation of the coupon was observed between the start and end

of testing. At 323 K, the highest achieved emissivity was 0.63 on August 3, 23:00, compared to only 0.54

at the same temperature on August 5, 21:30. This represents a loss of 17% performance at the coupon's

high-ε state, in less than 48 hours of continuous thermal vacuum in which only the heater settings and

electrochromic voltage settings were adjusted. Figures 9-4 through 9-10 present results from the

thermal vacuum testing. "High" and "Low" test points used the maximum/minimum (respectively)

voltage settings, which correspond to the maximum/minimum emissivity settings (respectively) for a

given set of conditions. Each "High" or "Low" set included test points at various surface temperatures.

The "Range" set used a constant surface temperature and voltage settings that ranged from the

minimum to maximum, with several interim voltages to establish a complete calibration curve. "Mixed"

sets involved setting two adjacent pixels to the low voltage and the other two pixels to the high setting,

creating a steady-state temperature gradient across the coupon; the B set simply reversed polarity of A.

Further details of each test point set are given in Table 9-1.
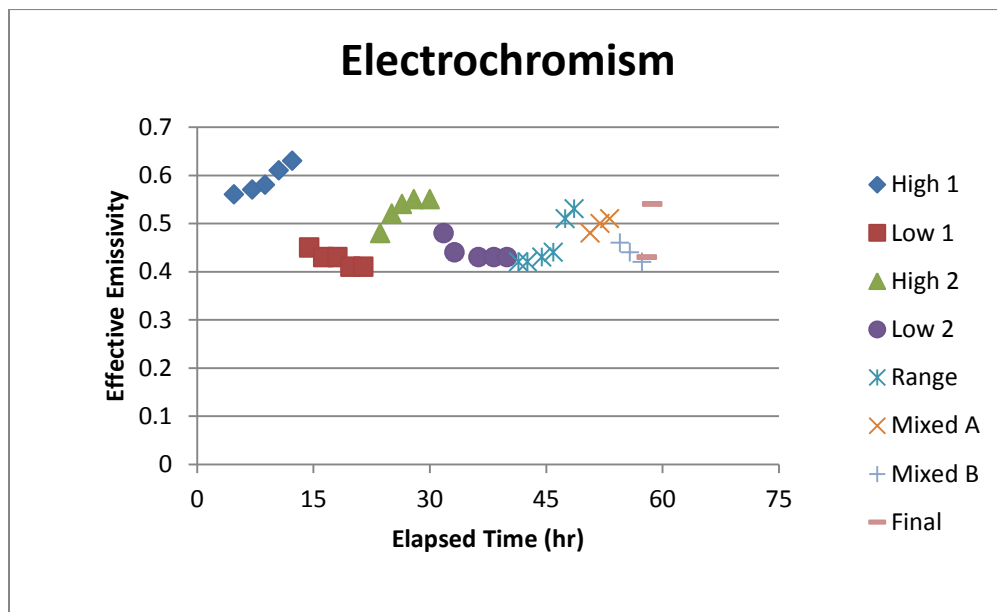
Figure 9-4: Emissivity Results for Various Test Points
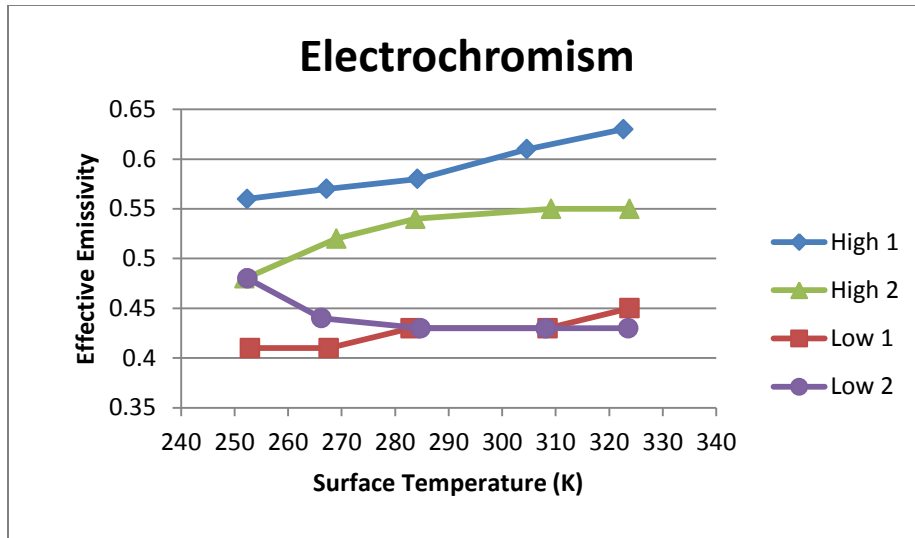
Figure 9-5: Emissivity Results and Temperature Variance for Primary Test Points
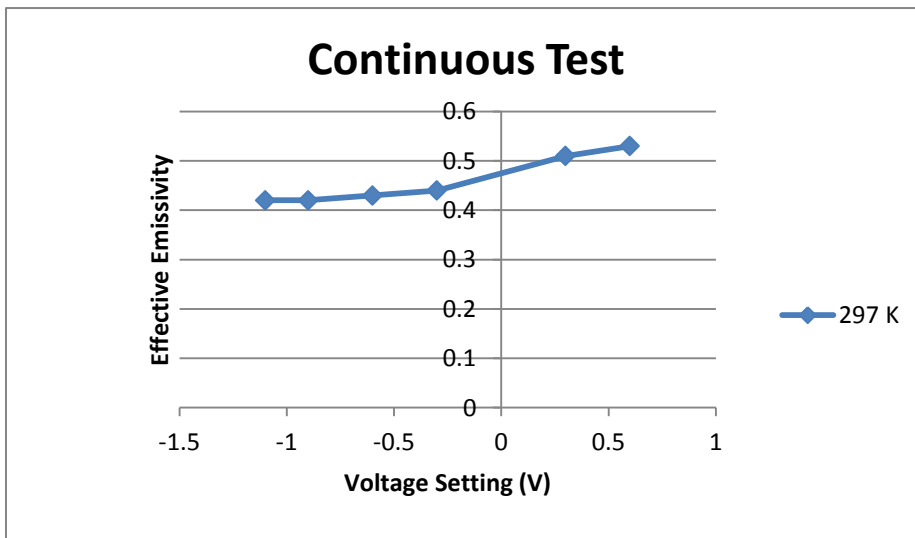
Figure 9-6: Emissivity Results for Continuous Operation (Variable Voltage) Testing
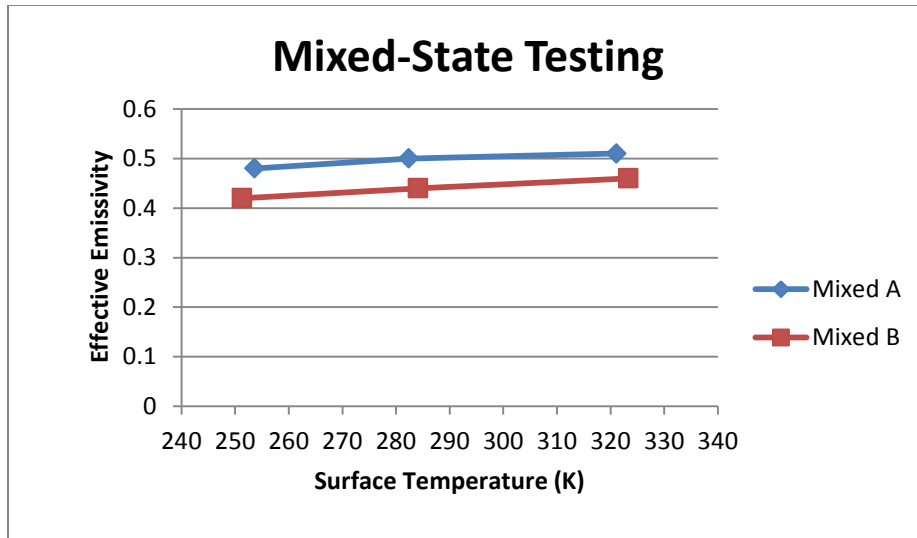
Figure 9-7: Emissivity Results and Temperature Variance for Mixed-State (Light/Dark) Testing
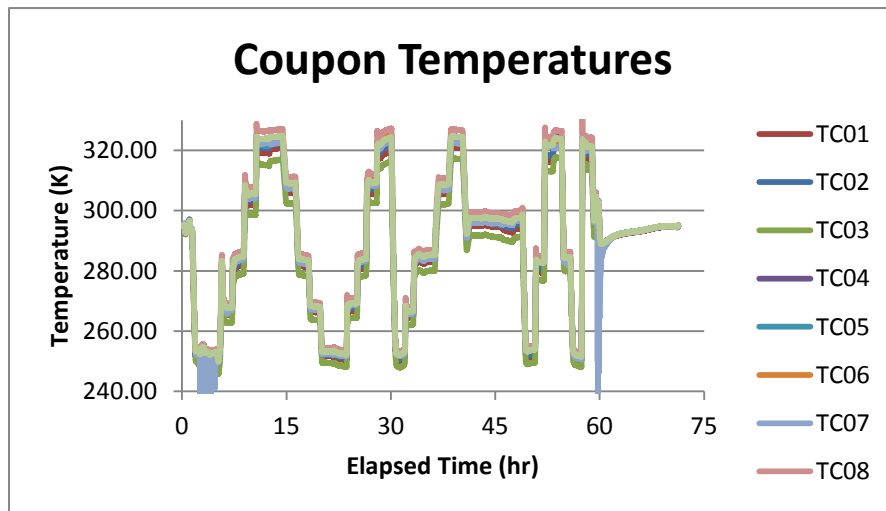
Figure 9-8: Local Coupon Temperatures at Each Thermocouple During Testing
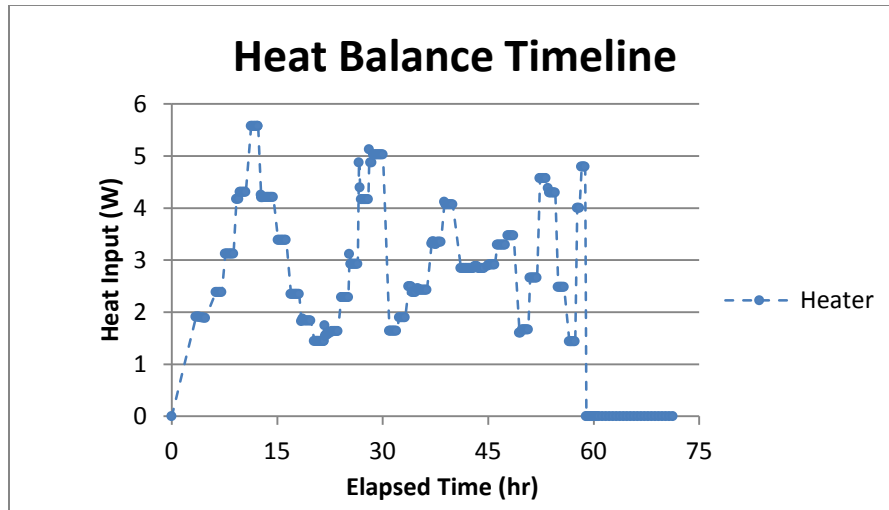
Figure 9-9: Electric Heater Input Power During Testing
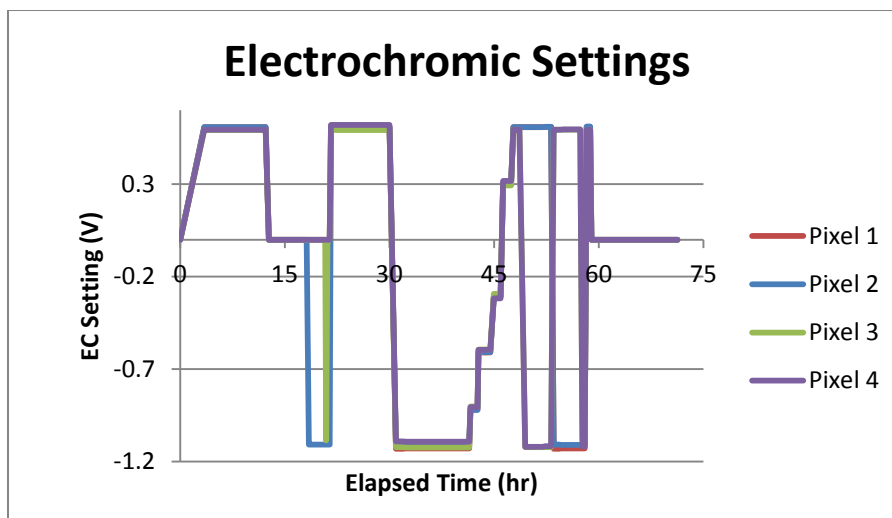
Figure 9-10: Electrochromic Coupon Input Voltage During Testing

Test points in the "Mixed" sets examined the effects of setting half the electrochromic pixels to one state, and half the pixels to the opposite state (Table 9-1). On a small scale, this represents an operational configuration that might be desirable for space suit radiators (part of the surface may be shaded while the other is not). Because the four pixels are adjacent, the expectation was that mixed-state settings would result in an overall emissivity between the low and high values. This compromise

value was indeed observed, but the effective emissivity was different between the two symmetrical configurations. Such a result suggests that, of the four pixels, at least one was off-nominal, causing disparate results when the pixels were paired up in different states. The mixed-state test points took place near the end of testing, so there is insufficient data to determine whether the pixels were fabricated inconsistently (performance varied per pixel throughout testing) or whether one or more pixels experienced disproportionate degradation over the course of testing. If any further testing is to be conducted with a similar electrochromic coupon, an array of mixed-state test points should be conducted both at the beginning and end of testing to identify underperforming pixels.

Electrochromic transition time was not measured in these tests, principally because it is not required for the steady-state emissivity calculation. However, observations by the test operators indicated that it too longer to reach steady-state at the coldest temperatures, possibly indicating an effect of temperature on the electrochromic transition response time. As electrochromic devices include both electrical and ion conductor thin films, the conductivity of these materials may be influenced by temperature (as is the case in many common materials), thus altering the response time.

Table 9-1: Summary of Test Points for ECD Thermal Vacuum Testing

Primary Test Points

T_s (C)	V
-20	
-5	
10	0.6
35	
50	
50	
35	
10	-1.1
-5	
-20	
-20	
-5	
10	0.6
35	
50	
-20	
-5	
10	-1.1
35	
50	

Vary Voltage

T_s (C)	V
	-1.1
	-0.9
	-0.6
25	-0.3
	0
	0.3
	0.6

Mixed State

T_s (C)	V
-20	Pixel 1, 2 @0.6V
10	
50	Pixel 3, 4 @-1.1V
50	Pixel 1, 2 @-1.1V
10	
-20	Pixel 3, 4 @0.6V

Final Check

T_s (C)	V
50	-1.1
50	0.6

In conclusion, the electrochromic materials demonstrated variable emissivity, but the range of this property did not meet expected requirements for radiator applications on human spacecraft or space suits. The materials exhibited considerable performance degradation over the test duration. Results also indicate inconsistent performance among the four pixels that were tested; the cause of this inconsistency is indeterminate. The vendor has reported problems with their fabrication equipment; when these problems are solved, testing on new material samples may indicate improved performance. Further testing is also needed to independently assess the performance of competing electrochromic materials, including those manufactured by Eclipse Thin Films (St. Petersburg, FL) and any other emerging commercial provider of infrared electrochromic devices. In future electrochromic testing,

asymmetric per-pixel test points should be included at the beginning and end to determine nominal variation and observe any localized degradation. Thermocouples should also be placed to measure discrete temperature for individual pixels as well as the interfaces between pixels.

Resulting Publications and Presentations:

Sheth, Rubik and Metts, Jonathan G., "Electrochromic Devices for Vehicle/Suit Radiators – Test Requirements and Test Plan", Johnson Space Center Document No. CTSD-ADV-736, 24 July 2009.

Metts, Jonathan G., "Electrochromic Radiator Testing Quick Look Report", NASA-JSC internal document, revised August 21, 2009.

9.2 EVA-Specific Electrochromic Test Objectives

In May 2010, a scheduling window became available to potentially enable a single working day (up to 12 hours, less cool-down and repress periods) of EVA-specific test points on a pair of previously installed Ashwin-Ushas electrochromic coupons in Thermal Vacuum Chamber N at NASA Johnson Space Center. Funding for this additional testing period was contingent upon delivery of EVA-specific test objectives and test points, with the caveat that the test articles could not be physically manipulated between prior testing and EVA-specific testing. (Opening the test chamber was associated with liquid nitrogen consumable loss, as well as labor costs.) Unrelated circumstances resulted in the original test period being terminated prior to completion and the subsequent cancellation of EVA-specific testing as well. However, this preliminary work is presented for the benefit of future testing.

EVA-specific test goals were identified as:

- Observation of electrochromic performance (steady-state thermal balance) with EVA suit internal heat loads applied to coupon (scaled down to radiator area as fraction of total available area on suit/PLSS).

- Observation of electrochromic performance during simulated, EVA-specific radiator operations such as "mixed-state" emissivity configurations.

- Observation of transient electrochromic performance during a rapid shift in environmental conditions, including investigation of time constants for electrochromic switching in response to such changes in sink temperature.

- Observation of electrochromic performance in EVA-specific, simulated thermal environments, such as a shadowed lunar crater or sloped, rough surface in the lunar highlands. *(This is not*

feasible with the given test setup, because sink temperatures higher than ~95 K require an array

of infrared heat lamps in the thermal vacuum chamber, and simulated terrain geometry would

require additional materials to achieve the desired view factors and environment properties.)

Proposed Test Points

All EVA-specific test points should include relevant heat loads. The internal heat load of an EVA suit, assuming no "heat leak" into or out of the suit, consists of metabolic heat and a constant PLSS heat of approximately 120 W. Reference values for metabolic heat are given below, in Watts.

Table 9-2: Standard EVA Metabolic Rates (NASA, 2006)

Environment	Min	Nom	Max
Microgravity	169	264	644
Apollo Surface	144	286	724
Adv. Walkback	491	696	880

The total internal heat loads, including constant 120 W for PLSS heat, are, in Watts:

Table 9-3: EVA Internal Heat Loads with 120 W PLSS Heat

Environment	Min	Nom	Max
Microgravity	289	384	764
Apollo Surface	264	406	844
Adv. Walkback	611	816	1000

To scale these heat loads down for the electrochromic test articles, an assumption must be made as to the total radiator area available on a future space suit. The natural boundary conditions are

PLSS external surface area (0.8547 m^2) at the minimum and total suit surface area (approximately 3.43 m^2) at the maximum. The most current electrochromic radiator test article owned by NASA Johnson Space Center (fabricated by Ashwin-Ushas Corp. with instrumentation by Paragon Space Development) has an active surface area of 0.0103 m^2. Thus, the scaled heat loads for the minimum radiator surface area (scale = 0.003) are:

Table 9-4: ECD Coupon Heat Loads Scaled for Minimum Radiator Surface Area (in Watts)

Environment	Min	Nom	Max
Microgravity	3.48	4.63	9.21
Apollo Surface	3.18	4.89	10.17
Adv. Walkback	7.36	9.83	12.05

The scaled heat loads for the maximum, full-suit radiator surface area (scale = 0.005) are:

Table 9-5: ECD Coupon Heat Loads Scaled for Maximum Radiator Surface Area (in Watts)

Environment	Min	Nom	Max
Microgravity	0.87	1.15	2.29
Apollo Surface	0.79	1.22	2.53
Adv. Walkback	1.83	2.45	3.00

The installed Kapton film heater is rated for up to 40 W total heat output (although the initial testing phase limits the heater to 8 W). Because emissivity range will have already been verified, and sink temperature is constant during full-flow thermal vacuum operation, the variable of interest in this kind of test is the radiator surface temperature, which is unconstrained. The investigation essentially determines whether the test article can withstand the surface temperatures required to maintain steady state at EVA-specific heat loads within the available emissivity range per coupon. If radiator surface

temperatures exceed material tolerances at a required heat load input, that means the electrochromic device is not capable of rejecting that particular heat load with the available emissivity performance.

Alternatively, the test points could be recalculated for some fraction of the scaled heat load, simulating an operating condition in which a portion of the internal heat load is diverted to a supplementary heat rejection system, such as a sublimator or evaporator. If the test article is found to be intolerant to simulated EVA-specific loading conditions, that indicates how emissivity capabilities need to be adjusted in order to enable practical electrochromic radiators for EVA.

For mixed-state operations, it is desirable to simulate EVA operations in which a suited crew member is facing a heat source (e.g. the sun) but is still able to reject heat from radiators facing a colder environment. Due to operational requirements, the crew member may need to reorient suddenly, which means the electrochromic radiators would need to reverse states very quickly in order to maintain thermal balance. Although mixed environments cannot be simulated with the given test setup, the surface temperature gradients and switching times can still be investigated.

This could be achieved by setting two adjacent pixels to the high emissivity state, with the other two pixels at the low emissivity state. At steady-state, a temperature gradient will exist across the radiator surface. First, it is useful to observe the maximum temperature difference and the transition temperature across the interface between pixel sets. Second, it is important to understand the time scale for the gradient to reverse when both pixel sets are reversed in polarity. This time scale is a function of both the electrochromic switching time (a complex material property that itself depends on surface temperature) as well as the thermodynamic environment, which will be constant. Emissivity switching is a consistent, periodic operation on orbital spacecraft, as the orbital environment has predictable thermal cycles. In contrast, crew members have more complex and often unpredictable movement patterns, especially during surface EVAs, and surface environments are also complex. (Even at the lunar poles, surface features like shadowed craters can produce large temperature swings as the

crew member moves through the environment.) For suit radiators, frequent electrochromic switching and on-demand heat rejection transitions are crucial. The required response time for electrochromic transitions will depend on the relative change in internal heat load and/or environment conditions, taking into account the crew member's allowable heat storage. The given test setup offers a good chance to begin investigating these EVA-specific operations and characteristics. An example test procedure to simulate a 180-degree turn:

1. Set heaters to one of the EVA simulation settings (e.g. Apollo nominal or Walkback minimal).

2. Set two adjacent pixels to the low emissivity state and the other two pixels to the high emissivity state.

3. Wait for steady state to be achieved and note the time and pixel temperatures (asymmetric).

4. Simultaneously reverse polarity on both sets of pixels.

5. Wait for a new steady state and note the time and pixel temperatures (asymmetric).

6. Repeat steps 4 and 5 to observe the opposite transition.

A variation on the above test is to simulate a 90-degree turn by following a similar procedure but only reversing polarity of one pixel in each set. The temperature gradient and transition time will be different than the above case, because there is less overall change in the surface conditions. Smaller turns cannot be simulated without a larger number of pixels (e.g. a more discretized radiator surface).

Chapter 10 – Conclusions and Suggestions for Future Work

10.1   Conclusions

This dissertation has been aimed at the goal of advancing the level of understanding of electrochromic radiator performance and how it may be used to increase EVA capabilities on future space missions. The original concept for this application, as identified in the Chameleon Suit report, provided the motivation for further evaluating the technology to assess its feasibility in meeting the needs of space suit heat rejection.

In Chapter 3, theoretical performance was predicted and bounded in multiple environments and for different metabolic rates. Required radiator emissivity ranges were then determined for various mission parameters. Because some of these emissivity ranges were reportedly achievable with current electrochromic technology, the application of a variable radiator concept for EVA cooling was deemed to be theoretically feasible.

In Chapter 4, detailed metabolic rates and lunar environment data from the Apollo program and Advanced Walkback Test were used to estimate water sublimation mass and predict hypothetical savings that could have been attained with an integrated electrochromic radiator. The radiator concept was found to reduce or eliminate water sublimation in most cases, with 69% savings over the entire Apollo program. Use of an electrochromic radiator could also reduce water sublimation in an emergency scenario such as that simulated by the Advanced Walkback Test, except in the hottest lunar environment conditions. Net impact of the radiator surface on consumable mass usage varies, however, and the use of a radiator was shown to increase required water sublimation in sufficiently hot cases due to heat absorption into the suit in those environments.

In Chapter 5, concepts are presented for integrating an electrochromic radiator with current and anticipated future space suit designs. Each concept was analyzed for thermal management and its potential challenges for implementation. One proposed concept, which includes a secondary fluid loop for transporting heat from the PLSS heat exchanger to exterior radiator surfaces, is compared to various other EVA cooling technologies by utilizing an Equivalent System Mass (ESM) analysis. The current formulation depends on preliminary design inputs for most of the technologies considered, so the ESM analysis should be revisited as the candidates mature in development. Results of the analysis at this stage suggested that electrochromic radiator concepts and other non-venting technologies may result in an overall mass savings break-even point within 12 or fewer EVAs. However, a more comprehensive system trade study would need to account for the varying levels of technology maturity and other operational factors in order to select the most desirable candidate for a particular mission.

In Chapter 6, various empirical tests are presented to observe and quantify performance and anticipated impact of electrochromic radiators used for EVA. A methodology combining experimental data and analytical results was developed to estimate emissivity modulation of electrochromic materials with a transient cooling test in a bench-top, laboratory environment. This method is relatively quick and inexpensive compared to thermal vacuum (simulated space environment) testing and can be used as a precursor to such work. The methodology was validated with fixed-emissivity materials and used to generate example results with prototype electrochromic materials. Concurrently, NASA conducted thermal vacuum testing on electrochromic radiator coupons, with test objectives geared for space vehicle applications, not space suits. Results from those tests are still considered relevant for aspects of the EVA application, but EVA-specific test objectives and simulated EVA operations for thermal vacuum testing were developed that currently remain to be conducted. Completion of these empirical tests is essential to characterizing the performance of electrochromic radiators for EVA applications.

The Technology Readiness Level (TRL) metric is used to quantify the advancements made over the course of this dissertation. Based on the Chameleon Suit report in 2004, the application of electrochromic radiators for EVA heat rejection best fit the definition of TRL-2, "Technology concept and/or application formulated." The subsequent work presented in this thesis, which began in late 2006, includes sufficient analysis to achieve TRL-3, "Analytical and experimental critical function and/or characteristic proof-of-concept." Furthermore, the experimental bench-top testing laid the groundwork for meeting the criteria for TRL-4, "Component and/or breadboard validation in laboratory environment." However, this validation is not yet complete; further bench-top testing is needed with more advanced prototypes or commercially available electrochromic materials, especially to evaluate thermal performance when flexed. Circumstances prevented completion of thermal vacuum testing required to meet TRL-5, "Component and/or breadboard validation in relevant environment." However, much of the test planning and precursor work has been done to enable thermal vacuum testing by defining EVA-specific heat loads and simulated operations (such as switching times and asymmetric loads). Thus, the testing needed to evaluate whether the concept meets the definition for TRL-5 should be achievable in the short-term with sufficient funding, high-quality test samples, and rigorous execution of the proposed experiments. Therefore, this thesis served to advance the application of variable emissivity electrochromic radiators for space suit thermal control from TRL 2 to a level of 3-4.

10.2 Recommendations

Future work should focus on completing the empirical testing, as actual performance of electrochromic radiators under thermal vacuum conditions remains the largest source of uncertainty for the continued development of this technology. Analytically, future studies should also incorporate Mars surface environments, given the long-standing programmatic and social interest in that destination.

Near-Earth objects (asteroids) represent another candidate EVA environment of recent interest that may be worth including in the analyses. All of these environments, including the lunar surface, present challenges such as dust and abrasion and, in some cases, atmospheric effects, that may impede an electrochromic radiator's thermal performance as well as impact its mechanical integrity. Finally, in addition to the radiator technology itself, work remains in defining the optimal heat pathway from the human skin to the surface of the spacesuit, and in developing and implementing a feedback control scheme that enables proper real-time adjustment of emissivity settings in order to maintain thermal equilibrium as the EVA astronaut conducts tasks on the lunar or planetary surface.

Bibliography

Anderson, Molly, Golliher, Eric, Leimkuehler, Thomas, and Quinn, Gregory, "Preliminary Trade Study of Evaporative Heat Sinks", SAE Paper No. 2006-01-2216, 36th International Conference on Environmental Systems, Norfolk, VA, 2006.

Arntz, F. O., Goldner, R.B., Morel, B., Hass, T. E., and Wong, K. K., "Near-infrared reflectance modulation with electrochromic crystalline WO_3 films deposited on ambient temperature glass substrates by an oxygen ion-assisted technique", *Journal of Applied Physics,* Volume 67, No. 6, pp. 3177-3179, 15 March 1990.

Ashwin-Ushas Corporation, "Our Unique, Patented Technology in a Nutshell", (http://www.ashwin-ushas.com/EleHome/IRElectro/index.html). Retrieved August 21, 2008.

Bannon, Erica T., "Ashwin 2010 Coupon Design", Paragon Space Development Corporation Document No. 803700022NC, 29 April 2010.

Bannon, Erica T., Bower, Chad E., Sheth, Rubik, and Stephan, Ryan, "Electrochromic Radiator Coupon Level Testing and Full Scale Thermal Math Modeling for Use on Altair Lunar Lander", AIAA-2010-6110, 40th International Conference on Environmental Systems, Barcelona, Spain, 2010.

Berland, Brian, Lanning, Bruce, Hodgson, Edward, Quinn, Gregory, Bue, Grant, and Trevino, Luis, "Multifunctional Fiber Batteries for Next Generation Space Suits", SAE Paper No. 2008-01-1996, 38th International Conference on Environmental Systems, San Francisco, CA, 2008.

Benedict, F.G., Miles, W.R., and Johnson, A., "The Temperature of the Human Skin", Procedures of the National Academy of Sciences of the United States of America, Volume 5, No. 6, pp. 218-222, June 1919.

Bessiere, A., Marcel, C., Morcrette, M., Tarascon, J-M., Lucas, V., Viana, B., and Baffier, N., "Flexible electrochromic reflectance device based on tungsten oxide for infrared emissivity control", *Journal of Applied Physics*, Volume 91, No. 3, 1 February 2002.

Bhandari, Pradeep, "Effective Solar Absorptance of Multilayer Insulation," SAE Paper No. 2009-01-2392, 39th International Conference on Environmental Systems, Savannah, GA, 2009.

Bue, Grant C., Trevino, Luis A., Hanford, Anthony J., and Mitchell, Keith, "Hollow Fiber Space Suit Water Membrane Evaporator Development for Lunar Missions," SAE Paper No. 2009-01-2371, 39th International Conference on Environmental Systems, Savannah, GA, 2009.

Bue, Grant C., Trevino, Luis, Tsioulos, Gus, and Hanford, Anthony, "Testing of Commercial Hollow Fiber Membranes for Spacesuit Water Membrane Evaporator," SAE Paper No. 2009-01-2427, 39th International Conference on Environmental Systems, Savannah, GA, 2009.

Byko, Maureen, "From Electric Corsets to Self-Cleaning Pants: The Materials Science and Engineering of Textiles", *JOM*, Vol 57, No. 7, 2005.

Campbell, Anthony B., French, Jonathan D., Nair, Satish S., and Miles, John B., "Thermal Analysis and Design of an Advanced Space Suit", *Journal of Thermophysics and Heat Transfer*, Vol. 14, No. 2, April–June 2000.

Carr, Christopher E. and Newman, Dava J., "Space Suit Bioenergetics: Cost of Transport During Walking and Running", *Aviation, Space, and Environmental Medicine*, Vol. 78, No. 12, December 2007.

Carr, Christopher E. and McGee, Jeremy, "The Apollo Number: Space Suits, Self-Support, and the Walk-Run Transition", *PLoS ONE*, Volume 4, Issue 8, August 2009.

Çengel, Yunus A., *Introduction to Thermodynamics and Heat Transfer*, The McGraw-Hill Companies, Inc., 1997.

Clark, C. S., "A Methodology for Calculation of EVA Suit Heat Leak", NAS9-17900/LESC-27794/CTSD-0491, submitted November 30, 1989.

Crawford, Sekou S., Mills, William, and Lusignan, Bruce, "Analysis of a Passive Thermal Control System for Use on a Lightweight Mars EVA Suit", SAE Paper No. 2000-01-2480, 30th International Conference on Environmental Systems, Toulouse, France.

Darrin, Ann Garrison, Osiander, Robert, Champion, John, Swanson, Ted, and Douglas, Donya, "Variable Emissivity Through MEMS Technology", American Institute of Physics, Space Technology and Applications International Forum 1-56396-919-X, pp. 803-808, 2000.

Demiryont, Hulya, Shannon, Kenneth III, and Ponnappan, Rengasamy, "Electrochromic Devices for Satellite Thermal Control", American Institute of Physics, Space Technology and Applications International Forum 0-7354-0305-8, pp. 64-73, 2006.

Demiryont, Hulya, Shannon, Kenneth III, and Williams, Andrew, "Emissivity Modulating Electrochromic Device", Eclipse Thin Films white paper, March 2008.

Demiryont, Hulya and Moorehead, David, "Electrochromic Emissivity Modulator for Spacecraft Thermal Management", *Solar Energy Materials & Solar Cells*, 2009.

Donnelly Corporation, "Electrochromic (EC) Rearview Mirror", (http://www.donnelly.com/products/interiorvisionsystems/ecrearview.asp). Retrieved January 16, 2008.

Drysdale, Alan, "ESM History, Capability, and Methods", SAE Paper No. 2003-01-2630, 33rd International Conference on Environmental Systems, Vancouver, British Columbia, Canada, 2003.

Duffield, Bruce E., "Exploration Life Support Basic Values and Assumptions", NASA Johnson Space Center, Document No. JSC-64367, October 31, 2008.

Eclipse Energy Systems, Inc., "Products and Services: Currently Available", (http://eclipsethinfilms.com/prodsservices_available.aspx). Retrieved April 8, 2010.

Fang, G., Liu, Z., and Yao, K. L., "Fabrication and characterization of electrochromic nanocrystalline WO_3/Si (111) thin films for infrared emittance modulation applications", *Journal of Physics D: Applied Physics*, Vol. 34, 2001.

Ferl, Janet, Hewes, Linda, Aitchison, Lindsay, Koscheyev, Victor, Leon, Gloria, Hodgson, Ed, and Sneeringer, Frank, "Trade Study of an Exploration Cooling Garment", SAE Paper No. 2008-01-1994, 38th International Conference on Environmental Systems, San Francisco, CA, 2008.

Gaier, James R., "The Effects of Lunar Dust on EVA Systems During the Apollo Missions", NASA Technical Memorandum 2005-213610/REV1, April 2007.

Gaier, James R. and Jaworske, Donald A., "Lunar Dust on Heat Rejection Surfaces: Problems and Prospects", NASA Technical Memorandum 2007-214814, June 2007.

Gaier, James R., "Effect of Illumination Angle on the Performance of Dusted Thermal Control Surfaces in a Simulated Lunar Environment," SAE Paper No. 2009-01-2420, 39th International Conference on Environmental Systems, Savannah, GA, 2009.

Ganapathi, Gani B., Sunada, Eric T., Birur, Gajanana C., Miller, Jennifer R., and Stephan, Ryan, "Design Description and Initial Characterization Testing of an Active Heat Rejection Radiator with Digital Turn-Down Capability," SAE Paper No. 2009-01-2419, 39th International Conference on Environmental Systems, Savannah, GA, 2009.

Gilmore, David G., *Spacecraft Thermal Control Handbook, Volume I: Fundamental Technologies*, Second Edition, The Aerospace Press / American Institute of Aeronautics and Astronautics, Inc., 2002.

Goldner, R. B., Mendelsohn, D. H., Alexander, J., Henderson, W. R., Fitzpatrick, D., Haas, T. E., Sample, H. H., Rauh, R. D., Parker, M. A., and Rose, T. L., "High near-infrared reflectivity modulation with polycrystalline electrochromic WO_3 films", *Applied Physics Letters*, Vol. 23, No. 12, December 15, 1983.

Granqvist, C. G., "Electrochromic tungsten oxide films: Review of progress 1993-1998", *Solar Energy Materials & Solar Cells*, Vol. 60, 2000.

Granqvist, C. G., *Handbook of Inorganic Electrochromic Materials*, Elsevier, 1995.

Guibert, A. and Taylor, C. L., "Radiation Area of the Human Body", *Journal of Applied Physiology*, 5(1), pp. 24-37, 1952.

Haddad, Emile, Kruzelecky, Roman V., Wong, Brian, and Jamroz, Wes, "Optimization of Tuneable Emittance Smart Coatings for Thermal Control in Small Satellites", SAE Paper No. 2007-01-3126, 37th International Conference on Environmental Systems, Chicago, IL, 2007.

Haddad, Emile, Kruzelecky, Roman V., Wong, Brian, and Jamroz, Wes, "Multilayer Tuneable Emittance Coatings with Low Solar Absorptance for Improved Smart Thermal Control in Space Applications", SAE Paper No. 2009-01-2575, 39th International Conference on Environmental Systems, Savannah, GA, 2009.

Hale, J. S., DeVries, M., Dworak, B., and Woollam, J. A., "Visible and infrared optical constants of electrochromic materials for emissivity modulation applications", *Thin Solid Films*, Vol. 313-314, pp. 205-209, 1998.

Hale, Jeffrey S. and Woollam, John A., "Prospects for IR emissivity control using electrochromic structures", *Thin Solid Films*, Vol. 339, pp. 174-180, 1999.

Hanford, A. J., "Advanced Life Support Basic Values and Assumptions", NASA Johnson Space Center, Document No. CTSD-ADV-484 A, August 16, 2004.

Heiken, Grant H., Vaniman, David T., and French, Bevan M., *Lunar Sourcebook: A User's Guide to the Moon*, Cambridge University Press, 1991.

Hodgson, Edward W., Jr., "A Chameleon Suit to Liberate Human Exploration of Space Environments: Final Report", NASA Institute for Advanced Concepts, Contract # 07600-067, December, 2001.

Hodgson, Jr., E. W., Bender, A., Goldfarb, J., Hansen, H., Quinn, J., Sribnik, F., Thibaud-Erkey, C., "A Chameleon Suit to Liberate Human Exploration of Space Environments", NASA Institute for Advanced Concepts, Contract # 07600-082, June 16, 2004.

Incropera, Frank P., DeWitt, David P., Bergman, Theodore L., and Lavine, Adrienne S., *Fundamentals of Heat and Mass Transfer*, Sixth Edition, John Wiley & Sons, 2007.

Iovine, John V. and Horton, Richard D., "Preliminary Design Review (PDR) Advanced Technology Spacesuit Thermal Module: Thermal Systems Analysis", *NASA/JSC Presentation*, 30 September, 1999.

Izenson, Michael G., Chen, Weibo, and Trevino, Luis, "Zero-Venting, Regenerable, Lightweight Heat Rejection for EVA Suits," SAE Paper No. 2005-01-2974, 35th International Conference on Environmental Systems, Rome, Italy, 2005.

Izenson, Michael G., Chen, Weibo, and Trevino, Luis A., "Lightweight, Flexible, and Freezable Heat Pump/Radiator for EVA Suits", SAE Paper No. 2008-01-2112, 38th International Conference on Environmental Systems, San Francisco, CA, 2008.

Izenson, Michael G., Chen, Weibo, Passow, Christian, Phillips, Scott, and Trevino, Luis, "Advanced Design Heat Pump/Radiator for EVA Suits," SAE Paper No. 2009-01-2406, 39th International Conference on Environmental Systems, Savannah, GA, 2009.

Jones, Eric M. & Glover, Ken, "Apollo Lunar Surface Journal", (http://www.hq.nasa.gov/alsj/frame.html), 1995. Retrieved May 21, 2010.

Jones, Harry, "Equivalent Mass versus Life Cycle Cost for Life Support Technology Selection", SAE Paper No. 2003-01-2635, 33rd International Conference on Environmental Systems, Vancouver, British Columbia, Canada, 2003.

Jones, Harry, "The Dynamic Impact of EVA on Lunar Outpost Life Support", SAE Paper No. 2008-01-2017, 38th International Conference on Environmental Systems, San Francisco, CA, 2008.

Jones, Harry, "Spacesuit Cooling on the Moon and Mars," SAE Paper No. 2009-01-2418, 39th International Conference on Environmental Systems, Savannah, GA, 2009.

Keddy, Michael D., "Geometric Radiator Surfaces for Spacecraft Thermal Control", AIAA TP 86-1291, 4th Thermophysics and Heat Transfer Conference, Boston, MA, 1986.

Kislov, Nikolai, Groger, Howard, and Ponnappan, Rengasamy, "All-Solid-State Electrochromic Variable Emittance Coatings for Thermal Management in Space", American Institute of Physics, Space Technology and Applications International Forum 0-7354-0114-4, pp. 172-179, 2003.

Kislov, Nikolai, Groger, Howard, Ponnappan, Rengasamy, Caldwell, Edmonia, Douglas, Donya, and Swanson, Theodore, "Electrochromic Variable Emittance Devices on Silicon Wafer for Spacecraft Thermal Control", American Institute of Physics, Space Technology and Applications International Forum 0-7354-0171-3, pp. 112-118, 2004.

Khanina, Elena, "Russian EVA Procedures", presentation to the Technical University of Munich, Institute of Astronautics, November 19, 2009.

Klaus, David M., "Regenerable Non-venting Thermal Sink (RNTS) II Final Test Report". *NASA/JSC Document* JSC-23055: pp. 1-527 (CTSD-SS-249), August 1988.

Kreith, Frank, *Radiation Heat Transfer for Spacecraft and Solar Power Plant Design*, International Textbook Company, 1962.

Kreith, Frank and Black, William Z., *Basic Heat Transfer,* Harper & Row, 1980.

Kuznetz, Lawrence H., "Control of Thermal Balance by a Liquid Circulating Garment Based on a Mathematical Representation of the Human Thermoregulatory System", University of California. Berkeley, 1975.

Lee, Siu-Chun and Kurtz, Joe, "Optical Extinction Properties of Space Suit Fabrics: Theory vs. Experiment", AEAA Paper No. 94-1967, 6th AIAA/ASME Joint Thermophysics and Heat Transfer Conference, Colorado Springs, CO, 1994.

Leimkuehler, Thomas O. and Stephan, Ryan A., "Development Status of the Contaminant Insensitive Sublimator", SAE Paper No. 2008-01-2168, 38th International Conference on Environmental Systems, San Francisco, CA, 2008.

Leimkuehler, Thomas O., Abounasr, Osama, and Stephan, Ryan A., "Design of a Sublimator Driven Coldplate Development Unit", SAE Paper No. 2008-01-2169, 38th International Conference on Environmental Systems, San Francisco, CA, 2008.

Leimkuehler, Thomas O., Powers, Aaron, Linrud, Chris, Bower, Chad, and Bue, Grant, "Demonstration of Super Cooled Ice as a Phase Change Material Heat Sink for Portable Life Support Systems," SAE Paper No. 2009-01-2405, 39th International Conference on Environmental Systems, Savannah, GA, 2009.

Leimkuehler, Thomas O., Sheth, Rubik, and Stephan, Ryan A., "Investigation of Transient Sublimator Performance," SAE Paper No. 2009-01-2480, 39th International Conference on Environmental Systems, Savannah, GA, 2009.

Leitch, Rob and Ambrose, Jay, "Transient Response of a Flexible High-Performance Variable Conductance Heat Pipe," SAE Paper No. 2009-01-2500, 39th International Conference on Environmental Systems, Savannah, GA, 2009.

Levri, J. A., Vaccari, D. A., and Drysdale, A. E., "Theory and Application of the Equivalent System Mass Metric," SAE Paper No. 2000-01-2395, 30th International Conference on Environmental Systems, Toulouse, France, July 10-13, 2000.

Levri, Julie A., and Drysdale, Alan E., "Clarifying Objectives and Results of Equivalent System Mass Analyses for Advanced Life Support", SAE Paper No. 2003-01-2631, 33rd International Conference on Environmental Systems, Vancouver, British Columbia, Canada, 2003.

Levri, Julie A., Fisher, John W., and Jones, Harry W., "Advanced Life Support Equivalent System Mass Guidelines Document", NASA/TM-2003-212278, September 2003.

Lunar and Planetary Institute, "Second Annual HEDS-UP Forum" Report, LPI Contribution No. 979, Houston, TX, May 1999.

Mankins, John C., "Technology Readiness Levels: A White Paper". NASA Office of Space Access and Technology / Advanced Concepts Office, April 6, 1995.

Metts, Jonathan G. and Klaus, David M., "Conceptual Analysis of Electrochromic Radiators for Space Suits", SAE Paper No. 2009-01-2570, 39th International Conference on Environmental Systems, Savannah, GA, 2009.

Metts, Jonathan G. and Klaus, David M., "Bench-Top Transient Cooling Testing of Electrochromic Radiator Material Performance", AIAA-2010-6160, 40th International Conference on Environmental Systems, Barcelona, Spain, July 2010.

Metts, Jonathan G., Nabity, James A., and Klaus, David M., "Theoretical Feasibility of Integrated Electrochromic Radiators for Space Suit Thermal Control", accepted for publication in *Advances in Space Research: The Official Journal of the Committee on Space Research (COSPAR), a Scientific Committee of the International Council for Science (ICSU)*, November 2010.

Modest, Michael F., *Radiative Heat Transfer*, 2nd Edition, Academic Press, 2003.

Mortimer, Roger J., "Electrochromic Materials", *Chemical Society Reviews*, Vol. 26, 1997.

Moran, Michael J., Shapiro, Howard N., Munson, Bruce R., and DeWitt, David P., *Introduction to Thermal Systems Engineering: Thermodynamics, Fluid Mechanics, and Heat Transfer*, John Wiley & Sons, Inc., 2003.

Nabity, James A., Mason, Georgia R., Copeland, Robert J., and Trevino, Luis A., "A Freezable Heat Exchanger for Space Suit Radiator Systems", SAE Paper No. 2008-01-2111, 38th International Conference on Environmental Systems, San Francisco, CA, 2008.

Nabity, James A., Mason, Georgia R., Copeland, Robert J., Libberton, Kerry A., Trevino, Luis A., Stephan, Ryan A., and Paul, Heather L., "Space Suit Radiator Performance in Lunar and Mars Environments", SAE Paper No. 2007-01-3275, 37th International Conference on Environmental Systems, Chicago, IL, 2007.

National Aeronautics and Space Administration (NASA), "NASA's Exploration Systems Architecture Study: Final Report", NASA-TM-2005-214062, November 2005.

National Aeronautics and Space Administration (NASA), "Constellation Program Human-Systems Integration Requirements", NASA CxP 70024 Baseline, Dec. 16, 2006.

National Aeronautics and Space Administration (NASA), "Apollo 17 PLSS/OPS/BLSS Briefing", NASA Historical Document, http://history.nasa.gov/alsj/a17/A17LifeSpprtBrief.html, Retrieved Feb. 8, 2010.

Newman, Dava, J., Bethke, Kristen, Carr, Christopher, Hoffman, Jeffrey, and Trotti, Guillermo, "Astronaut Bio-Suit System to Enable Planetary Exploration", IAC-04-U.1.03, 55th International Astronautical Congress, Vancouver, Canada, 2004.

Norcross, Jason R., Lee, Lesley R., Clowers, Kurt G., et al., "Feasibility of Performing a Suited 10-km Ambulation on the Moon – Final Report of the EVA Walkback Test (EWT)", NASA Technical Report TP-2009-214796.

Norcross, Jason R., Clowers, Kurt G., Clark, Tim, et al., "Metabolic Costs and Biomechanics of Level Ambulation in a Planetary Suit", NASA Technical Report TP-2010-216115, February 2010.

Nunneley, Sarah A., "Water Cooled Garments: A Review", *Space Life Sciences 2*, pp. 335-360, 1970.

Ochoa, Dustin A., Miranda, Bruno M., Conger, Bruce C., and Trevino, Luis A., "Lunar EVA Thermal Environment Challenges," SAE Paper No. 2006-01-2231, 36th International Conference on Environmental Systems, Norfolk, VA, 2006.

Ochoa, Dustin A., Vogel, Matthew R., Trevino, Luis A., and Stephan, Ryan A., "Potential of a New Lunar Surface Radiator Concept for Hot Lunar Thermal Environments", SAE Paper No. 2008-01-1960, 38th International Conference on Environmental Systems, San Francisco, CA, 2008.

Paris, Anthony, Anderson, Kevin, Chandrasekhar, Prasanna, Zay, Brian, and McQueeney, Terrance, "Electrochromic Radiators for Microspacecraft Thermal Control", 10 August 2005.

Pisacane, V.L, Kuznetz, L.H., Logan, J.S., Clark, J.B., and Wissler, E.H., "Thermoregulatory models of safety-for-flight issues for space operations", *Acta Astronautica*, Vol. 59, pp. 531-546, 2006.

Pitts, B., Brensinger, C., Saleh, J., Carr, C., Schmidt, P., Newman, D., "Astronaut Bio-Suit for Exploration Class Missions", NASA Institute for Advanced Concepts, Phase 1 Report, 2001.

Planck, Max, *The Theory of Heat Radiation*, American Institute of Physics, 1988. (German text originally published in 1906; translated to English in 1914 by Morton Masius).

138

Pu, Zhengxiang, Kapat, Jay, Chow, Louis, Recio, Jose, Rini, Dan, and Trevino, Luis, "Personal Cooling for Extra-Vehicular Activities on Mars", Space 2004 Conference and Exhibit, San Diego, CA, September 28-30, 2004.

Reid, Charles D. and McAlister, E. D., "Measurement of Spectral Emissivity from 2μ to 15μ", *Journal of the Optical Society of America*, Vol. 49, No. 1, 1959.

Ruzza, Paulo, Molina, Marco, and Gröller, Marcus, "AMS-02 Radiators Thermal Model Correlation Using In-Air Test," SAE Paper No. 2009-01-2429, 39th International Conference on Environmental Systems, Savannah, GA, 2009.

Sapp, S. A., Sotzing, G. A., and Reynolds, J. R., "High Contrast Ratio and Fast-Switching Dual Polymer Electrochromic Devices", *Chemical Materials*, Vol. 10, pp. 2101-2108, 1998.

Shannon, Kenneth III, Demiryont, Hulya, Groger, Howard, Sheets, Judd, and Williams, Andrew, "Thermal Management Integration Using Plug-and-Play Variable Emissivity Devices", 49th AIAA/ASME/ASCE/AHS/ASC Structures, Structural Dynamics, and Materials Conference, AIAA-2008-1962, Schaumburg, IL, April 2008.

Sheth, Rubik and Metts, Jonathan G., "Electrochromic Devices for Vehicle/Suit Radiators – Test Requirements and Test Plan", Johnson Space Center Document No. CTSD-ADV-736, 24 July 2009.

Siegel, Robert and Howell, John, *Thermal Radiation Heat Transfer*, 4th Edition, Taylor & Francis Publishing, 2002.

Silva, C., Schuller, M., and Marotta, E., "Radiator Heat Pump Subsystem for the Space Suit Portable Life Support," SAE Paper No. 2009-01-2407, 39th International Conference on Environmental Systems, Savannah, GA, 2009.

Sompayrac, Robert and Conger, Bruce, "Portable Life Support System Heat Rejection Study – Constellation Space Suit Element," NASA Johnson Space Center, Document No. CTSD-ADV-675, September 2008.

Sompayrac, Robert, Conger, Bruce, and Trevino, Luis, "Lunar Portable Life Support System Heat Rejection Study," SAE Paper No. 2009-01-2408, 39th International Conference on Environmental Systems, Savannah, GA, 2009.

Streckert, Liz and Ambrose, Jay, "Steady State Performance Results for a Flexible High-Performance Variable Conductance Heat Pipe," SAE Paper No. 2009-01-2502, 39th International Conference on Environmental Systems, Savannah, GA, 2009.

Tachikawa, Sumitaka, Ohnishi, Akira, Matsumoto, Kan, Nakamura, Yasuyuki, and Okamoto, Akira, "Multi-layer Coating for Smart Radiation Device with Solar Absorptance 0.13," SAE Paper No. 2009-01-2574, 39th International Conference on Environmental Systems, Savannah, GA, 2009.

Tepper, Edward H., Trevino, Luis A., and Anderson, James E., "Results of Shuttle EMU Thermal Vacuum Tests Incorporating an Infrared Imaging Camera Data Acquisition System", SAE Paper No. 1991-01-1388, 21st International Conference on Environmental Systems, San Diego, CA, 1991.

Tongue, Stephen and Dingell, Charles W., "The Porous Plate Sublimator as the X-38/CRV (Crew Return Vehicle) Orbital Heat Sink", SAE Paper No. 1999-01-2004, 29th International Conference on Environmental Systems, Denver, CO, 1999.

Trevino, Luis A. and Orndoff, Evelyne S., "Advanced Space Suit Insulation Feasibility Study", SAE Paper No. 2000-01-2479, 30th International Conference on Environmental Systems, Toulouse, France, 2000.

Trevino, Luis A., Copeland, Robert J., Elliot, Jeannine E., and Weislogel, Mark, "Freeze Tolerant Radiator for Advanced EMU", SAE Paper No. 2004-01-388, 34th International Conference on Environmental Systems, Colorado Springs, CO, 2004.

Trimble, C. L., Franke, E., Hale, J. S., and Woollam, J. A., "Electrochromic Emittance Modulation Devices For Spacecraft Thermal Control", American Institute of Physics, Space Technology and Applications International Forum 1-56396-919-X, pp. 797-802, 2000.

Tuan, George C. and Birur, Gajanana, "Evaluation of Material and Coating Coupons for Lightweight Radiator", NASA Johnson Space Center, Document No. CTSD-ADV-610, July 28, 2006.

Tuan, George C. and Stephan, Ryan A., "Development and Testing of the Advanced Lightweight Radiator Development Unit (ALRDU)", SAE Paper No. 2008-01-2151, 38th International Conference on Environmental Systems, San Francisco, CA, 2008.

U.S. Department of Energy, "Radiant Barrier Fact Sheet", (http://www.ornl.gov/sci/roofs+walls/radiant/rb_01.html), published in 1991. Retrieved March 24, 2008.

Vogel, Matthew R., Peterson, Keith, Zapata, Felipe III, Dillon, Paul, and Trevino, Luis A., "Spacesuit Water Membrane Evaporator Development for Lunar Missions", SAE Paper No. 2008-01-2114, 38th International Conference on Environmental Systems, San Francisco, CA, 2008.

Vogt, Greg, and Haynes, Robert, "Spacesuit Guidebook", NASA PED-117, January 1990.

Vogt, Gregory L. and George, Jane A., "Suited for Spacewalking: A Teacher's Guide with Activities for Technology Education, Mathematics, and Science", NASA Document #EG-1998-03-112-HQ.

Vos, Jessica R., Gernhardt, Michael L, and Lee, Lesley, "The Walkback Test: A Study to Evaluate Suit and Life Support System Performance Requirements for a 10 Kilometer Lunar Traverse in a Planetary Suit", SAE Paper No. 2007-01-3133, 37th International Conference on Environmental Systems, Chicago, IL, 2007.

Waligora, James M., "Apollo Experience Report: Assessment of Metabolic Expenditures", NASA Technical Document #TN-D-7883, March, 1975.

Waligora, J.M. and Horrigan, D.J., "Metabolism and Heat Dissipation During Apollo EVA Periods", Biomedical Results of Apollo, Edited by Johnston, Richard S., Dietlein, Lawrence F., and Berry, Charles A., National Aeronautics and Space Administration (NASA), 1975, pp. 115-128.

Wang, C., Shim, M., Guyot-Sionnest, P., "Electrochromic Nanocrystal Quantum Dots", *Science*, Vol. 291, pp. 2390-2392, March 23, 2001.

Webb, Paul and Annis, James F., "The Principle of the Space Activity Suit," NASA Contractor Report CR-973, December, 1967.

Webb, Paul, "The Space Activity Suit: An Elastic Leotard for Extravehicular Activity," *Aerospace Medicine*, Vol. 39, No. 4, April, 1968.

Webb, Paul, "Work, Heat, and Oxygen Cost", *Bioastronautics Data Book*, 2nd Edition, Edited by Parker, James F. and West, Vita R., National Aeronautics and Space Administration (NASA), 1973, pp. 847-879.

Wertz, James R. and Larson, Wiley J., *Space Mission Analysis and Design*, 1st Edition, Kluwer Academic Publishers, 1991.

Wiebelt, J. A., *Engineering Radiation Heat Transfer*, Holt Rinehart and Winston, Inc., 1966.

Wilde, Richard C., Abramov, Isaak P., McBarron, James W. II, "Extravehicular Individual Life Support: A Comparison of American and Russian Systems", SAE Technical Paper #932223, 23rd International Conference on Environmental Systems, Colorado Springs, CO, July 1993.

Wilde, Richard C., McBarron, James W., and Faszcza, Jeffrey J., "Identification and Status of Design Improvements for the NASA Shuttle EMU for International Space Station Application", *Acta Astronautica* Vol. 40, No. 11, pp. 797-805, 1997.

Wilde, Richard, Hodgson, Edward, and Mumford, Robert, "What Does It Take to Work on Mars? A New Direction in Spacesuit Systems", AIAA 2004-5967, Space 2004 Conference and Exhibit, San Diego, CA, 2004.

Appendix A – Apollo Lunar Surface EVA Metabolic Data

This data was originally compiled by James Waligora (NASA-JSC) during and after the Apollo program; it was excerpted in a few reports but never fully published. Christopher Carr (MIT), while researching Apollo EVA metabolic rates for a separate study, discovered these records, correlated timestamps to specific activities via the online Apollo Lunar Surface Journal (Jones & Glover, 2010) and formatted them into an electronic spreadsheet. This invaluable data is included here for posterity, with all due credit to the original researchers and Dr. Carr, who requested that this data be accompanied by the citation, which is also included in the comprehensive list of references:

Carr and Newman. Space suit bioenergetics: framework and analysis of unsuited and suited activity. Aviation, Space, and Environmental Medicine (2007) vol. 78 (11) pp. 1013-22.

Mission [XX]	Role [CDR/LMP]	EVA [X]	Activity [Description]	Start MET [hhh:mm:ss]	Duration [mm]	Stop MET [hhh:mm:ss]	Work Rate [Btu/hr]
11	CDR	1	Initial extravehicular activity	109:13:00	11	109:24:00	900
11	CDR	1	Environmental familiarization	109:24:00	3	109:27:00	800
11	CDR	1	Photography	109:27:00	7	109:34:00	875
11	CDR	1	Contingency sample collection	109:34:00	5	109:39:00	675
11	CDR	1	Monitor and photograph LMP	109:39:00	4	109:43:00	850
11	CDR	1	Deploy television camera on surface	109:43:00	23	110:06:00	750
11	CDR	1	Flag and President's message	110:06:00	12	110:18:00	825
11	CDR	1	Bulk sample collection	110:18:00	23	110:41:00	850
11	CDR	1	Lunar module inspection	110:41:00	18	110:59:00	675
11	CDR	1	Experiment package deployment	110:59:00	12	111:11:00	775
11	CDR	1	Documented sample collection	111:11:00	19	111:30:00	1250
11	CDR	1	Transfer sample return containers	111:30:00	7	111:37:00	1450
11	CDR	1	Terminate extravehicular activity	111:37:00	2	111:39:00	1400
11	LMP	1	Assist and monitor Commander	109:13:00	26	109:39:00	1200
11	LMP	1	Initial extravehicular activity	109:39:00	5	109:44:00	1950
11	LMP	1	Environmental familiarization; deploy televisi	109:44:00	14	109:58:00	1200
11	LMP	1	Deploy solar wind experiment	109:58:00	6	110:04:00	1275
11	LMP	1	Flag and President's message	110:04:00	14	110:18:00	1350
11	LMP	1	Evaluation of extravehicular mobility unit	110:18:00	16	110:34:00	850
11	LMP	1	Lunar module inspection	110:34:00	19	110:53:00	875
11	LMP	1	Experiment package deployment	110:53:00	18	111:11:00	1200
11	LMP	1	Documented sample collection; recovery of	111:11:00	12	111:23:00	1450
11	LMP	1	Terminate extravehicular activity; ingress, a	111:23:00	14	111:37:00	1650
11	LMP	1	Assist and monitor Commander	111:37:00	2	111:39:00	1100

12	CDR	1	Extravehicular preparation	115:14:00	2	115:16:00	350
12	CDR	1	Egress	115:16:00	6	115:22:00	1250
12	CDR	1	Environmental familiarization	115:22:00	3	115:25:00	1250
12	CDR	1	Contingency sample collection	115:25:00	5	115:30:00	1100
12	CDR	1	Equipment bag transfer	115:30:00	16	115:46:00	1200
12	CDR	1	Contingency photography	115:46:00	6	115:52:00	1050
12	CDR	1	S-band antenna deployment	115:52:00	18	116:10:00	1250
12	CDR	1	U.S. Flag deployment	116:10:00	10	116:20:00	950
12	CDR	1	Panoramic photography	116:20:00	12	116:32:00	800
12	CDR	1	Unload experiment package	116:32:00	20	116:52:00	800
12	CDR	1	Transfer experiment package	116:52:00	9	117:01:00	1000
12	CDR	1	Deploy experiment package	117:01:00	59	118:00:00	700
12	CDR	1	Return traverse	118:00:00	27	118:27:00	1050
12	CDR	1	Sample container packing	118:27:00	25	118:52:00	1250
12	CDR	1	Equipment transfers	118:52:00	10	119:02:00	950
12	CDR	1	Ingress	119:02:00	6	119:08:00	1300
12	LMP	1	Safety Monitoring	115:14:00	35	115:49:00	1050
12	LMP	1	Egress	115:49:00	3	115:52:00	1225
12	LMP	1	Television deployment	115:52:00	18	116:10:00	1050
12	LMP	1	Deploy solar wind experiment	116:10:00	5	116:15:00	1000
12	LMP	1	Lunar module inspection	116:15:00	17	116:32:00	1225
12	LMP	1	Unload experiment package	116:32:00	20	116:52:00	1075
12	LMP	1	Transfer experiment package	116:52:00	9	117:01:00	1450
12	LMP	1	Activate experiment package	117:01:00	59	118:00:00	775
12	LMP	1	Return traverse	118:00:00	35	118:35:00	1050
12	LMP	1	Core-tube sample	118:35:00	16	118:51:00	925
12	LMP	1	Ingress	118:51:00	1	118:52:00	1275
12	LMP	1	Safety Monitoring	118:52:00	16	119:08:00	850
12	CDR	2	Extravehicular preparation	131:35:00	2	131:37:00	500
12	CDR	2	Egress	131:37:00	2	131:39:00	1250
12	CDR	2	Equipment bag transfer	131:39:00	5	131:44:00	850
12	CDR	2	Traverse preparations	131:44:00	16	132:00:00	650
12	CDR	2	Initial geological traverse	132:00:00	83	133:23:00	875
12	CDR	2	Core-tube sampling	133:23:00	13	133:36:00	850
12	CDR	2	Final geological traverse	133:36:00	17	133:53:00	900
12	CDR	2	Surveyor inspection	133:53:00	41	134:34:00	825
12	CDR	2	Return to spacecraft	134:34:00	12	134:46:00	1050
12	CDR	2	Sample container packing	134:46:00	25	135:11:00	900
12	CDR	2	Equipment transfers	135:11:00	9	135:20:00	875
12	CDR	2	Ingress	135:20:00	3	135:23:00	1500
12	LMP	2	Safety Monitoring	131:35:00	9	131:44:00	875
12	LMP	2	Egress	131:44:00	5	131:49:00	1150
12	LMP	2	Contrast chart photography	131:49:00	22	132:11:00	975
12	LMP	2	Initial geological traverse	132:11:00	72	133:23:00	975
12	LMP	2	Core-tube sampling	133:23:00	13	133:36:00	1075
12	LMP	2	Final geological traverse	133:36:00	17	133:53:00	975
12	LMP	2	Surveyor inspection	133:53:00	41	134:34:00	950
12	LMP	2	Return to spacecraft	134:34:00	12	134:46:00	1275
12	LMP	2	Closeup photography	134:46:00	22	135:08:00	1100
12	LMP	2	Ingress	135:08:00	3	135:11:00	1300
12	LMP	2	Equipment transfers	135:11:00	12	135:23:00	925

14	CDR	1	Cabin depressurization	113:39:00	8	113:47:00	0
14	CDR	1	Egress	113:47:00	4	113:51:00	712
14	CDR	1	Environmental familiarization, modular equipr	113:51:00	21	114:12:00	1201
14	CDR	1	S-band antenna deployment	114:12:00	10	114:22:00	1052
14	CDR	1	Transferal of expendables	114:22:00	19	114:41:00	717
14	CDR	1	U.S. Flag deployment and photography	114:41:00	6	114:47:00	726
14	CDR	1	Lunar module and site inspection	114:47:00	18	115:05:00	587
14	CDR	1	Television transfer to scientific equipment b	115:05:00	3	115:08:00	868
14	CDR	1	Experiment package offloading	115:08:00	13	115:21:00	690
14	CDR	1	Unknown activity	115:21:00	1	115:22:00	651
14	CDR	1	Television positioning	115:22:00	3	115:25:00	840
14	CDR	1	Modular equipment transporter loading	115:25:00	15	115:40:00	733
14	CDR	1	Unknown activity	115:40:00	6	115:46:00	581
14	CDR	1	Traverse to experimental package deployme	115:46:00	15	116:01:00	984
14	CDR	1	Unknown activity	116:01:00	3	116:04:00	677
14	CDR	1	Experimental package system interconnect,	116:04:00	26	116:30:00	794
14	CDR	1	Charged particle lunar environment experime	116:30:00	5	116:35:00	496
14	CDR	1	Deployment of experiment package antenna	116:35:00	63	117:38:00	517
14	CDR	1	Return traverse	117:38:00	16	117:54:00	1273
14	CDR	1	Unknown activity	117:54:00	6	118:00:00	1735
14	CDR	1	Sample collection	118:00:00	3	118:03:00	1165
14	CDR	1	Extravehicular activity closeout	118:03:00	16	118:19:00	1029
14	CDR	1	Ingress	118:19:00	4	118:23:00	1098
14	CDR	1	Cabin repressurization	118:23:00	4	118:27:00	793
14	LMP	1	Cabin depressurization	113:39:00	8	113:47:00	0
14	LMP	1	Pre-egress operations	113:47:00	8	113:55:00	711
14	LMP	1	Egress	113:55:00	2	113:57:00	1582
14	LMP	1	Environmental familiarization, contingency sa	113:57:00	15	114:12:00	901
14	LMP	1	Deployment of solar wind composition experi	114:12:00	2	114:14:00	1045
14	LMP	1	Laser ranging retro-reflector unloading	114:14:00	9	114:23:00	1061
14	LMP	1	Ingress	114:23:00	2	114:25:00	1265
14	LMP	1	S-band antenna switching	114:25:00	12	114:37:00	1195
14	LMP	1	Egress	114:37:00	2	114:39:00	889
14	LMP	1	Camera setup	114:39:00	4	114:43:00	883
14	LMP	1	U.S. flag deployment and photography	114:43:00	4	114:47:00	948
14	LMP	1	Traverse to television	114:47:00	3	114:50:00	747
14	LMP	1	Television panorama	114:50:00	10	115:00:00	620
14	LMP	1	Modular equipment transporter deployment	115:00:00	8	115:08:00	746
14	LMP	1	Experiment package offloading	115:08:00	38	115:46:00	1038
14	LMP	1	Traverse to experiment package deployment	115:46:00	15	116:01:00	1098
14	LMP	1	Unknown activity	116:01:00	2	116:03:00	786
14	LMP	1	Experiment package system interconnect, tl	116:03:00	23	116:26:00	786
14	LMP	1	Mortar offload	116:26:00	3	116:29:00	972
14	LMP	1	Unknown activity	116:29:00	5	116:34:00	778
14	LMP	1	Suprathermal ion detector experiement unlo	116:34:00	11	116:45:00	905
14	LMP	1	Penetrometer activity	116:45:00	2	116:47:00	795
14	LMP	1	Geophone deployment	116:47:00	15	117:02:00	941
14	LMP	1	Thumper activity	117:02:00	32	117:34:00	707
14	LMP	1	Unknown activity	117:34:00	3	117:37:00	634
14	LMP	1	Mortar pack arming	117:37:00	4	117:41:00	695
14	LMP	1	Unknown activity	117:41:00	1	117:42:00	721
14	LMP	1	Return traverse	117:42:00	12	117:54:00	1041
14	LMP	1	Extravehicular activity closeout	117:54:00	21	118:15:00	1111
14	LMP	1	Ingress	118:15:00	3	118:18:00	1231
14	LMP	1	Extravehicular activity termination	118:18:00	5	118:23:00	1248
14	LMP	1	Cabin repressurization	118:23:00	4	118:27:00	915

14	CDR	2	Cabin depressurization	131:08:00	5	131:13:00	486
14	CDR	2	Egress	131:13:00	7	131:20:00	750
14	CDR	2	Familiarization and transferal of equipment t	131:20:00	8	131:28:00	423
14	CDR	2	Modular equipment transporter loading	131:28:00	10	131:38:00	410
14	CDR	2	Lunar portable magnetometer offloading	131:38:00	5	131:43:00	465
14	CDR	2	Evaluation of modular equipment transporter	131:43:00	5	131:48:00	423
14	CDR	2	Lunar module to A traverse	131:48:00	6	131:54:00	562
14	CDR	2	Station A activity	131:54:00	32	132:26:00	509
14	CDR	2	A to B traverse	132:26:00	8	132:34:00	761
14	CDR	2	Station B activity	132:34:00	5	132:39:00	772
14	CDR	2	B to Delta traverse	132:39:00	3	132:42:00	844
14	CDR	2	Station Delta activity	132:42:00	3	132:45:00	928
14	CDR	2	Delta to B1 traverse	132:45:00	3	132:48:00	1068
14	CDR	2	Station B1 activity	132:48:00	4	132:52:00	1228
14	CDR	2	B1 to B2 traverse	132:52:00	5	132:57:00	1362
14	CDR	2	Station B2 activity	132:57:00	3	133:00:00	1455
14	CDR	2	B2 to B3 traverse	133:00:00	14	133:14:00	1492
14	CDR	2	Station B3 activity	133:14:00	2	133:16:00	1655
14	CDR	2	B3 to C' activity	133:16:00	6	133:22:00	1810
14	CDR	2	Station C' activity	133:22:00	16	133:38:00	1020
14	CDR	2	C' to C1 traverse	133:38:00	2	133:40:00	970
14	CDR	2	Station C1 activity	133:40:00	6	133:46:00	1272
14	CDR	2	C1 to C2 traverse	133:46:00	6	133:52:00	945
14	CDR	2	Station C2 activity	133:52:00	2	133:54:00	896
14	CDR	2	C2 to E traverse	133:54:00	6	134:00:00	1244
14	CDR	2	Station E activity	134:00:00	2	134:02:00	1128
14	CDR	2	E to F traverse	134:02:00	4	134:06:00	1281
14	CDR	2	Station F activity	134:06:00	3	134:09:00	940
14	CDR	2	F to G traverse	134:09:00	2	134:11:00	1118
14	CDR	2	Station G activity	134:11:00	36	134:47:00	779
14	CDR	2	G to G1 traverse	134:47:00	2	134:49:00	1065
14	CDR	2	Station G1 activity	134:49:00	3	134:52:00	935
14	CDR	2	G1 to Lunar Module	134:52:00	3	134:55:00	1209
14	CDR	2	Extravehicular ativity closeout	134:55:00	40	135:35:00	1108
14	CDR	2	Extravehicular activity termination	135:35:00	6	135:41:00	903
14	CDR	2	Post-Extravehicular activity operations and	135:41:00	2	135:43:00	1180

14	LMP	2	Cabin depressurization	131:08:00	12	131:20:00	410
14	LMP	2	Egress	131:20:00	1	131:21:00	633
14	LMP	2	Modular equipment transporter preparation	131:21:00	18	131:39:00	633
14	LMP	2	Lunar portable magnetometer offloading	131:39:00	5	131:44:00	756
14	LMP	2	Lunar portable magnetometer operation	131:44:00	2	131:46:00	921
14	LMP	2	Lunar module to A traverse	131:46:00	8	131:54:00	829
14	LMP	2	Station A activity	131:54:00	32	132:26:00	606
14	LMP	2	A to B traverse	132:26:00	8	132:34:00	840
14	LMP	2	Station B activity	132:34:00	5	132:39:00	555
14	LMP	2	B to Delta traverse	132:39:00	3	132:42:00	893
14	LMP	2	Station Delta activity	132:42:00	2	132:44:00	1013
14	LMP	2	Delta to B1 traverse	132:44:00	4	132:48:00	1272
14	LMP	2	Station B1 activity	132:48:00	4	132:52:00	824
14	LMP	2	B1 to B2 traverse	132:52:00	5	132:57:00	1154
14	LMP	2	Station B2 activity	132:57:00	3	133:00:00	1336
14	LMP	2	B2 to B3 traverse	133:00:00	14	133:14:00	1251
14	LMP	2	Station B3 activity	133:14:00	2	133:16:00	1973
14	LMP	2	B3 to C' traverse	133:16:00	6	133:22:00	2064
14	LMP	2	Station C' activity	133:22:00	16	133:38:00	1142
14	LMP	2	C' to C1 traverse	133:38:00	2	133:40:00	1283
14	LMP	2	Station C1 activity	133:40:00	6	133:46:00	1160
14	LMP	2	C1 to C2 traverse	133:46:00	6	133:52:00	1057
14	LMP	2	Station C2 activity	133:52:00	2	133:54:00	1177
14	LMP	2	C2 to E traverse	133:54:00	6	134:00:00	1337
14	LMP	2	Station E activity	134:00:00	2	134:02:00	1341
14	LMP	2	E to F traverse	134:02:00	4	134:06:00	1463
14	LMP	2	Station F activity	134:06:00	3	134:09:00	1640
14	LMP	2	F to G traverse	134:09:00	2	134:11:00	1551
14	LMP	2	Station G activity	134:11:00	36	134:47:00	993
14	LMP	2	G to G1 traverse	134:47:00	2	134:49:00	1504
14	LMP	2	Station G1 activity	134:49:00	3	134:52:00	1260
14	LMP	2	G1 to Lunar Module	134:52:00	3	134:55:00	1558
14	LMP	2	Unknown activity	134:55:00	2	134:57:00	1415
14	LMP	2	Extravehicular activity closeout	134:57:00	28	135:25:00	1082
14	LMP	2	Extravehicular activity termination	135:25:00	10	135:35:00	1102
14	LMP	2	Post-Extravehicular activity operations and	135:35:00	8	135:43:00	996
15	CDR	1	Pre-egress operations	119:39:00	12	119:51:00	1485
15	CDR	1	Egress	119:51:00	8	119:59:00	1635
15	CDR	1	Television deployment	119:59:00	12	120:11:00	1795
15	CDR	1	Lunar roving vehicle offload and deployment	120:11:00	21	120:32:00	1386
15	CDR	1	Lunar roving vehicle configuration	120:32:00	73	121:45:00	1173
15	CDR	1	Lunar roving vehicle traverse (LM-Station 1)	121:45:00	26	122:11:00	486
15	CDR	1	Station 1 Activity - Geological site selection	122:11:00	4	122:15:00	990
15	CDR	1	Station 1 Activity - Radial sample	122:15:00	9	122:24:00	807
15	CDR	1	Station 1 Activity - Traverse preparation	122:24:00	5	122:29:00	1272
15	CDR	1	Lunar roving vehicle traverse (station 1 to s	122:29:00	6	122:35:00	460
15	CDR	1	Station 2 Activity - Description and docume	122:35:00	22	122:57:00	1061
15	CDR	1	Station 2 Activity - Comprehensive sample	122:57:00	8	123:05:00	1148
15	CDR	1	Station 2 Activity - Double core tube	123:05:00	11	123:16:00	1053
15	CDR	1	Station 2 Activity - 500 mm photography &	123:16:00	10	123:26:00	1368
15	CDR	1	Lunar roving vehicle traverse (station 2 to l	123:26:00	34	124:00:00	584
15	CDR	1	Experiments package offload	124:00:00	24	124:24:00	998
15	CDR	1	Experiments package traverse (lunar roving	124:24:00	9	124:33:00	753
15	CDR	1	Heat flow experiment deployment	124:33:00	51	125:24:00	1121
15	CDR	1	Lunar ranging retro reflector deployment	125:24:00	9	125:33:00	1320
15	CDR	1	Photography & traverse preparation	125:33:00	5	125:38:00	1320
15	CDR	1	Lunar roving vehicle traverse (experiments p	125:38:00	5	125:43:00	1272
15	CDR	1	Extravehicular activity closeout	125:43:00	15	125:58:00	1236
15	CDR	1	Solar wind composition deployment & extrav	125:58:00	13	126:11:00	1611

15	LMP	1	Pre-egress operations	119:39:00	21	120:00:00	854
15	LMP	1	Egress	120:00:00	4	120:04:00	1035
15	LMP	1	Contingency sample collection	120:04:00	10	120:14:00	1308
15	LMP	1	Lunar roving vehicle offload and deployment	120:14:00	17	120:31:00	1211
15	LMP	1	Lunar roving vehicle configuration	120:31:00	45	121:16:00	976
15	LMP	1	Pallet transfer & power down	121:16:00	29	121:45:00	1380
15	LMP	1	Lunar roving vehicle traverse (lunar module	121:45:00	26	122:11:00	459
15	LMP	1	Station 1 activity - photography panorama	122:11:00	4	122:15:00	465
15	LMP	1	Station 1 Activity - Radial sample	122:15:00	9	122:24:00	587
15	LMP	1	Station 1 Activity - Traverse preparation	122:24:00	5	122:29:00	744
15	LMP	1	Lunar roving vehicle traverse (station 1 to s	122:29:00	6	122:35:00	360
15	LMP	1	Station 2 Activity - Photography panorama	122:35:00	22	122:57:00	502
15	LMP	1	Station 2 Activity - Comprehensive sample	122:57:00	8	123:05:00	840
15	LMP	1	Station 2 Activity - Double core tube	123:05:00	11	123:16:00	835
15	LMP	1	Station 2 Activity - 70 mm photography and	123:16:00	10	123:26:00	732
15	LMP	1	Lunar roving vehicle traverse (station 2 to l	123:26:00	34	124:00:00	360
15	LMP	1	Experiments package offload	124:00:00	24	124:24:00	1055
15	LMP	1	Experiments package traverse (walking)	124:24:00	4	124:28:00	1995
15	LMP	1	Experiments package interconnect	124:28:00	15	124:43:00	1440
15	LMP	1	Passive seismic experiment deployment	124:43:00	8	124:51:00	1455
15	LMP	1	Solar wind experiment deployment	124:51:00	4	124:55:00	1290
15	LMP	1	Lunar surface magnetometer deployment	124:55:00	15	125:10:00	1180
15	LMP	1	Sunshield deployment	125:10:00	8	125:18:00	1470
15	LMP	1	Antenna installation	125:18:00	7	125:25:00	1251
15	LMP	1	Suprathermal ion detector experiment deploy	125:25:00	9	125:34:00	1427
15	LMP	1	Central station activation	125:34:00	5	125:39:00	1128
15	LMP	1	Lunar roving vehicle traverse (experiment pa	125:39:00	4	125:43:00	630
15	LMP	1	Extravehicular activity closeout	125:43:00	11	125:54:00	1456
15	LMP	1	Extravehicular activity termination	125:54:00	17	126:11:00	1444
15	CDR	2	Pre-egress operations	142:15:00	9	142:24:00	707
15	CDR	2	Egress	142:24:00	5	142:29:00	1380
15	CDR	2	Equipment preparation	142:29:00	35	143:04:00	1207
15	CDR	2	Lunar roving vehicle navigation initialization	143:04:00	7	143:11:00	1114
15	CDR	2	Lunar roving vehicle traverse (lunar module	143:11:00	43	143:54:00	441
15	CDR	2	Station 6 Activity - Documented sample	143:54:00	31	144:25:00	1014
15	CDR	2	Station 6 Activity - Soil mechanics trench	144:25:00	10	144:35:00	1032
15	CDR	2	Station 6 Activity - Single core tube	144:35:00	4	144:39:00	1050
15	CDR	2	Station 6 Activity - Documented sample	144:39:00	5	144:44:00	1308
15	CDR	2	Station 6 Activity - 500 mm photography ar	144:44:00	14	144:58:00	1170
15	CDR	2	Lunar roving vehicle traverse (station 6 to s	144:58:00	3	145:01:00	980
15	CDR	2	Station 6A Activities	145:01:00	22	145:23:00	1470
15	CDR	2	Lunar roving vehicle traverse (station 6A to	145:23:00	3	145:26:00	800
15	CDR	2	Station 7 Activity - Documented Sample	145:26:00	31	145:57:00	1034
15	CDR	2	Station 7 Activity - Comprehensive Sample	145:57:00	9	146:06:00	1127
15	CDR	2	Station 7 Activity - Documented sample and	146:06:00	9	146:15:00	1320
15	CDR	2	Lunar roving vehicle traverse (station 7 to s	146:15:00	13	146:28:00	743
15	CDR	2	Station 4 Activity - Documented Sample	146:28:00	14	146:42:00	1144
15	CDR	2	Station 4 Activity - Traverse Preparation	146:42:00	4	146:46:00	1635
15	CDR	2	Lunar roving vehicle traverse (station 4 to l	146:46:00	22	147:08:00	554
15	CDR	2	Lunar roving vehicle configuration	147:08:00	12	147:20:00	805
15	CDR	2	Lunar roving vehicle traverse (lunar module	147:20:00	1	147:21:00	420
15	CDR	2	Experiments package site activity - heat flo	147:21:00	36	147:57:00	878
15	CDR	2	Experiments package site activity - geologic	147:57:00	17	148:14:00	1112
15	CDR	2	Experiments package site activity - deep co	148:14:00	18	148:32:00	1000
15	CDR	2	Extravehicular activity closeout - Closeout a	148:32:00	21	148:53:00	1254
15	CDR	2	Extravehicular activity closeout - Flag deplo	148:53:00	5	148:58:00	1176
15	CDR	2	Extravehicular activity closeout - Closeout a	148:58:00	21	149:19:00	1214
15	CDR	2	Extravehicular activity termination	149:19:00	9	149:28:00	1140

15	LMP	2	Pre-egress operations	142:15:00	21	142:36:00	780
15	LMP	2	Egress	142:36:00	2	142:38:00	1380
15	LMP	2	Equipment preparation	142:38:00	26	143:04:00	1089
15	LMP	2	Lunar roving vehicle navigation initialization	143:04:00	7	143:11:00	814
15	LMP	2	Lunar roving vehicle traverse (lunar module	143:11:00	43	143:54:00	360
15	LMP	2	Station 6 Activity - Photography panorama	143:54:00	4	143:58:00	675
15	LMP	2	Station 6 Activity - Documented sample	143:58:00	28	144:26:00	690
15	LMP	2	Station 6 Activity - Soil mechanics trench	144:26:00	9	144:35:00	993
15	LMP	2	Station 6 Activity - Single core tube	144:35:00	4	144:39:00	975
15	LMP	2	Station 6 Activity - Documented sample	144:39:00	5	144:44:00	1248
15	LMP	2	Station 6 Activity - 70 mm magazine change	144:44:00	14	144:58:00	776
15	LMP	2	Lunar roving vehicle traverse (station 6 to s	144:58:00	3	145:01:00	380
15	LMP	2	Station 6A Activty - Photography panorama	145:01:00	18	145:19:00	816
15	LMP	2	Station 6A Activity - Traverse preparation	145:19:00	4	145:23:00	645
15	LMP	2	Lunar roving vehicle traverse (station 6A to	145:23:00	3	145:26:00	360
15	LMP	2	Station 7 Activity - Photography panorama	145:26:00	9	145:35:00	587
15	LMP	2	Station 7 Activity - Documented sample	145:35:00	21	145:56:00	640
15	LMP	2	Station 7 Activity - Comprehensive Sample	145:56:00	10	146:06:00	702
15	LMP	2	Station 7 Activity - Documented sample and	146:06:00	9	146:15:00	820
15	LMP	2	Lunar roving vehicle traverse (station 7 to s	146:15:00	13	146:28:00	351
15	LMP	2	Station 4 Activity - Photography panorama	146:28:00	14	146:42:00	699
15	LMP	2	Station 4 Activity - Traverse Preparation	146:42:00	4	146:46:00	660
15	LMP	2	Lunar roving vehicle traverse (station 4 to lı	146:46:00	22	147:08:00	350
15	LMP	2	Lunar roving vehicle configuration	147:08:00	22	147:30:00	908
15	LMP	2	Traverse to experiments package site (walki	147:30:00	5	147:35:00	876
15	LMP	2	Experiments package site activities - Experir	147:35:00	13	147:48:00	808
15	LMP	2	Experiments package site activities - Sample	147:48:00	7	147:55:00	1174
15	LMP	2	Experiments package site activities - Photog	147:55:00	7	148:02:00	720
15	LMP	2	Experiments package site activities - Soil me	148:02:00	16	148:18:00	1290
15	LMP	2	Experiments package site activities - Penetr	148:18:00	10	148:28:00	1134
15	LMP	2	Traverse to lunar module (walking)	148:28:00	5	148:33:00	1224
15	LMP	2	Extravehicular activity closeout - Closeout a	148:33:00	19	148:52:00	1143
15	LMP	2	Extravehicular activity closeout - Flag deplo	148:52:00	6	148:58:00	1050
15	LMP	2	Extravehicular activity closeout - Closeout a	148:58:00	6	149:04:00	980
15	LMP	2	Extravehicular activity termination	149:04:00	24	149:28:00	1328
15	CDR	3	Pre-egress operations	163:18:00	10	163:28:00	642
15	CDR	3	Egress	163:28:00	4	163:32:00	1275
15	CDR	3	Equipment preparation	163:32:00	32	164:04:00	943
15	CDR	3	Lunar roving vehicle traverse (lunar module	164:04:00	3	164:07:00	840
15	CDR	3	Experiments package site activity - Remove	164:07:00	11	164:18:00	1315
15	CDR	3	Experiments package site activity - Disasser	164:18:00	19	164:37:00	973
15	CDR	3	Experiments package site activity - Lunar ro	164:37:00	8	164:45:00	810
15	CDR	3	Lunar roving vehicle navigation initialization	164:45:00	3	164:48:00	820
15	CDR	3	Lunar roving vehicle traverse (experiments p	164:48:00	14	165:02:00	429
15	CDR	3	Station 9 activities	165:02:00	15	165:17:00	1012
15	CDR	3	Lunar roving vehicle traverse (station 9 to s	165:17:00	2	165:19:00	660
15	CDR	3	Station 9A activity - Geological description	165:19:00	17	165:36:00	829
15	CDR	3	Station 9A activity - Documented sample	165:36:00	17	165:53:00	896
15	CDR	3	Station 9A activity - Comprehensive sample	165:53:00	8	166:01:00	945
15	CDR	3	Station 9A activity - Double core tube	166:01:00	8	166:09:00	840
15	CDR	3	Station 9A activity - Undocumented sample	166:09:00	5	166:14:00	1428
15	CDR	3	Lunar roving vehicle traverse (station 9A to	166:14:00	3	166:17:00	740
15	CDR	3	Station 10 activities	166:17:00	12	166:29:00	1055
15	CDR	3	Lunar roving vehicle traverse (station 10 to	166:29:00	15	166:44:00	476
15	CDR	3	Lunar roving vehicle traverse (experiments p	166:44:00	2	166:46:00	660
15	CDR	3	Extravehicular activity closeout - Closeout a	166:46:00	29	167:15:00	1219
15	CDR	3	Extravehicular activity closeout - Stamp car	167:15:00	8	167:23:00	1380
15	CDR	3	Extravehicular activity closeout - Lunar rovi	167:23:00	30	167:53:00	1438
15	CDR	3	Extravehicular activity closeout - Closeout a	167:53:00	8	168:01:00	1845
15	CDR	3	Extravehicular activity termination	168:01:00	7	168:08:00	1714

15	LMP	3	Pre-egress operations	163:18:00	14	163:32:00	947
15	LMP	3	Egress	163:32:00	2	163:34:00	1380
15	LMP	3	Equipment preparation	163:34:00	29	164:03:00	799
15	LMP	3	Traverse to experiments package site (walki	164:03:00	3	164:06:00	1340
15	LMP	3	Experiments package site activity - Remove	164:06:00	12	164:18:00	920
15	LMP	3	Experiments package site activity - Disasser	164:18:00	4	164:22:00	1005
15	LMP	3	Experiments package site activity - Photogr	164:22:00	7	164:29:00	806
15	LMP	3	Experiments package site activity - Disasser	164:29:00	8	164:37:00	953
15	LMP	3	Experiments package site activity - Photogr	164:37:00	8	164:45:00	743
15	LMP	3	Lunar roving vehicle navigation initialization	164:45:00	3	164:48:00	820
15	LMP	3	Lunar roving vehicle traverse (experiments p	164:48:00	14	165:02:00	373
15	LMP	3	Station 9 activities	165:02:00	15	165:17:00	624
15	LMP	3	Lunar roving vehicle traverse (station 9 to s	165:17:00	2	165:19:00	570
15	LMP	3	Station 9A activity - Documented sample	165:19:00	34	165:53:00	702
15	LMP	3	Station 9A activity - Comprehensive sample	165:53:00	8	166:01:00	938
15	LMP	3	Station 9A activity - Double core tube	166:01:00	8	166:09:00	848
15	LMP	3	Station 9A activity - Undocumented sample	166:09:00	5	166:14:00	864
15	LMP	3	Lunar roving vehicle traverse (station 9A to	166:14:00	3	166:17:00	360
15	LMP	3	Station 10 Activity - 70 mm Photography pa	166:17:00	3	166:20:00	920
15	LMP	3	Station 10 Activity - Sample Collection	166:20:00	9	166:29:00	733
15	LMP	3	Lunar roving vehicle traverse (station 10 to	166:29:00	15	166:44:00	384
15	LMP	3	Core tube retrieval	166:44:00	1	166:45:00	660
15	LMP	3	Traverse to lunar module (walking)	166:45:00	2	166:47:00	1020
15	LMP	3	Extravehicular activity closeout	166:47:00	67	167:54:00	895
15	LMP	3	Extravehicular activity termination	167:54:00	14	168:08:00	1281
16	CDR	1	Overhead - Egress and television deploymen	119:05:00	19	119:24:00	
16	CDR	1	Overhead - Lunar roving vehicle offload and	119:24:00	20	119:44:00	
16	CDR	1	Overhead - Lunar roving vehicle checkout	119:44:00	8	119:52:00	
16	CDR	1	Overhead - Far ultraviolet camera deployme	119:52:00	18	120:10:00	
16	CDR	1	Overhead - Lunar roving vehicle load up	120:10:00	21	120:31:00	1104
16	CDR	1	Overhead - Flag deployment	120:31:00	7	120:38:00	1200
16	CDR	1	ALSEP activity - ALSEP offload	120:38:00	4	120:42:00	1212
16	CDR	1	ALSEP activity - Far Ultraviolet camera rese	120:42:00	15	120:57:00	855
16	CDR	1	ALSEP activity - ALSEP traverse (walking)	120:57:00	9	121:06:00	479
16	CDR	1	ALSEP activity - ALSEP Interconnect	121:06:00	8	121:14:00	936
16	CDR	1	ALSEP activity - Passive seismic experiment	121:14:00	25	121:39:00	839
16	CDR	1	ALSEP activity - Central station deployment	121:39:00	17	121:56:00	690
16	CDR	1	ALSEP activity - Lunar surface magnetomet	121:56:00	10	122:06:00	646
16	CDR	1	ALSEP activity - Thumer/Geophone deploym	122:06:00	11	122:17:00	909
16	CDR	1	ALSEP activity - Geophone Deployment	122:17:00	17	122:34:00	642
16	CDR	1	ALSEP activity - Mortar package deploymen	122:34:00	19	122:53:00	859
16	CDR	1	ALSEP activity - Geology configure	122:53:00	15	123:08:00	950
16	CDR	1	Traverse to Station 1	123:08:00	29	123:37:00	742
16	CDR	1	Geology Station 1	123:37:00	49	124:26:00	910
16	CDR	1	Traverse to Station 2	124:26:00	5	124:31:00	531
16	CDR	1	Geology Station 2	124:31:00	27	124:58:00	761
16	CDR	1	Traverse to Station 3	124:58:00	8	125:06:00	586
16	CDR	1	Traverse to LM	125:06:00	13	125:19:00	757
16	CDR	1	Overhead	125:19:00	57	126:16:00	1045

16	LMP	1	Overhead - Pre-Egress and Egress Operation	119:05:00	19	119:24:00	
16	LMP	1	Overhead - Lunar roving vehicle offload and	119:24:00	20	119:44:00	
16	LMP	1	Overhead - Lunar roving vehicle inspection	119:44:00	8	119:52:00	
16	LMP	1	Overhead - Lunar roving vehicle load up	119:52:00	36	120:28:00	885
16	LMP	1	Overhead - Flag deployment	120:28:00	10	120:38:00	1227
16	LMP	1	ALSEP activity - ALSEP offload	120:38:00	6	120:44:00	1234
16	LMP	1	ALSEP activity - ALSEP traverse (walking)	120:44:00	10	120:54:00	1722
16	LMP	1	ALSEP activity - Heat flow experiment Deplc	120:54:00	38	121:32:00	895
16	LMP	1	ALSEP activity - Deep core	121:32:00	31	122:03:00	1211
16	LMP	1	ALSEP activity - Geophone Deployment	122:03:00	4	122:07:00	1261
16	LMP	1	ALSEP activity - ALSEP Photography	122:07:00	28	122:35:00	740
16	LMP	1	ALSEP activity - Geology configure	122:35:00	33	123:08:00	1134
16	LMP	1	Traverse to Station 1	123:08:00	29	123:37:00	603
16	LMP	1	Geology Station 1	123:37:00	49	124:26:00	1046
16	LMP	1	Traverse to Station 2	124:26:00	5	124:31:00	467
16	LMP	1	Geology Station 2	124:31:00	27	124:58:00	1107
16	LMP	1	Traverse to Station 3	124:58:00	8	125:06:00	840
16	LMP	1	Station 3	125:06:00	5	125:11:00	1034
16	LMP	1	Traverse to LM (walking)	125:11:00	4	125:15:00	1590
16	LMP	1	Solar wing composition deployment	125:15:00	4	125:19:00	1326
16	LMP	1	Overhead	125:19:00	57	126:16:00	1158
16	CDR	2	Overhead - Egress	142:51:00	8	142:59:00	
16	CDR	2	Overhead - Traverse preparation	142:59:00	44	143:43:00	715
16	CDR	2	Traverse to Station 4	143:43:00	36	144:19:00	388
16	CDR	2	Geology station 4	144:19:00	56	145:15:00	824
16	CDR	2	Traverse to Station 5	145:15:00	8	145:23:00	650
16	CDR	2	Geology station 5	145:23:00	47	146:10:00	830
16	CDR	2	Traverse to Station 6	146:10:00	9	146:19:00	519
16	CDR	2	Geology station 6	146:19:00	22	146:41:00	846
16	CDR	2	Traverse to Station 8	146:41:00	11	146:52:00	382
16	CDR	2	Geology station 8	146:52:00	68	148:00:00	936
16	CDR	2	Traverse to Station 9	148:00:00	4	148:04:00	424
16	CDR	2	Geology station 9	148:04:00	37	148:41:00	990
16	CDR	2	Traverse to Station 10	148:41:00	25	149:06:00	465
16	CDR	2	Geology station 10	149:06:00	29	149:35:00	857
16	CDR	2	Overhead	149:35:00	39	150:14:00	1083
16	LMP	2	Overhead - Egress	142:51:00	10	143:01:00	
16	LMP	2	Overhead - Traverse preparation	143:01:00	42	143:43:00	721
16	LMP	2	Traverse to Station 4	143:43:00	36	144:19:00	378
16	LMP	2	Geology station 4	144:19:00	56	145:15:00	1035
16	LMP	2	Traverse to Station 5	145:15:00	8	145:23:00	524
16	LMP	2	Geology station 5	145:23:00	47	146:10:00	900
16	LMP	2	Traverse to Station 6	146:10:00	9	146:19:00	379
16	LMP	2	Geology station 6	146:19:00	22	146:41:00	986
16	LMP	2	Traverse to Station 8	146:41:00	11	146:52:00	500
16	LMP	2	Geology station 8	146:52:00	68	148:00:00	960
16	LMP	2	Traverse to Station 9	148:00:00	4	148:04:00	365
16	LMP	2	Geology station 9	148:04:00	37	148:41:00	871
16	LMP	2	Traverse to Station 10	148:41:00	25	149:06:00	417
16	LMP	2	Geology station 10	149:06:00	26	149:32:00	1103
16	LMP	2	Overhead	149:32:00	42	150:14:00	1142
16	CDR	3	Overhead - Egress	165:43:00	8	165:51:00	
16	CDR	3	Overhead - Traverse preparation	165:51:00	26	166:17:00	894
16	CDR	3	Traverse to Station 12	166:17:00	40	166:57:00	390
16	CDR	3	Geology station 12	166:57:00	83	168:20:00	952
16	CDR	3	Traverse to station 13	168:20:00	9	168:29:00	578
16	CDR	3	Geology station 13	168:29:00	29	168:58:00	900
16	CDR	3	Traverse to station 10'	168:58:00	29	169:27:00	455
16	CDR	3	Geology station 10'	169:27:00	34	170:01:00	878
16	CDR	3	Traverse to LM	170:01:00	2	170:03:00	966
16	CDR	3	Geology at LM	170:03:00	6	170:09:00	672
16	CDR	3	Overhead	170:09:00	74	171:23:00	943

17	CDR	1	Egress	117:01:00	9	117:10:00	1192
17	CDR	1	Egress Operations Completed	117:10:00	12	117:22:00	1164
17	CDR	1	LRV deploy	117:22:00	11	117:33:00	1276
17	CDR	1	Set up LRV	117:33:00	8	117:41:00	1722
17	CDR	1	LRV test drive	117:41:00	13	117:54:00	1081
17	CDR	1	configure LRV	117:54:00	25	118:19:00	1345
17	CDR	1	Flag deploy	118:19:00	7	118:26:00	1094
17	CDR	1	LRV misc ops	118:26:00	40	119:06:00	1150
17	CDR	1	ALSEP Trav.	119:06:00	7	119:13:00	1194
17	CDR	1	ALSEP Deploy	119:13:00	144	121:37:00	1249
17	CDR	1	Traverse to Station 1 (Via SEP site)	121:37:00	27	122:04:00	394
17	CDR	1	Station 1 Geology	122:04:00	30	122:34:00	1166
17	CDR	1	Traverse to SEP site	122:34:00	16	122:50:00	581
17	CDR	1	SEP Deploy	122:50:00	24	123:14:00	976
17	CDR	1	Traverse to LM	123:14:00	2	123:16:00	646
17	CDR	1	EVA closeout (repress time)	123:16:00	57	124:13:00	984
17	LMP	1	Egress	117:01:00	12	117:13:00	492
17	LMP	1	Egress Operations Completed	117:13:00	12	117:25:00	1184
17	LMP	1	LRV deploy	117:25:00	8	117:33:00	1406
17	LMP	1	Set up LRV	117:33:00	8	117:41:00	1406
17	LMP	1	LM Area Description & Photo	117:41:00	13	117:54:00	1517
17	LMP	1	Configure LRV	117:54:00	25	118:19:00	1020
17	LMP	1	Flag deploy	118:19:00	7	118:26:00	1206
17	LMP	1	LM Inspection	118:26:00	11	118:37:00	1094
17	LMP	1	ALSEP offload	118:37:00	13	118:50:00	1132
17	LMP	1	ALSEP Traverse (walking, carring ALSEP pac	118:50:00	8	118:58:00	1762
17	LMP	1	ALSEP deploy	118:58:00	126	121:04:00	1095
17	LMP	1	Sample collection & Traverse preparation	121:04:00	29	121:33:00	1148
17	LMP	1	Traverse to LM (walking, carring core stems	121:33:00	3	121:36:00	1556
17	LMP	1	Offload SEP	121:36:00	2	121:38:00	1964
17	LMP	1	Traverse to SEP site (walking carrying SEP p	121:38:00	12	121:50:00	1074
17	LMP	1	Traverse to Station 1	121:50:00	14	122:04:00	370
17	LMP	1	Station 1 Geology	122:04:00	30	122:34:00	1073
17	LMP	1	Traverse to SEP site	122:34:00	16	122:50:00	702
17	LMP	1	SEP deploy	122:50:00	22	123:12:00	841
17	LMP	1	Traverse to LM (walking)	123:12:00	2	123:14:00	1594
17	LMP	1	EVA closeout (repress time)	123:14:00	59	124:13:00	1168
17	CDR	2	Egress	134:35:00	9	134:44:00	1031
17	CDR	2	Traverse Preparations	134:44:00	40	135:24:00	1310
17	CDR	2	Traverse to Station 2	135:24:00	80	136:44:00	414
17	CDR	2	Station 2 Geology	136:44:00	64	137:48:00	855
17	CDR	2	Traverse to Station 3	137:48:00	6	137:54:00	688
17	CDR	2	LRV Sample (crewmen remain seated)	137:54:00	11	138:05:00	939
17	CDR	2	Continue Traverse to Station 3	138:05:00	24	138:29:00	437
17	CDR	2	Station 3 Geology	138:29:00	36	139:05:00	968
17	CDR	2	Traverse to Station 4	139:05:00	18	139:23:00	578
17	CDR	2	Station 4 Geology	139:23:00	34	139:57:00	1251
17	CDR	2	Traverse to Station 5	139:57:00	9	140:06:00	573
17	CDR	2	LRV Photos	140:06:00	4	140:10:00	462
17	CDR	2	Continue Traverse to Station 5	140:10:00	6	140:16:00	434
17	CDR	2	LRV Sample (crewmen remain seated)	140:16:00	3	140:19:00	406
17	CDR	2	Continue Traverse to Station 5	140:19:00	7	140:26:00	406
17	CDR	2	Station 5 Geology	140:26:00	28	140:54:00	1103
17	CDR	2	Travel to LM VIA ALSEP Site	140:54:00	19	141:13:00	518
17	CDR	2	EVA closeout (repress time)	141:13:00	59	142:12:00	1076

17	LMP	2	Egress	134:35:00	11	134:46:00	713
17	LMP	2	Traverse Preparations	134:46:00	33	135:19:00	1009
17	LMP	2	Traverse to SEP site (walking)	135:19:00	2	135:21:00	1565
17	LMP	2	SEP activities	135:21:00	9	135:30:00	1343
17	LMP	2	Traverse to Station 2	135:30:00	74	136:44:00	237
17	LMP	2	Station 2 Geology	136:44:00	64	137:48:00	1087
17	LMP	2	Traverse to Station 3	137:48:00	6	137:54:00	433
17	LMP	2	LRV Sample (crewmen remain seated)	137:54:00	11	138:05:00	1655
17	LMP	2	Continue Traverse to Station 3	138:05:00	24	138:29:00	321
17	LMP	2	Station 3 Geology	138:29:00	36	139:05:00	1020
17	LMP	2	Traverse to Station 4	139:05:00	18	139:23:00	279
17	LMP	2	Station 4 Geology	139:23:00	34	139:57:00	1528
17	LMP	2	Traverse to Station 5	139:57:00	9	140:06:00	606
17	LMP	2	LRV Photos	140:06:00	4	140:10:00	754
17	LMP	2	Continue Traverse to Station 5	140:10:00	6	140:16:00	495
17	LMP	2	LRV Sample (crewmen remain seated)	140:16:00	3	140:19:00	569
17	LMP	2	Continue Traverse to Station 5	140:19:00	7	140:26:00	680
17	LMP	2	Station 5 Geology	140:26:00	28	140:54:00	857
17	LMP	2	Traverse to ALSEP site	140:54:00	14	141:08:00	450
17	LMP	2	ALSEP Activities	141:08:00	6	141:14:00	857
17	LMP	2	Traverse to LM	141:14:00	3	141:17:00	672
17	LMP	2	EVA closeout (repress time)	141:17:00	55	142:12:00	1097
17	CDR	3	Egress	163:33:00	9	163:42:00	1350
17	CDR	3	Traverse Preparations	163:42:00	34	164:16:00	1490
17	CDR	3	Traverse to Station 6	164:16:00	18	164:34:00	904
17	CDR	3	LRV Sample (crewmen remain seated)	164:34:00	2	164:36:00	883
17	CDR	3	Continue Traverse to Station 6	164:36:00	16	164:52:00	716
17	CDR	3	Station 6 Geology	164:52:00	70	166:02:00	1161
17	CDR	3	Traverse to Station 7	166:02:00	7	166:09:00	462
17	CDR	3	Station 7 Geology	166:09:00	22	166:31:00	1047
17	CDR	3	Traverse to Station 8	166:31:00	17	166:48:00	278
17	CDR	3	Station 8 Geology	166:48:00	47	167:35:00	1114
17	CDR	3	Traverse to Station 9	167:35:00	18	167:53:00	459
17	CDR	3	Station 9 Geology	167:53:00	56	168:49:00	872
17	CDR	3	Traverse to LM	168:49:00	29	169:18:00	385
17	CDR	3	EVA closeout (repress time)	169:18:00	90	170:48:00	950
17	LMP	3	Egress	163:33:00	13	163:46:00	585
17	LMP	3	Traverse Preparations	163:46:00	35	164:21:00	1178
17	LMP	3	Traverse to Station 6	164:21:00	13	164:34:00	363
17	LMP	3	LRV Sample (crewmen remain seated)	164:34:00	2	164:36:00	642
17	LMP	3	Continue Traverse to Station 6	164:36:00	16	164:52:00	308
17	LMP	3	Station 6 Geology	164:52:00	70	166:02:00	1123
17	LMP	3	Traverse to Station 7	166:02:00	7	166:09:00	976
17	LMP	3	Station 7 Geology	166:09:00	22	166:31:00	976
17	LMP	3	Traverse to Station 8	166:31:00	17	166:48:00	443
17	LMP	3	Station 8 Geology	166:48:00	47	167:35:00	1184
17	LMP	3	Traverse to Station 9	167:35:00	18	167:53:00	352
17	LMP	3	Station 9 Geology	167:53:00	56	168:49:00	1561
17	LMP	3	Traverse to SEP site	168:49:00	25	169:14:00	338
17	LMP	3	Sample collection	169:14:00	2	169:16:00	894
17	LMP	3	Traverse to LM (walking)	169:16:00	2	169:18:00	1784
17	LMP	3	EVA closeout (repress time)	169:18:00	90	170:48:00	1130

Note that data for Apollo 16, Lunar Module Pilot EVA-3 are missing from the above tables. For unknown reasons, that EVA is missing from the original documentation. Therefore, metabolic data for this EVA has been compiled with a different methodology, by correlating three categories of metabolic rates to specific activities identified in the Apollo Lunar Surface Journal. This analysis is included below for completeness.

Cross-Referenced Metabolic Accounting for Apollo 16 LMP/EVA-3 (Duke)

Metabolic Rates from Waligora (1975); Timestamps from Apollo Lunar Surface Journal (Jones & Glover, 2010)

Activity	Met. (kJ/hr)	Met. (W)	Notes
Overhead	1107	307.7	Miscellaneous tasks (e.g. egress/ingress, rover setup, and simple walking traverse)
Geology	1013	281.6	Primary EVA science tasks (e.g. instrument setup, photography, and sample collection)
Rover	430	119.5	Sitting operation of the rover (hence low metabolic rate)

Timestamp	Dur. (min)	Type	Met. (W)	Notes
165:33:12				LM at vacuum; begin egress
166:09:08	36	Overhead	307.7	Walked out to LRV and buckled in
166:47:12	38	Rover	119.5	LRV has arrived at Station 11
167:35:30	48	Geology	281.6	LMP has been taking photos and samples around North Ray Crater
168:08:16	33	Geology	281.6	LMP has been taking photos and samples around House Rock
168:17:37	9	Rover	119.5	LRV has arrived at Station 13
168:46:11	29	Geology	281.6	LMP has been taking photos and samples around Station 13
169:17:10	31	Rover	119.5	LRV has returned to Station 10' (near the LM landing site)
169:51:07	34	Geology	281.6	LMP has been taking photos and samples around Station 10'
170:23:31	32	Overhead	307.7	LMP has been stowing tools and materials for EVA-3 closeout
171:11:58	48	Overhead	307.7	LMP has completed ingress and cabin repressurization

Subject 1

Time (min)	Δt (min)	VO$_2$ (L/min)	Met. (W)	Energy (kJ)	w/ PLSS (W)	Energy (kJ)
4.00	4.00	1.18	411.70	98.81	531.70	127.61
9.00	5.00	1.64	572.20	171.66	692.20	207.66
12.00	3.00	1.84	641.98	115.56	761.98	137.16
16.00	4.00	2.01	701.29	168.31	821.29	197.11
21.00	5.00	1.59	554.75	166.43	674.75	202.43
26.00	5.00	1.89	659.42	197.83	779.42	233.83
31.00	5.00	1.68	586.15	175.85	706.15	211.85
32.00	1.00	1.37	477.99	28.68	597.99	35.88
37.00	5.00	1.58	551.26	165.38	671.26	201.38
40.00	3.00	1.81	631.51	113.67	751.51	135.27
45.00	5.00	1.42	495.44	148.63	615.44	184.63
48.00	3.00	1.59	554.75	99.86	674.75	121.46
53.00	5.00	1.55	540.80	162.24	660.80	198.24
58.00	5.00	1.24	432.64	129.79	552.64	165.79
63.00	5.00	1.57	547.77	164.33	667.77	200.33
68.00	5.00	1.98	690.82	207.25	810.82	243.25
73.00	5.00	1.53	533.82	160.15	653.82	196.15
74.00	1.00	1.23	429.15	25.75	549.15	32.95
79.00	5.00	1.69	589.64	176.89	709.64	212.89
84.00	5.00	1.99	694.31	208.29	814.31	244.29
89.00	5.00	1.51	526.84	158.05	646.84	194.05
92.00	3.00	1.27	443.10	79.76	563.10	101.36
97.00	5.00	1.68	586.15	175.85	706.15	211.85
100.00	3.00	1.88	655.93	118.07	775.93	139.67
105.00	5.00	1.49	519.86	155.96	639.86	191.96
110.00	5.00	1.61	561.73	168.52	681.73	204.52
115.00	5.00	1.36	474.50	142.35	594.50	178.35
118.00	3.00	1.48	516.37	92.95	636.37	114.55

Totals:	118.00			3976.83		4826.43
Equivalent Water Mass (kg):				1.76		2.14

Subject 2

Time	Δt (min)	VO₂ (l/min)	Met. (W)	Energy (kJ)	w/ PLSS (W)	Energy (kJ)
5.00	5.00	1.85	645.47	193.64	765.47	229.64
8.00	3.00	2.04	711.76	128.12	831.76	149.72
13.00	5.00	2.22	774.56	232.37	894.56	268.37
15.00	2.00	2.30	802.47	96.30	922.47	110.70
20.00	5.00	2.32	809.45	242.83	929.45	278.83
25.00	5.00	2.36	823.40	247.02	943.40	283.02
30.00	5.00	2.44	851.32	255.39	971.32	291.39
35.00	5.00	2.24	781.54	234.46	901.54	270.46
40.00	5.00	2.36	823.40	247.02	943.40	283.02
45.00	5.00	2.54	886.21	265.86	1006.21	301.86
46.00	1.00	2.57	896.67	53.80	1016.67	61.00
51.00	5.00	2.39	833.87	250.16	953.87	286.16
56.00	5.00	2.32	809.45	242.83	929.45	278.83
60.00	4.00	2.25	785.03	188.41	905.03	217.21
65.00	5.00	2.06	718.73	215.62	838.73	251.62
70.00	5.00	2.19	764.09	229.23	884.09	265.23
75.00	5.00	2.16	753.62	226.09	873.62	262.09
80.00	5.00	2.05	715.25	214.57	835.25	250.57
85.00	5.00	2.06	718.73	215.62	838.73	251.62
86.00	1.00	1.72	600.11	36.01	720.11	43.21
Totals:	86.00			4015.35		4634.55
Equivalent Water Mass (kg):				1.78		2.05

Subject 3

Time	Δt (min)	VO$_2$ (l/min)	Met. (W)	Energy (kJ)	w/ PLSS (W)	Energy (kJ)
5.00	5.00	2.06	718.73	215.62	838.73	251.62
10.00	5.00	2.19	764.09	229.23	884.09	265.23
15.00	5.00	2.22	774.56	232.37	894.56	268.37
20.00	5.00	2.22	774.56	232.37	894.56	268.37
25.00	5.00	2.21	771.07	231.32	891.07	267.32
30.00	5.00	2.18	760.60	228.18	880.60	264.18
35.00	5.00	2.19	764.09	229.23	884.09	265.23
40.00	5.00	2.16	753.62	226.09	873.62	262.09
45.00	5.00	2.21	771.07	231.32	891.07	267.32
50.00	5.00	2.31	805.96	241.79	925.96	277.79
55.00	5.00	2.23	778.05	233.41	898.05	269.41
60.00	5.00	2.24	781.54	234.46	901.54	270.46
65.00	5.00	2.27	792.00	237.60	912.00	273.60
70.00	5.00	2.30	802.47	240.74	922.47	276.74
75.00	5.00	2.21	771.07	231.32	891.07	267.32
80.00	5.00	2.20	767.58	230.27	887.58	266.27
85.00	5.00	2.13	743.16	222.95	863.16	258.95
90.00	5.00	2.14	746.65	223.99	866.65	259.99
95.00	5.00	2.16	753.62	226.09	873.62	262.09
100.00	5.00	2.13	743.16	222.95	863.16	258.95
105.00	5.00	2.23	778.05	233.41	898.05	269.41
110.00	5.00	1.99	694.31	208.29	814.31	244.29

Totals:	110.00			5043.00		5835.00
Equivalent Water Mass (kg):				2.23		2.58

Subject 4

Time	Δt (min)	VO$_2$ (l/min)	Met. (W)	Energy (kJ)	w/ PLSS (W)	Energy (kJ)
3	3.00	1.49	519.86	93.57	639.86	115.17
8	5.00	1.85	645.47	193.64	765.47	229.64
13	5.00	1.86	648.95	194.69	768.95	230.69
15	2.00	1.83	638.49	76.62	758.49	91.02
20	5.00	1.88	655.93	196.78	775.93	232.78
25	5.00	1.87	652.44	195.73	772.44	231.73
30	5.00	1.91	666.40	199.92	786.40	235.92
35	5.00	1.81	631.51	189.45	751.51	225.45
40	5.00	1.83	638.49	191.55	758.49	227.55
45	5.00	1.9	662.91	198.87	782.91	234.87
50	5.00	1.82	635.00	190.50	755.00	226.50
55	5.00	1.94	676.87	203.06	796.87	239.06
60	5.00	1.82	635.00	190.50	755.00	226.50
65	5.00	1.89	659.42	197.83	779.42	233.83
70	5.00	1.89	659.42	197.83	779.42	233.83
75	5.00	1.86	648.95	194.69	768.95	230.69
80	5.00	1.94	676.87	203.06	796.87	239.06
85	5.00	1.88	655.93	196.78	775.93	232.78
86	1.00	2.05	715.25	42.91	835.25	50.11
91	5.00	2.02	704.78	211.43	824.78	247.43
93	2.00	2.05	715.25	85.83	835.25	100.23
97	4.00	2.08	725.71	174.17	845.71	202.97
100	3.00	2.23	778.05	140.05	898.05	161.65

Totals:	100.00			3959.46		4679.46
Equivalent Water Mass (kg):				1.75		2.07

Subject 5

Time	Δt (min)	VO$_2$ (l/min)	Met. (W)	Energy (kJ)	w/ PLSS (W)	Energy (kJ)
5	5.00	1.62	565.22	169.57	685.22	205.57
10	5.00	1.8	628.02	188.41	748.02	224.41
15	5.00	1.76	614.06	184.22	734.06	220.22
20	5.00	1.7	593.13	177.94	713.13	213.94
21	1.00	1.78	621.04	37.26	741.04	44.46
26	5.00	1.82	635.00	190.50	755.00	226.50
31	5.00	1.73	603.60	181.08	723.60	217.08
32	1.00	1.79	624.53	37.47	744.53	44.67
37	5.00	1.87	652.44	195.73	772.44	231.73
42	5.00	1.82	635.00	190.50	755.00	226.50
45	3.00	1.85	645.47	116.18	765.47	137.78
50	5.00	1.89	659.42	197.83	779.42	233.83
55	5.00	1.89	659.42	197.83	779.42	233.83
60	5.00	1.98	690.82	207.25	810.82	243.25
65	5.00	2.06	718.73	215.62	838.73	251.62
70	5.00	2.03	708.27	212.48	828.27	248.48
75	5.00	2.04	711.76	213.53	831.76	249.53
80	5.00	1.99	694.31	208.29	814.31	244.29
85	5.00	2.02	704.78	211.43	824.78	247.43
90	5.00	2.04	711.76	213.53	831.76	249.53
91	1.00	1.99	694.31	41.66	814.31	48.86
92	1.00	1.94	676.87	40.61	796.87	47.81

Totals:	92.00			3628.91		4291.31
Equivalent Water Mass (kg):				1.61		1.90

Subject 6

Time	Δt (min)	VO$_2$ (l/min)	Met. (W)	Energy (kJ)	w/ PLSS (W)	Energy (kJ)
5	5.00	2.03	708.27	212.48	828.27	248.48
10	5.00	2.27	792.00	237.60	912.00	273.60
15	5.00	2.13	743.16	222.95	863.16	258.95
16	1.00	1.98	690.82	41.45	810.82	48.65
21	5.00	2.15	750.14	225.04	870.14	261.04
26	5.00	2.23	778.05	233.41	898.05	269.41
30	4.00	2.19	764.09	183.38	884.09	212.18
35	5.00	2.11	736.18	220.85	856.18	256.85
36	1.00	2.12	739.67	44.38	859.67	51.58
41	5.00	2.17	757.11	227.13	877.11	263.13
46	5.00	2.16	753.62	226.09	873.62	262.09
51	5.00	2.13	743.16	222.95	863.16	258.95
54	3.00	2.18	760.60	136.91	880.60	158.51
59	5.00	2.21	771.07	231.32	891.07	267.32
60	1.00	2.23	778.05	46.68	898.05	53.88
65	5.00	2.29	798.98	239.69	918.98	275.69
70	5.00	2.46	858.29	257.49	978.29	293.49
71	1.00	2.46	858.29	51.50	978.29	58.70
75	4.00	2.44	851.32	204.32	971.32	233.12
79	4.00	2.55	889.70	213.53	1009.70	242.33
84	5.00	2.48	865.27	259.58	985.27	295.58

Totals:	84.00			3938.73		4543.53
Equivalent Water Mass (kg):				1.74		2.01

Appendix C – Equivalent System Mass Technology Dossiers

The following data were compiled for each candidate technology, if available:

- Heat rejection capacity (in Watts) – scale system for 8-hr lunar surface EVA as needed
- System mass (m_s)
- System volume (V_s)
- Consumable mass, if applicable (m_c)
- Consumable volume, if applicable (V_c)
- Power consumption, if applicable (P_c)
- Crew time for operation and/or regeneration, if applicable (t_c)
- Estimated Technology Readiness Level (TRL; based on definitions in Mankins, 1995)
- Known reliability problems
- Backup/contingency options

Apollo/EMU Sublimator

Heat Rejection Capacity: 3500 Btu/hr = 1026 W max (Tongue, 1999) OR ~2000 Btu/hr = 586 W for Apollo A7L-B model (Vos, 2007)

m_s = 3.38 kg (includes plate, tubing, pump, and feed tank) (Izenson, 2008; Lovine & Horton, 1999; Trevino, 1999)

      OR = 2.17 kg (scaled from X-38 data in Tongue, 1999 as suggested by Greg Quinn of H-S)

V_s = 124.124 in3 = 0.00203 m^3 = 2.03 L (sublimator assembly)

      + 4.59 L = 0.00459 m^3 (feed tank, assuming equal to feed water volume)

m_c = 4.57 kg (NASA, "Suited for Spacewalking", 1998) + some condensate from PLSS (no cost)

V_c = 4.57 kg / 995 kg/m^3 = 0.00459 m^3 = 4.59 L

t_c = 0.5 hour (refill feed water; my estimate)

TRL = 9

Reliability – Minor contamination issues over long periods (reduced performance) (Leimkuehler et al., 2008); not effective in atmospheric conditions (Mars)

Backup – Secondary O2 tank purge for ~30 minutes of cooling and ventilation; can refill feed water with umbilical connection to vehicle (during EVA)

Spacesuit Water Membrane Evaporator (SWME)

Heat Rejection Capacity: 81-870 W range (Bue et al., 2009)

m_s = 1.36 kg (evaporator only) (Sompayrac et al., 2009)
      + 0.91 kg for empty 8-hour feed water tank (Sompayrac et al., 2009)

V_s = 2.05 L = 0.00205 m^3 (evaporator)
      + 6.38 L = 0.00638 m^3 (feed tank, assuming equal to feed water volume)

m_c = ~14 lbm = 6.35 kg for 8-hour EVA (Sompayrac et al., 2009)
      or = 13.36 to 15.44 lbm (6.06 to 7.00 kg) for 8-hour EVA (Sompayrac et al., 2009)

V_c = 6.38 L = 0.00638 m^3

P_c = TBD (pump from LCVG bypass junction to SWME)

t_c = 0.5 hour (recharge LCVG tank; my estimate)

TRL = 6 (system prototype testing in thermal vacuum)

Reliability = Insensitive to contaminants; potential leakage issues; operates in a wider range of environmental pressures than the sublimator (e.g. remains effective on Mars surface, although these specs are based on lunar surface EVA)

Backup = Buddy-system bypass for multi-crew EVA; contingency O_2 purge

Kapton Substrate Mass/Volume Calculations for Electrochromic Radiator Options

5 mil = 125 μm (microns)
Density = 1.42 g/mL = 1420 kg/m^3 (DuPont)
Volume = (125 microns)*(3.43 m^2) = 0.000429 m^3
Mass = (1420 kg/m^3)*(0.000429 m^3) = 0.609 kg

Integrated Electrochromic Radiator (A = 3.43 m^2 and 0.1 < ε < 0.9 and T_s = 300 K)

Heat Rejection Capacity: (Metts & Klaus, 2010)
      Q_{rad} > 700 W in most lunar environments, specifics depend on sink temperature

Q_{abs} < 144 W at lunar sub-solar point (set to minimum emissivity)

Ashwin-Ushas:

0.06 g/cm^2 = 0.6 kg/m^2 = 2.06 kg (ECD only) (Ashwin-Ushas)

Total Mass = 2.669 kg + 3 kg (coolant loop) = 5.669 kg

P_c = 40 μW/cm^2 = 0.08 W (Ashwin-Ushas)

Eclipse:

5 g/m^2 = 0.0172 kg (ECD only)

Total Mass = 0.626 kg + 3 kg (coolant loop) = 3.626 kg

P_c = 0.1 mW/cm^2 = 1 W/m^2 = 3.43 W (Demiryont, 2009)

m_s = ECD/substrate plus tubing/support (estimate equal to LCVG, 3 kg dry mass) (Pisacane, 2006)

V_s = estimate equal to LCVG tubing + substrate (see above)

= (3 kg)/(0.93 spec gravity for ethyl vinyl-acetate tubing)/(1000 kg/m^3 for water) = 0.00323 m^3

+ substrate = 0.003659 kg total (volume of ECD itself is negligible)

Estimated TRL = 4 (Component validation in laboratory/relevant environment)

Reliability – Potential degradation at thermal vacuum; lunar dust effects (both thermal and abrasive); structural vulnerability due to position in suit fabric; built-in redundancy (with reduced performance) with parallel matrix of electrochromic pixels; performance depends on radiator sink conditions

Backup –Contingency O_2 purge

Combined ECD Radiator & Sublimator Approach

m_s = sum of ECD (averaged Ashwin and Eclipse values) and Sublimator options

V_s = see above

m_c = 30% of Sublimator value*

V_c = 30% of Sublimator value*

P_c = same as ECD (averaged Ashwin and Eclipse values)

t_c = 30% of Sublimator value*

*Based on Apollo water consumption study (Metts & Klaus, 2010)

This is a more realistic implementation of the ECD radiator concept, as a Sublimator will likely be retained for additional heat rejection during high-load activities, for backup in case of radiator failure, or in adverse thermal conditions (radiator heat absorption). It also best fits NASA's crew safety

requirements, as there are multiple, dissimilar systems. There is some water consumption, but less than the Sublimator-only configuration.

Sub-Cooled Phase Change Material (SPCM)

Heat Rejection Capacity = 400 W nominal, 800 W max (Leimkuehler et al., 2009a)

m_s = 12 kg (ice) + ~18 kg (fins and container) – ice is half of "20 to 25 kg" for 8-hr EVA; hardware is average of "one to two times" the PCM mass (Leimkuehler et al., 2009a)

        = 30 kg for each 4-hour unit

        = 60 kg for baseline 8-hour EVA

V_s = 15.93 L = 0.01593 m^3 for each 4-hour unit (entire SPCM unit based on current PLSS add-on dimensions) (Leimkuehler et al., 2009a)

    = 31.86 L = 0.03186 m^3 for baseline 8-hour EVA (two packs)

P_c = 0 (separate radiator for regeneration

t_c = 0.5 hour (for regeneration and unit-switching; my estimate)

TRL = 4 (component validation in laboratory)

Reliability: Limited capacity (4 hours) per unit; crew must carry a second unit, stay near vehicle, or limit EVA duration

Backup: Designed for fast switching with multiple extension/backup units

Creare Regenerable Absorption Heat Pump with Radiator and Evaporative Cooling Garment (ECG)

Heat Rejection Capacity = 192 W (Start) / 162 W (End) max rejection; with absorber bed, heat storage potential should be adequate to maintain crew member's thermal equilibrium; 1280 W-hr (460.8 kJ) overall capacity (8-hour EVA)

m_s = 9.0 kg – does not include ECG, since LCVG is standard for other candidates (personal communication with Michael Izenson, 2010; updated from previously published data)

V_s = (12 x 17 x 1.1 inches per 300 W-hr module) = 224.4 in^3 per module = 0.0037 m^3 per module

    = 0.0147 m^3 total for four modules (approx. 1200 W-hr capacity)

P_c = 0 (separate or built-in radiator for regeneration between EVAs)

t_c = 0.5 hr (regeneration; my estimate)

TRL = 5 (multiple components validated in thermal vacuum)

Reliability: Some dependency on radiator sink conditions; higher risk than other concepts due to combination of several new components (such as replacing the legacy LCVG)

Backup: Purge mode from ECG for additional cooling (consumable penalty); absorber unit may be modular and replaceable during EVA

Appendix D – Author's Notes

This research began in August 2006, when I began the Ph.D. program at the University of Colorado at Boulder with a general desire to work on something related to human spaceflight. The then-recent announcement of the Vision for Space Exploration implied development of new space suits for extravehicular activity (EVA), and NASA's subsequent architecture study that resulted in formation of the Constellation program called for space suit technologies that would eventually enable long-term habitation on the lunar surface as well as exploration of Mars. Professor David Klaus, my research advisor, saw the developments as an opportunity for academic research to address certain fundamental problems that will face the next generation space suits. After evaluating several possible technologies and areas of need, we focused on the idea of using electrochromic materials as a flexible radiator for space suits, a concept that Dr. Klaus had first heard about at the NASA Institute for Advanced Concepts (NIAC) 2005 Annual Meeting in nearby Broomfield, Colorado. We confirmed with the original study's authors that their work on the concept had concluded, and we began to identify areas in which the electrochromic radiator concept could be further developed in ways that would be meaningful both academically and practically. The potential value to NASA was quickly realized, and a proposal for NASA's Graduate Student Researchers Program (GSRP) was initiated.

While the GSRP proposal was being written and submitted, I was also taking courses and working on other research projects that served as introductions to the thesis topic. During the fall of 2006, Dr. Klaus taught a graduate course called "Space Life Support" that covered many topics pertaining to space suits, including thermal control. The design project for this course resulted in the entire class contributing concepts and preliminary analysis for a unified Constellation lunar suit architecture. A paper summarizing that group project was presented at the 2007 International Conference on Environmental Systems (ICES). During the spring and summer of 2007, I joined other

students and Dr. Klaus to write a paper on lunar outpost life support requirements for the Pacific International Space Center for Exploration Systems (PISCES) Conference.

Research on the electrochromic radiator concept began in earnest upon acceptance of the GSRP award in late summer 2007. The first task was developing a rationale through literature review and first principles, as a way to begin asking and answering the question of whether this technology could be used for EVA. A simple thermal model was created to predict radiator performance, and this model would be refined several times over the course of the research as I obtained better parameters and learned more about radiative heat transfer. An early version of this work was presented in the student poster competition at the 2008 ICES conference and received 4th place.

The project's NASA Technical Mentor through GSRP was Luis A. Trevino at Johnson Space Center, who provided considerable assistance in obtaining historical documents, internal NASA studies, and technical insight into space suit thermal control. Trevino was working on a new technology for NASA, called the Space Suit Water Membrane Evaporator (SWME), which is intended to replace existing sublimator technology and is essentially a competitor to the electrochromic radiator concept. Upon further review, we learned of several other technologies being developed either by NASA, university research groups, or private companies to address the problem of EVA water consumption. This marketplace of ideas led us to consider a system trade analysis that could fairly compare multiple candidates despite the wide range of technologies. The Equivalent System Mass (ESM) is a metric developed by NASA for just such a purpose. Using ESM not only allows for comparative analysis of multiple technologies but can also help identify areas for improvement within each candidate and may even lead to suggestions for combining certain technologies into hybrid systems.

Testing was always part of the research plan, and it presented significant challenges even from the outset. The electrochromic technology being studied, which is specially tuned for infrared modulation, is not commercially available as of this writing, and attempting to fabricate our own version

at the university would have proven to be highly expensive and distracting from the original research scope. Our discussions with electrochromic manufactures indicated that samples either were not ready for independent testing, or their cost would far exceed the GSRP materials budget. Nevertheless, we obtained a Beverly Sears Graduate Award from the CU-Boulder Graduate School and, during the summer of 2008, used those funds to build up a laboratory station devoted to testing for this research project. Testing methodologies were developed using standard, off-the-shelf materials in anticipation of later electrochromic material acquisition. This work led to a 2nd place prize in the student poster competition at the 2009 ICES conference.

In summer 2009, I spent ten weeks at Johnson Space Center in fulfillment of a GSRP requirement. Coincidentally, the Crew and Thermal Systems Division (CTSD) had purchased electrochromic samples from Ashwin-Ushas Corp. for study as a possible radiator technology on the Altair lunar lander vehicle. NASA engineers were scheduled to test the devices in a thermal vacuum chamber during that same period of time. I was allowed to participate in the final stages of planning and the actual test conduction, as well as post-testing analysis and documentation that eventually led to a NASA-authored paper at the 2010 ICES conference. Unfortunately, the test conditions did not translate well to the space suit problem, and the test results were not directly applicable to this research.

In December 2009, I met with an electrochromic manufacturer that had previously been unprepared to deliver functional samples for testing. The company had recently been awarded new funding and had begun producing prototypes of a new, commercial electrochromic material that would later be mass produced for terrestrial applications. This company graciously provided a pair of electrochromic devices, at no charge, for testing at CU-Boulder. While these devices were early prototypes and not representative of final performance, and they are not specifically developed for space applications, their small size, simple configuration, and demonstrable electrochromic properties were very helpful in validating and improving the test hardware and procedure in our laboratory. A

paper summarizing the test development and establishing a "bench-top" test approach as an inexpensive alternative to thermal vacuum testing for electrochromics was presented at the 2010 ICES conference.

Predicting actual water savings with the electrochromic radiator had always been a top goal for this study, but the scarcity of actual metabolic data from the Apollo program meant that any such analysis would be based on ground studies, at best. In spring of 2010, I was introduced to Dr. Christopher Carr of MIT, who had compiled extensive and highly detailed Apollo metabolic data for a previous study. The data had been recorded by NASA engineers and physicians during the Apollo program but had never been fully archived; Carr searched through the original documents and correlated the physiological data with minute-by-minute EVA timelines from the Apollo Lunar Surface Journal. The resulting database, which Carr graciously shared with me, could be combined with lunar environment data to calculate rigorous sublimator water consumption and hypothetical radiator performance for every Apollo EVA. Preliminary results of this study were presented at the 2010 ICES conference and received 1st place in the student poster competition.

I returned to Johnson Space Center in summer 2010, and this second trip was intentionally scheduled around follow-up electrochromic testing in the thermal vacuum chamber. NASA engineers had consulted the author on certain aspects of the test setup, but this second round of testing was still focused on vehicle applications. However, Luis Trevino was able to arrange additional funding for one extra day of EVA-specific testing, using the same electrochromic test samples and the same thermal vacuum chamber. I quickly developed EVA-specific test points that could be run within these constraints. Unfortunately, the real-time data indicated a problem with the test sample after less than 24 hours in the chamber, and the test was terminated before either Altair or EVA test routines could be executed. The delicate electrochromic devices were likely damaged during shipping to Houston, causing certain

layers to delaminate at vacuum. This outcome is an example of the inherent difficulty and iterative

nature to laboratory testing, especially when dealing with advanced, unproven technology.

While I would have liked to have more experimental results for this dissertation, I am confident

the analytical work achieves the original goal of advancing the knowledge of this EVA life support

technology so that future engineering decisions will be more informed. Moreover, the limited

experiments that were conducted during this period did lead to a better understanding of objectives,

requirements, and precautions needed to enable future, more advanced experimental testing.